CONDITIONS IN BLACK ASH STANDS AT VARYING STAGES OF EAB INVASION: VEGETATION, RADIAL GROWTH, AND CERAMBYCIDAE

By

River Daniel Raymond Mathieu

A THESIS

Submitted to
Michigan State University
in partial fulfillment of the requirements
for the degree of

Entomology – Master of Science

2025

ABSTRACT

This thesis, presented in four chapters, focuses on differences in forest vegetation, black ash (*Fraxinus nigra*) dendroecology across 24 black ash stands, and longhorn beetle (Coleoptera: Cerambycidae) species assemblages across eight stands, representing different stages of the emerald ash borer (EAB) (*Agrilus planipennis* Fairmaire) invasion referred to as: Post-, Mid-, and Pre-Invasion stands. Chapter one consists of a comprehensive assessment of forest vegetation across EAB Invasion Strata. Post-Invasion stands in the Lower Peninsula and eastern Upper Peninsula have experienced extensive overstory black ash mortality and Mid-Invasion stands have experienced some black ash mortality, while black ash in Pre-Invasion stands were predominately healthy. Black ash recruits (trees DBH 2.5-10 cm) in Post-Invasion stands exhibited high rates of mortality, and many recruits in Post- and Mid-Invasion stands were infested with EAB larvae. Chapter two focuses on the dendroecology of black ash overstory trees and recruits in 24 stands. Age of black ash recruits also varied but one recruit was 98 years old. In Post-Invasion stands, increases in annual ring width following overstory black ash mortality indicated release of black ash recruits. Chapter three examines cerambycid beetle species assemblages in eight black ash stands in Michigan's Upper Peninsula, in stands representing Mid and Pre-Invasion conditions. We recorded 43 new county records for 22 species of cerambycids and captured two species not previously reported from the Upper Peninsula. Finally, chapter four presents results from a 15-year common garden study in which survival and EAB infestations were tracked for four North American ash species: black ash, blue ash (*Fraxinus quadrangulata*), green ash (*Fraxinus pennsylvanica*), and white ash (*Fraxinus americana*), along with two Asian ash species: Chinese ash (*Fraxinus chinensis*) and Manchurian ash (*Fraxinus mandshurica*).

ACKNOWLEDGMENTS

First, I would like to acknowledge my advisor, Dr. Deb McCullough for her constant support and encouragement throughout my time at MSU. Deb's mentorship has made me a better scientist, and writer, and without her guidance I would not be where I am today. I would also like to thank my guidance committee: Dr. Eric Benbow and Dr. Andrew Finley for their assistance and expertise.

Second, I would like to thank Dr. Nate Siegert for introducing me to the world of forest entomology and dendrochronology. Without his mentorship before I arrived at MSU, I would never have pursued this research, and I cannot thank him enough for showing me the black ash forests of the northeast and encouraging me to be curious about the natural world.

This project would not have been possible without the technicians who helped collect data and process samples. Specifically, Drew LaCommare and Tim Harrison, who spent countless hours in the woods with me, and endured conditions that were, at times, brutal. I am grateful to have shared time in black ash stands with them both and am grateful for their friendship.

I would like to thank my partner Kelly Waters, for her constant support and encouragement during my time at MSU. Your love and support carried me through some of the most difficult times, and I am grateful to have you by my side.

Finally, I would like to thank my parents and my brother for introducing me to nature and exploring the forests with me when I was young. Your love and support has driven me to pursue a career that I truly love, and I will forever cherish the moments in the hemlock groves and beech maple forests where we spent countless hours.

PREFACE

Emerald ash borer (EAB) (*Agrilus planipennis* Fairmaire) is the most destructive forest insect pest to ever invade North America, killing hundreds of millions of ash trees since its introduction in the mid-1990s (Herms and McCullough 2014, Siegert et al. 2014). Of particular concern, is the impact that EAB will have on black ash (*Fraxinus nigra*), the most vulnerable and preferred host EAB has encountered to date (Engelken and McCullough 2020, Mathieu and McCullough 2025, Siegert et al. 2021, Smith et al. 2015). Black ash, found growing in forested wetlands and generally wet stands (Gucker 2005a), comprises an important component of the landscape in the Great Lakes States, often dominating especially wet stands. Additionally, black ash is a cultural keystone species used by Indigenous people throughout its range for traditional basketry practices (Costanza et al. 2017, Diamond and Emery 2011, Siegert et al. 2023). Given the species importance, and the threat posed by emerald ash borer, understanding the ecology of black ash forests is paramount to facilitating preservation and EAB management efforts.

This thesis, presented in four chapters, seeks to understand the impacts of EAB on black ash forests by comparing forest vegetation composition and radial growth of black ash overstory trees and recruits across 24 stands representing varying EAB invasion conditions. Cerambycid species assemblages are also explored in eight black ash stands in Michigan's Upper Peninsula. Results from a long-term study established in 2007 to investigate host preference and vulnerability of multiple ash species exposed to EAB are presented in Chapter 4.

Chapter one consists of a comprehensive assessment of forest vegetation, in which I explore differences in overstory, recruit, sapling, and seedling densities, as well as shrub and herbaceous plant composition in black ash stands across three broad Invasion Strata, representing Post-, Mid-, and Pre-Invasion conditions. In addition to vegetation assessments, we debarked

black ash recruits in stands where black ash regeneration was abundant, to understand if and to what degree EAB is infesting younger black ash. Overall, the majority of overstory black ash in our Post-Invasion stands have succumbed to EAB, and nearly 55% of overstory black ash in Mid-Invasion are dead, with the rest in decline. Overstory black ash in Pre-Invasion stands appeared healthy. There were no differences in regeneration densities (recruits and saplings) across broad Invasion Strata, however five Post-Invasion stands had low densities of recruits, saplings, and seedlings. Over half of the total black ash recruit stems present in Post-Invasion stands were dead, a significantly higher proportion than percent mortality of black ash recruits in Pre-Invasion stands. Furthermore, high proportions of live black ash recruits in Post- and Mid-Invasion stands exhibited signs of EAB infestation (i.e. epicormic shoots and woodpecker holes), suggesting that EAB infests and kills recruits during the middle stages of infestation and after overstory black ash trees die. We observed EAB galleries on black ash recruits across all Invasion Strata, with the highest gallery density present on recruits in Mid-Invasion stands. Bareground and graminoid percent coverage did not differ by Invasion Strata, however seedling density was negatively correlated with graminoid percent coverage across all stands. Multivariate analysis of overstory, recruit, and sapling species showed few differences in tree communities across Invasion Strata.

Despite mortality and EAB infestations on black ash recruits in Post- Invasion stands and Mid- Invasion stands, chapter two explores the release of black ash recruits across Invasion Strata, shedding light on black ash stand dynamics in the wake of EAB. Through collection of increment cores from live overstory black ash trees in Pre- and Mid-Invasion stands, and live black ash recruits across Invasion Strata, we characterize the dendroecology of black ash in Michigan forests. Old overstory black ash trees were present in Pre- and Mid-Invasion stands, with one stand containing two overstory black ash over the age of 200, and the oldest at 283 years old. We

expect that this one stand represents old growth conditions. Age class distribution of overstory black ash trees across Pre- and Mid-Invasion stands represents uneven aged forests, with multiple different cohorts present in the overstory. Black ash recruits across all stands were variable in age, however, we did not observe very old recruits in some instances. The oldest black ash recruit was 98 years old, and 16 recruits were over 75 years old across all stands, contributing to the mounting evidence that black ash is a shade tolerant species and can remain in the understory for decades. Black ash recruits appeared to release in Post-Invasion stands following the loss of overstory black ash, with average annual ring width increasing by 95% on average across our Post-Invasion sites. We also noted the absence of older black ash recruits in Post-Invasion stands where EAB had been present longer, suggesting a shift in the age class of regenerating black ash in the wake of EAB. Finally, increment cores collected from balsam fir recruits, where it co-occurred with black ash at relatively high densities, showed no significant increases in balsam fir radial growth following the loss of overstory black ash in Post-Invasion stands.

Chapter three explores cerambycid communities in black ash forests of Michigan's Upper Peninsula, contributing to the literature on the biodiversity of these unique forest systems. Native woodboring beetles are often overlooked in our forests, and they play important roles in nutrient cycling and decomposition. Cross vane panel traps baited with 3R* lures and UHR ethanol were deployed across eight black ash stands representing varying levels of EAB infestation. Coarse woody debris in these stands was quantified, and multivariate analysis conducted to understand how changes in snag density and CWD volume from EAB caused black ash mortality impacts cerambycid species assemblages. We captured a total of 705 beetles over 2 years of trap deployment, representing 28 species. The most commonly caught beetles were *Clytus ruricola* (Olivier) and *Xylotrechus colonus* (Fabricius), representing almost 80% of beetle captures

combined. There were no differences in beetle species assemblages based on EAB Invasion Strata, and no stand level data (i.e. CWD volume, snag basal area) were significant predictors of cerambycid species assemblages. Despite these insignificant results, upon lengthy review of Michigan cerambycid county record literature, we recorded 43 new county records for 22 cerambycid species in Michigan's Upper Peninsula, and one new state record.

Chapter four, currently published in the journal of Environmental Entomology, details the results of a 15 yearlong common garden study, in which the survival and growth of multiple ash species was recorded. This common garden study, linked to the previous chapters through the inclusion of black ash, contributes to the literature on EAB host preference and vulnerability. Four North American ash species were included in this study: black ash (*F. nigra*), blue ash (*F. quadrangulata*), green ash (*F. pennsylvanica*), and white ash (*F. americana*), along with two Asian ash species: Chinese ash (*F. chinensis*), and Manchurian ash (*F. mandshurica*), were planted in in 2007, protected from EAB with tree wrap until 2011, and then monitored until 2022. The study focuses on data from 2017-2022, tracking tree survival, DBH, woodpecker hole and exit hole density, and tree annual increment over time. All black ash died within the first year of exposure to EAB, and the majority of Chinese ash (86%) and green ash (63%) where dead by 2022. Only 12 % of white ash were dead in 2022, and all blue ash were alive. We also observed high densities of woodpecker holes and EAB exit holes on green, white, and Chinese ash, but low densities on blue ash. Furthermore, live Manchurian ash appeared healthy, with few signs of EAB infestation. Low mortality of blue ash, and clearly low densities of exit holes and woodpecks contributes to the evidence that blue ash are less vulnerable to and less preferred by EAB its other North American counterparts.

In all, this thesis provides information on the status of black ash forests before, during, and after EAB invasion, shedding light on the impacts that EAB has had on Michigan's black ash forests. Although most overstory black ash trees in Post-Invasion stands have been killed, substantial differences amongst regenerating tree communities were not observed across Invasion Strata, suggesting that regenerating tree communities remain relatively unchanged in the wake of EAB. Furthermore, high proportions of dead black ash recruits hint toward the eventual demise of black ash through the interactions between the orphaned black ash cohort and EAB. Because the loss of overstory black ash will result in severely depressed seed production, the future of black ash depends on the black ash regeneration. Colonization by EAB makes it unlikely that black ash regeneration will reach a size and age where they are capable of producing seed, despite the apparent ability to release of black ash recruits following overstory ash mortality observed in our study. More research is needed to continually monitor the status of regenerating black ash present in aftermath forests to determine if releasing black ash recruits eventually produce seed.

TABLE OF CONTENTS

CHAPTER ONE: FOREST VEGETATION OF MICHIGANS BLACK ASH FORESTS ACROSS THREE EAB INVASION STRATA

Introduction

First detected in 2002, emerald ash borer (EAB) (*Agrilus planipennis* Fairmaire), a phloem-feeding beetle from Asia introduced into Michigan in the early 1990s (Siegert et al. 2014), has become the most destructive forest insect to invade North America (Herms and McCullough 2014, McCullough 2020, Ward et al. 2021). To date, EAB is established in 37 U.S. States and six Canadian Provinces (USDA Aphis, 2025) and has killed hundreds of millions of ash trees (Herms and Mccullough 2014). As EAB continues to spread, millions more are at risk (Herms and McCullough 2014, Klooster et al. 2018, Ward et al. 2021), as all major North American ash species (*Fraxinus spp.*) can be colonized by EAB. During early stages of infestation, individual trees exhibit few or no external signs or symptoms (Cappaert et al. 2005). As densities of larval galleries build over time, thin or yellowing foliage, canopy dieback, epicormic shoots, and holes left by woodpeckers feeding on late instar and pre-pupal larvae become apparent (Anulewicz et al. 2007, Herms and McCullough 2014). Most overstory ash trees succumb within four to six years following EAB infestation (Herms and McCullough 2014, Klooster et al. 2014, Smith et al. 2015).

Although all ash species EAB has encountered in North America to date can be colonized and killed, variation in EAB host preference and vulnerability among North American ash species is consistently observed (Engelken and McCullough 2020a, Mathieu and McCullough 2025, Rebek et al. 2008, Robinett and McCullough 2019, Tanis and McCullough, 2012, 2015). Blue ash (*F. quadrangulata*) is the least preferred and vulnerable EAB host, followed by white ash (*F. americana*) which is intermediately vulnerable, and green ash (*F. pennsylvanica*) which is considered highly vulnerable (Rebek et al. 2014, Tanis and McCullough, 2012, 2015, Robinett

and McCullough 2019, Engelken and McCullough 2020, Mathieu and McCullough 2025). Black ash (*F. nigra*) is consistently the most preferred and vulnerable host of the major North American ash species encountered by EAB (Smith et al. 2015, Engelken and McCullough 2020, Mathieu and McCullough 2025, Siegert et al. 2021). Mortality rates of 80% or higher for overstory black ash were reported in Michigan stands following EAB invasion (Klooster et al. 2014, Engelken and McCullough 2020, Siegert et al. 2021). By 2040, projections suggest > 90% of black ash basal area across nearly its entire native range is likely to be dead (Siegert et al. 2023), generating concerns about the ecological and cultural impacts of losing black ash entirely.

Commonly found in forested wetlands of North America's Great Lakes region, the northeastern US, and southeastern Canada, black ash is considered an ecologically foundational species. Traits including hypertrophied lenticels, adventitious roots, shallow rooting depth and vegetive sprouting facilitate black ash growth in boggy, swampy, or ephemerally flooded stands where many other trees species cannot survive (Erdman et al. 1987, Tardiff and Bergeron 1993, 1999, Gucker 2005a, Benedict and Frelich 2008, Shannon et al. 2018, COSEWIC 2020). In stands dominated by black ash, evapotranspiration by overstory trees facilitates hydrological regulation (D'Amato et al. 2018, Palik et al. 2012, 2021), senescent leaves provide an input of high-quality nutrients in autumn (Toczydlowski et al. 2019, Youngquist et al. 2017) and trees provide habitat for wildlife, including, birds, amphibians, deer, and ground beetles (COSEWIC 2018, Kolka et al. 2018). Although black ash is typically associated with hydric conditions, it can also grow in mesic or well-drained area (Benedict and Frelich 2008, Costanza et al. 2017, Gucker 2005a, Palik et al. 2021), where it is generally a minor or co-dominant overstory component.

Black ash trees can co-occur with numerous tree species across its native range and, until the EAB invasion, were most frequently a component of lowland hardwood forests (Gucker 2005a, Rudolf, 1970). Other associates noted in the Lakes States region include white cedar (*Thuja occidentalis*), basswood (*Tillia americana*), balsam fir (*Abies balsamea*), silver maple (*Acer saccharinum*), balsam poplar (*Populus balsamifera*), and black spruce (*Picea mariana*) (Erdman et al.1987, Weber et al. 2007, Wright and Rauscher 1990, Zogg and Burton 1995). Multiple shrubs including various alder species (*Alnus spp.*) and Michigan holly (*Ilex verticulata*) often grow in patches within black ash forests (Weber et al. 2007, Zogg and Burton 1995). An array of understory plant species flourish in light gaps that can be common in black ash stands, including multiple species of sedges (*Carex spp.*) and rushes (*Juncaceae spp.*), forbs including dwarf red raspberry (*Rubus pubescens*), marsh marigold (*Caltha palustris*), *Impatiens spp*, and multiple fern species (Weber et al. 2007).

Along with its ecological importance, black ash is considered a cultural keystone species, serving as a significant cultural and spiritual resource for members of many Native American and First Nations people throughout the eastern US and Canada. For millennia, indigenous basketmakers have harvested black ash to craft utilitarian and artistic baskets from sapwood (Benedict and David 2004, Costanza et al. 2017, Diamond and Emery 2011, Siegert et al. 2023), an arduous process that takes years to master (Costanza et al. 2017, Diamond and Emery 2011, Siegert et al. 2023). Basket making begins with the careful selection of a suitable tree which is felled, then cut to a 2-3 m length and hauled out of the forest. Logs are debarked, then must be pounded with the back of an axe or similar tool to separate individual growth rings, which are shaved further down to splints that can be woven together (Costanza et al. 2017, Diamond and Emery 2011). This practice has been passed down through generations, and in modernity, has

become an essential aspect of cultural preservation for tribes that practice black ash basketry (Costanza et al. 2017, Frey and Greenlaw 2019). Furthermore, black ash plays a role in the spiritual aspects and traditions of multiple tribal cultures, including the W8banaki creation story and has medicinal traits (Costanza et al. 2017, Siegert et al. 2023).

Ongoing spread of EAB and high levels of black ash mortality sustained in post-invasion stands have intensified interest in and concern regarding the status of black ash regeneration, along with condition of other vegetation in affected stands. Results from studies attempting to simulate potential impacts of EAB, e.g., by felling large numbers of black ash trees in winter (Cianciolo et al. 2021, Davis et al. 2016, D'Amato et al. 2018, Kolka et al. 2018, Slesak et al. 2014, Windmuller-Camppione et al. 2020) have reported changes in hydrology, tree species composition, and increases in shrub and sedge cover. While these studies provide insight into black ash ecology, direct impacts of EAB on overstory composition and tree regeneration in black ash stands have yet to be explored.

Michigan, the original epicenter of the EAB invasion in North America (Cappaert et al. 2005, Siegert et al. 2014), provides a unique opportunity to assess conditions in black ash stands at different stages of invasion. Post-Invasion sites where the majority of overstory black ash have died are primarily present in the Lower and eastern Upper Peninsula. Parts of the eastern and central Upper Peninsula contain stands representing Mid-Invasion conditions, where overstory black ash are declining, dying, and dead. Pre-Invasion stands, present in the central and western Upper Peninsula, are the last healthy black ash stands in Michigan, where there are few to no signs of infestation and no EAB-caused tree mortality.

To document and understand the broad impacts of EAB invasion on vegetation in forest stands dominated by black ash, we quantified species composition, abundance, and condition of

overstory trees and regeneration, along with shrub and herbaceous plant communities in stands representing different stages of EAB invasion. Here, we describe how overstory tree communities have changed in the wake of EAB, and the extent of overstory black ash mortality in our Mid- and Post-Invasion stands. We then examine the density and condition of regenerating trees, with emphasis on differences in density and condition of black ash recruits (DBH 2.5-10 cm), saplings (height > 1 m; diam < 2.5 cm), and seedlings (height < 1 m) across Invasion Strata. Finally, we assess differences in shrub and herbaceous plant percent coverage across Invasion Strata.

Methods

Stand Selection: We selected 24 stands where black ash is currently or was historically present (Table S1). Stands were identified by accessing maps and data from EAB impact surveys conducted between 2019-2022, Michigan forest cover maps (MI DNR 2022) (ArcGIS Pro; ESRI, Redlands CA), and forest inventory data provided by the Hiawatha National Forest. Potential stands were visited to confirm the presence of black ash, assess invasion status and stand size. We classed stands into three broad Invasion Strata: Post-Invasion where > 80% of overstory black ash had been killed by EAB (n = 12 stands), representative of overstory black ash mortality cited in lower Michigan as of 2020 by Engelken and McCullough 2020 and Siegert et al. 2021, Mid-Invasion where 20 to 80% of overstory black ash were killed (n = 5 stands) and Pre-Invasion stands where < 20% of overstory black ash were dead (n = 7 stands) (Fig. 1.1). Seven Post-Invasion stands represented sites with abundant regeneration of all species (>500 recruit stems/ ha), while the other five Post-invasion stands had low or negligible regeneration (<500 recruit stems /ha). These stands are referred to henceforth as Post-Invasion Ample Regeneration, and Post-Invasion Minimal Regeneration. Post-Invasion stands are pooled for most analysis, but

separated to understand if and how differences in overstory tree basal area and density may impact tree regeneration in Post-Invasion conditions.

Survey Design: We delineated boundaries of stands using Google Earth imagery (Google Inc, Mountain View, CA, 2023), then overlaid a 50 m x 50 m grid using the fishnet tool in ArcGIS Pro (ESRI, Redlands, CA, 2023). We identified grid cells within each stand where overstory black ash or recruits occurred, then randomly selected three of those grid cells for surveys (Fig. 1.2A). At the center of selected grid cells, we established nested, fixed radius plots comprised of a macroplot (11.4 m radius) and a subplot centered within the macroplot (8 m radius). If center plots did not include a minimum of six overstory black ash trees or six black ash recruits (alive or dead), we randomly selected a new grid cell. To evaluate herbaceous vegetation, a 1x1 m quadrat was oriented diagonally away from the center point in a random compass heading and two additional 1x1 m quadrats were located on the northern and southern perimeter of each subplot. Two 25 x 2 m transects to quantify coarse woody debris were established from the center of each plot in random compass headings; one was located between 0-180° and the other was located between 180-360°, ensuring transects did not overlap.

Overstory assessments: In macroplots (Fig. 1.2B), we measured diameter at breast height (DBH) (1.3 m aboveground) and visually estimated canopy condition (percent transparency; percent dieback) of live and dead overstory trees (DBH > 10 cm) by species. We recorded external signs of EAB infestation including the number of distinct holes left by woodpeckers preying on late-instar EAB larvae and counted live epicormic shoots up to 2 m high on the trunk, as well as basal sprouts. Density of overstory trees standardized per ha, and proportion of live and dead overstory black ash trees were calculated for each species and for all species combined in each stand and averaged for stands representing Pre-, Mid- and Post-Invasion strata. Overstory

trees were further grouped into 5 cm size classes (starting at 10 cm DBH) to document size class structure within stands. Basal area of overstory trees by species was calculated for each stand then averaged by Invasion Strata to assess relative dominance by species. Relative importance values (RIV), defined as the sum of relative density, relative dominance, and relative frequency, were calculated for each tree species tallied in each stand and averaged by Invasion Strata. Species richness of overstory trees was also calculated for each site.

Regeneration assessments: We recorded DBH of live and dead recruits (DBH 2.5 to 10 cm) in subplots (Fig. 1.2B), estimated canopy condition of live recruits, counted woodpecks and live epicormic shoots and up to 2 m high and tallied live basal sprouts. Live and dead saplings (height > 1 m; DBH < 2.5 cm) within subplots were tallied by species. Percent coverage of *Alnus* spp. and abundant shrub species within subplots or numbers of individual stems of occasional shrub species were recorded. Densities of live and dead recruits and saplings along with the proportion of live black ash recruits with external signs of EAB infestation (≥ 3 epicormic sprouts or ≥ 1 woodpeck) were calculated, standardized per ha for each stand and averaged by Invasion Strata.

Emerald ash borer colonization of recruits: We randomly selected and felled three live black ash recruits (1 per plot) in stands where ample regeneration was present (≥ 6 black ash recruits within plots or within 10 m of plots). Each recruit was cut into three ~1 m bolts, beginning just above the root flare. Bolts were transported back to the lab and carefully debarked within five days. Numbers of EAB galleries and live larvae were recorded. We calculated phloem area following McCullough and Siegert (2007) using measurements of the length and circumference of each bolt end and standardized galleries and larvae per m^2 of phloem area. Average densities of galleries and larvae were then calculated for each stand.

Tree seedings and herbaceous plants: We recorded the number of tree seedlings present by species or genera in the three microplots (1x1 m) established in each macroplot. In the microplot centered in each macroplot (Fig. 1.2 B), we identified herbaceous plants minimally to family and to genus or species when possible and estimated percent cover. Herbaceous plants were identified using field guides (Chadde 2016, 2017) and mobile applications (Seek by iNarualist, 2023, v2.17.0) (Hart et al. 2023). To further increase sampling effort, we established two microplots on the perimeter of the macroplots (Fig 1.2. B), and estimated percent cover of sedges, grasses, forbs, ferns, bare ground, bryophytes, and woody plants. Invasive plant species, excluding ferns and graminoids, were noted.

***Coarse woody debris*:** In each of the two 25 x 2 m transects (Fig. 1.2 B), we measured diameter of coarse wood debris (CWD) pieces (≥ 4.0 cm), the length of the piece within the transect and recorded species or genera (when possible). Pieces of CWD were assigned to one of four decay classes following Engelken and McCullough (2020a): (1) bark present to mostly present and firm, few areas of solid wood exposed; (2) bark loose and sloughing off in multiple spots, exposed wood mostly firm with some soft areas; (3) bark absent or loose in some areas, mix of firm and soft exposed wood; (4) bark absent, exposed wood soft and spongy. Pre-EAB black ash basal area and density was estimated in Post- and Mid-Invasion sites using the DBH of the trunks of fallen ash trees (DBH > 10 cm) encountered in transects and basal area of standing dead overstory ash (snags) in macroplots. Pre-EAB basal area and densities were averaged by site and Invasion Strata.

Statistical analysis: Analysis and data management were conducted using R (R Core Team, 2024; Version 4.3.2). Generalized linear models (GLMs) and mixed models were constructed using the glmmTMB package (Brooks et al. 2017; Version 1.1.9), and likelihood

ratio tests were used to evaluate significance of GLMs and GLMMs (Bolker 2025). All model assumptions were checked using simulated residual plots from the DHARMa package (Hartig 2022, v0.4.6), and model contrasts and model estimates were obtained using the emmeans package (Lenth 2024; Version 1.10.2).

To evaluate differences in recruit density (all species) among stands representing different invasion strata, we conducted one-way ANOVA, with log transformed stand average density as the response, and Invasion Strata as the predictor. One-way ANOVA was also used to test for differences among Invasion Strata in density of black ash recruits (square root transformed). We tested for significant differences in relative black ash recruit density, alive and dead, across Invasion Strata using beta regression. These analyses were repeated for saplings of all species (square root transformed) and black ash recruits.

Differences in the proportion of black ash basal area before EAB and basal area of all live species between two types of Post-Invasion stands (Post-Invasion Ample Regeneration and Post-Invasion Minimal Regeneration) were assessed using two-sample t-tests. To further assess these relationships, we used linear regression to predict average recruit density (all species) by proportion of black ash basal area before EAB and residual tree basal area separately.

To evaluate differences in average proportion of black ash recruits that were dead and live black ash recruits with signs of EAB infestation across Invasion Strata (Post, Mid, Pre), we used quasi-binomial GLMs, accounting for overdispersed binomial data, with the proportion of dead black ash recruits or the proportion of infested black ash recruits as response variables and Invasion Strata (three-level factor) as the predictor in separate models. Differences in density of EAB galleries on black ash recruits by Invasion Strata were assessed using a one-way ANOVA, with square root transformed average gallery density as a response and Invasion Strata as a

factor. The number of EAB larval galleries recorded on recruits was regressed against live black ash basal area recorded in each stand using a negative binomial GLM, to account for overdispersed count data, with phloem area sampled as a model offset.

Differences in percent cover of shrubs, bare ground, and graminoids among Invasion Strata were assessed using beta regression separately for microplots and for data from auxiliary plots to examine the impacts of canopy loss on the herbaceous plant layer. To assess potential competition between regenerating tree species and shrubs, sapling density was regressed against percent cover of shrubs (all species) with simple linear regression using combined data from microplots and auxiliary plots.

We tested for differences in densities of total seedlings and black ash seedlings across Invasion Strata separately, using negative binomial GLMMs with plot seedling density as a response, Invasion Strata as a fixed effect and Stand as a random effect, and total area sampled as a model offset (Table S1.1). To understand how percent cover of graminoids impacted total seedling density, and if the relationships between seedling density changed across Invasion Strata, we compared three models negative binomial models: one with mean percent graminoid cover as the sole predictor, a second with mean percent graminoid cover and Invasion Status as a three level factor as predictors, and a third with mean percent graminoid cover and an interaction with Invasion Status as predictors, all with total stand seedling counts as a response, with area sampled as a model offset.

Total counts of overstory trees, recruits, and saplings by species from each stand were assessed to understand black ash forest community structure within Post-, Mid-, and Pre-Invasion stands. Using the vegan package in R (Oksanen et al. 2022; Version 2.6.4), we calculated species alpha diversity of overstory trees, recruits, and saplings separately used a one-

way ANOVA to test for differences in alpha diversity across Invasion Strata. Species counts were then Hellinger transformed (Legendre and Gallagher 2001) and principal component analysis (PCA) was conducted for overstory, recruit and sapling communities separately. Given recent research projecting the impending loss of black ash as EAB advances (Siegert et al. 2023), we ran additional PCAs to explore forest communities in the absence of black ash for overstory, recruit, and sapling communities. We used redundancy analysis (RDA) and ANOVA with permutations to test for significant differences in overstory tree communities among Invasion Strata (Legendre and Gallagher 2001).

Similarity of overstory / recruits, and overstory / sapling species were assessed with Co-Inertia Analysis (CoIA) conducted on PCA objects obtained from the dudi function from the ade4 package in R (Dray et al. 2007; Version 1.10.0). Co-Inertia of overstory / recruit and overstory / sapling distance matrices within stands were assessed and permutation tests were conducted to determine significance of individual CoIA. These tests were conducted twice, once with ash species included in the distance matrix and once with ash excluded from the distance matrix to evaluate the influence of ash on relationships between overstory and regenerating communities. We calculated similarity of overstory / recruit and overstory / saplings, represented by the distance between points from the CoIA for each stand, and conducted a one-way ANOVA to discern differences in the similarity of overstory and regeneration species by Invasion Strata.

Results

Overstory: Black ash had the highest relative importance values within all Pre- and Mid-Invasion sites, whereas northern white cedar and balsam fir were more important species in Post-Invasion stands (Table 1.1). Diameter class distributions of black ash in Mid- and Pre-Invasion sites represented uneven-aged forests, with some large overstory trees and many trees in smaller

and intermediate size classes (Fig. 1.3; Table S1.2). This trend was less pronounced in Post-Invasion stands, presumably due to EAB-caused mortality of overstory black ash, which also contributed to lower basal area of live black ash in Post- and Mid-Invasion stands compared to Pre-Invasion stands. Overstory tree species richness was lower in Post-Invasion stands (5.25 ± 0.637) than in Pre-Invasion (8 ± 0.834) stands (F = 3.654; d.f. = 2, 21; $P = 0.043$), and species richness in Mid-Invasion stands did not differ among other Strata. This difference in overstory tree species diversity, was likely drive by the mortality of overstory black ash in Post-Invasion stands, which averaged 89.2 ± 6.4%, compared with 52.4 ± 12.0% and 4.4 ± 1.3% in Mid-Invasion and Pre-Invasion stands, respectively.

Recruits: Live recruits were observed in every stand, although density and composition varied (Fig. 1.4). Common recruit species across all stands included black ash and balsam fir, with red maple, white cedar, green ash, and balsam poplar occurring less frequently (Figure 1.4). Recruit species richness did not differ by Invasion Strata (F = 1.626; d.f. = 2,21; $P = 0.2205$), and the median species richness across all stands was four. Average density of total live recruits was similar among Post-, Mid- and Pre-Invasion stands (Fig. 1.5A) (F = 0.68; d.f. = 2, 21; $P = 0.516$). Post-Invasion stands with minimal regeneration had on average 116 ± 35 recruits per ha, significantly lower than average recruit densities of other Invasion Strata (F = 11.35; d.f. = 3, 20; $P < 0.001$) (Fig. 1.5B). Similarly, there was no difference in density of dead recruits across Invasion strata (F = 0.84; d.f. = 2, 21; $P = 0.447$). Mean current live basal area of all species in Post-Invasion sites with Ample Regeneration (10.94 m^2/Ha; 95% CI [7.44, 14.44]) was 2.3 times higher than in Post-Invasion Stands with Minimal Regeneration (4.72 m^2/Ha; 95% CI [.574, 8.86]) (F = 6.53; d.f. = 1, 10; $P = 0.029$), and recruit density in Post-Invasion stands was significantly correlated with live tree basal area (F = 5.43; d.f. = 1, 10; $P = 0.0419$; *Adj.* R^2 =

0.29), however there was no significant difference in Pre-EAB black ash relative basal area (F = 4.06; d.f. = 1, 10; $P = 0.072$).

We observed live black ash recruits in all stands, except for two Post-Invasion Minimal Regeneration stands that had few live recruits of any species. Black ash consistently comprised a large proportion of live recruit stems, and density did not differ across Invasion Strata (F = 0.57; d.f. = 2, 21; $P = 0.576$) (Fig. 1.5A). Generally, density of dead black ash recruits was similar among all Post-, Mid-, and Pre-Invasion stands (F = 2.57; d.f. = 2, 21; $P = 0.1$) (Fig. 1.5A), however we observed differences in the proportion of black ash recruits that were dead among Invasion Strata (χ^2 =14.197; d.f. = 2; $P < 0.001$). The proportion of dead black ash recruits was 2.4 times higher in Post-Invasion stands than in Mid-Invasion stands, and 4.8 times higher than in Pre-Invasion stands (Fig 1.6A).

EAB infestation of recruits: Live black ash recruits with signs of EAB infestation (epicormic shoots or woodpecker holes) were observed in all Post- and Mid-Invasion stands, and in four Pre-Invasion stands (57%). However, in three of the four Pre-Invasion stands where EAB signs were observed, only 3% of recruits in each stand had one or more epicormic shoots, likely reflecting natural stress. Overall, a higher proportion of live black ash recruits had signs of EAB infestation in Post- and Mid-Invasion sites than in Pre-Invasion sites (χ^2 = 10.96; d.f. = 2; $P = 0.004$) (Fig. 1.6B).

Black ash recruits were felled and debarked in 16 of the 24 stands including six, three, and seven Pre-, Mid-, and Post-Invasion stands, respectively. We recorded EAB galleries and live larvae on debarked black ash recruits in each of these Post-Invasion and Mid-Invasion stands, compared with only two of the Pre-Invasion stands (33%). On average, 81 ± 10% and 78 ± 11% of debarked recruits in Post-Invasion and Mid-Invasion stands, respectively, had EAB

galleries, compared to 39.8 ± 20% of recruited in Pre-Invasion stands. Densities of EAB galleries differed among invasion strata (F = 4.86: d.f. = 2, 13; $P = 0.0265$). Recruits in Mid-Invasion stands had the highest and most variable density of galleries, followed by Post-, and Pre-Invasion stands (Fig. 1.7A). Density of EAB galleries on recruits was negatively related to basal area of live black ash trees ($\chi^2 = 8.55$; d.f. = 1; $P = 0.0035$) (Fig. 1.7B).

Saplings and Shrubs: Live saplings were present at varying densities in all stands, with the exception of one Post-Invasion stand, and represented 20 tree species (Fig. 1.8). Black ash and balsam fir were common sapling species, frequently encountered in all Invasion Strata (Fig. 1.8). Sapling species richness did not differ among Invasion Strata (F = 1.007; d.f. = 1, 21; $P = 0.832$), and the median species richness was four. Density of live saplings (all species) was highest and most variable in Mid-Invasion stands, compared to Post-, and Pre-Invasion stands but differences among Invasion Strata were not significant (F = 0.545; d.f. = 2, 21; $P = 0.6$) (Fig 1.5B). Dead saplings were present in 18 of 24 stands but densities were generally low, and total dead sapling density did not differ by Invasion Strata (F = 0.397; d.f. = 2, 21, $P > 0.5$) (Fig. 1.5B).

Black ash, the most common and abundant sapling species, was tallied in 21 stands and was only absent from two Post-Invasion and one Pre-Invasion stand, all of which had few saplings of any species. Density of black ash saplings was highest in Mid-Invasion stands followed by Post and Pre-Invasion stands, but did not differ among Invasion Strata (F = 0.45; d.f. = 2, 21; $P > 0.5$). On average 43 ± 6 %, 50 ± 10%, and 37 ± 12% of live saplings were black ash in Post-, Mid-, and Pre-Invasion stands, respectively. Dead black ash saplings were present in 14 stands; however, their densities were similarly low across all Invasion Strata (F = 0.177; d.f. = 2 and 21; $P = 0.8$) (Fig. 1.5B)

Shrub species were present in all 24 stands, but species composition varied. Alder (*Alnus spp*.) was present in 19 stands while Michigan holly (*Ilex verticulata*), and cherry species (*Prunus spp.*) were each present in six stands (Table 1.2). Other shrubs occurring less frequently and at lower densities included buckthorn species (*Rhamnaceae spp.),* and mountain maple *(Acer spicatum).* Percent cover of all shrub species differed among Invasion Strata ($F = 4.251$; d.f. = 2, 21; $P = 0.028$), and was highest in Post- and Mid-Invasion stands which did not differ from each other, and lowest in Pre-Invasion stands (Table 1.2). There was no relationship between shrub percent cover and sapling density ($F = 1.704$; d.f. = 3, 20; $P = 0.198$). Two common invasive shrubs in Michigan, multi-flora rose (*Rosa multiflora*) and autumn olive (*Elaeagnus umbellata*), were present at low densities in one Post-Invasion stand in the central Lower Peninsula.

***Seedlings and Herbaceous Plants*:** Ten seedling species were observed in microplots, with seedlings being observed in 87% of stands (Table 1.3), and only not present in two Post-Invasion stands. Average total seedling density ranged from 0 seedlings/Ha to 142,000 ± 59,389 seedlings/Ha and differed significantly by Invasion Strata ($\chi^2 = 10.3$; d.f. = 2; $P = 0.006$). Total seedling density was 7.2 times greater in Pre-Invasion stands (60872 seedling/Ha; 95% CI [24056,154032]) than in Post-Invasion stands (8346 seedling/Ha; 95% CI [3791,18377]) and there was no significant difference among seedling densities in Mid-Invasion stands and other Invasion strata (17264 seedling/Ha, 95% CI [5518,54010]) (Table 2). Seedling density was negatively correlated with mean percent cover of graminoids, regardless of Invasion Strata ($F = \chi^2 = 3.98$; d.f. = 1; $P = 0.046$) (Fig. 1.9; Table 1.5).

The most prevalent seedling species was black ash, which occurred in 20 stands at varying densities. Black ash seedling density differed significantly by Invasion Strata ($\chi^2 = 9.7$;

d.f. = 2; P = 0.0078) and was highest in Pre-Invasion Stands followed by Mid-Invasion and Post-Invasion stands (Table 1.3).

Frequently observed herbaceous plant species in microplots were similar across Invasion strata although percent cover varied (Table 1.4). We found no difference in bare ground percent coverage across Invasion Strata (χ^2 = 5.68; d.f. = 2; P = 0.0582), and the average total percent coverage of graminoids did not differ significantly (χ^2 = 2.5; d.f. = 2; P = 0.276) (Table 1.4). In auxiliary microplots, we also found no difference in total graminoid cover by Invasion Strata (χ^2 = 0.358; d.f. = 2; P = 0.836*)*. It is important to note that auxiliary plots in three Post-Invasion stands with Minimal Regeneration and one Mid-Invasion stand contained *Typha spp.*, contributing to graminoid percent cover in those stands. There was a significant difference in the percent cover of bare ground found in auxiliary plots (χ^2 = 8.87; d.f. = 2; P = 0.0174), however, post-hoc tests revealed that percent cover only differed significantly in Mid- and Pre-Invasion stands. Multivariate analysis of auxiliary plot communities revealed no significant differences in plant community coverage by Invasion Strata (Fig. 1.10).

***Tree Communities - Beta Diversity*:** Species composition of overstory trees differed among Invasion Strata when ash species were included in analysis (F = 2.145; d.f. = 2, 21; P = 0.006), and this pattern was largely driven by the lack of live overstory black ash in Post-Invasion stands (Fig. 1.11A). When black ash was excluded, overstory tree beta diversity did not differ among Invasion Strata (F = 1.078; d.f. = 2, 21; P = 0.362) (Fig. 1.11B). Beta diversity of recruit communities did not differ by Invasion Strata when ash species were included in analysis (F = 1.258; d.f. = 2, 21; P = 0.198) (Fig. 1.11C), or excluded from analysis (F = 1.585; d.f. = 2, 21, P = 0.085) (Fig. 1.11C). Sapling community beta diversity did not differ among Invasion

Strata when ash was included in analysis (F = 1.175; d.f. = 2, 21; $P = 0.261$) (Fig. 1.11D), nor when ash was excluded from analysis (F = 1.462; d.f. = 2, 21; $P = 0.095$) (Fig 1.11E).

Co-inertia analysis demonstrated similarities between overstory and recruit communities when ash species were included ($RV = 0.53$; $P = 0.001$) (Fig. 1.12A), but also when ash species were excluded ($RV = 0.55$; $P = 0.001$) (Fig. 1.12B). When ash was included, balsam fir, black ash and green ash contributed substantially to the structure of the CoIA plot, indicating these overstory and recruit species were generally correlated (Fig S1.2). When ash was excluded, balsam fir, red maple, and white cedar influenced the CoIA plot, and like species were also generally correlated with one another. Sapling communities appeared to be less related to overstory communities than recruit communities when ash was included ($RV = 0.44$; $P = 0.002$) (Fig. 1.12 C), and more closely related to overstory communities when ash was excluded based on RV value ($RV = 0.5$; $P > 0.001$) (Fig 1.12D). Species influencing overstory-sapling CoIA were similar to the overstory-recruit CoIA regardless of whether ash was included or excluded (Fig. S1.2). For all CoIA, except the CoIA assessing Overstory-Sapling similarity when black ash was included, similarity between communities (Overstory-Recruit, Overstory-Sapling), did not differ by Invasion Strata (Table 1.7). Similarity of overstory trees to sapling species was significantly higher in Mid-Invasion stands, and Post-Invasion stands with Minimal Regeneration appeared to have the lowest and most variable similarity, albeit not significantly lower (Table 1.7).

Discussion

We recorded near complete mortality of overstory black ash in all Post-Invasion stands, and extensive black ash decline was underway in Mid-Invasion stands, consistent with previous reports (Klooster et al. 2014, 2018, Engelken et al. 2020a, Siegert et al. 2021). Overstory

mortality has not yet occurred in Pre-Invasion stands. We also observed EAB larvae and galleries on black ash recruits indicating these small trees are likely to succumb within the next few years. Lower densities of recruits, saplings, and seedlings in five Post-Invasion stands suggests unfavorable conditions for all regenerating tree species in some instances. Furthermore, larval galleries on live black ash recruits and the presence of dead black ash recruits demonstrate that EAB is still present at residual densities within Post-Invasion stands and has caused significant mortality of black ash recruits. Together, these results demonstrate that future changes in forest vegetation composition following EAB infestation are affected by cascading impacts of losing overstory black ash and by continued mortality of advanced regeneration.

Density and composition of regeneration in black ash forests in different states or regions varies considerably (Windmuller-Campione et al. 2021, Springer and Dech 2021, Palik et al. 2012, D'Amato et al. 2018), and we similarly noted variability in recruits and saplings in our stands. In some Post-Invasion stands we observed significantly lower densities of regeneration (recruits, saplings, and seedlings). Combined with significantly lower basal area of live non-ash trees compared to other Post-Invasion stands, there is the potential that lower regeneration could be linked to the more pronounced loss of black ash. It is, however, difficult to discern whether the loss of overstory black ash from these stands created unfavorable conditions for regeneration, or if regeneration conditions were poor prior to EAB infestation. Windmuller-Campione et al. (2021) observed no significant relationship between residual basal area of trees and regeneration density post-harvest in black ash stands in Minnesota. Similar results were reported from surveys in stands dominated by young white ash regeneration, where Pre-EAB ash basal area was not correlated with recruit or sapling densities (Wilson et al. 2025). We expect that regeneration conditions were poor in our Post-Invasion stands with Minimal Regeneration prior to EAB

infestation due to the lack of advanced tree regeneration observed, signaling low rates of seedling establishment and growth prior to EAB. These poor growing conditions are likely compounded by changes associated with the loss of overstory black ash, including increased sun exposure through canopy gap formation, hydrological changes (Krezmein et al. 2024; Slesak et al. 2014), and reduced black ash seed production (Klooster et al 2014).

Despite the low densities of regeneration in five Post-Invasion stands, overall, we did not observe differences in regeneration density amongst Post-, Pre-, and Mid-Invasion stands. Black ash was a dominant regeneration species in these Post-Invasion stands and in Pre- and Mid-Invasion sites, along with other species that were abundant in the regeneration layer. These results provide evidence supporting the intuitive hypothesis described by Bowen and Stevens (2014), that conditions in hardwood swamps with a lower component of ash prior to EAB will experience less pronounced changes with respect to forest composition as non-ash species are already present in the understory and overstory, and therefore capable of replacing ash following mortality. Much of the work to monitor regeneration dynamics of black ash was conducted in northern Minnesota, where extensive stands of black ash, which often comprises over 80% of overstory trees, occur. These stands tend to have few non-ash tree species regenerating and regeneration is primarily dominated by black ash and shrubs (Palik et al. 2012; D'Amato et al. 2018). Most black ash stands in lower Michigan, and portions of the eastern Upper Peninsula contain a lower component of overstory black ash compared to the large, forested wetland stands in Minnesota, which may contribute to the common presence of non-ash regeneration in these stands.

Presence of non-ash overstory trees and regeneration is especially important given the interaction between residual populations of EAB and regenerating black ash in Post-Invasion

conditions. Along with relatively high densities of black ash recruits, saplings, and seedlings in most of our Post-Invasion stands, we also observed high proportions of both dead black ash recruits and live recruits exhibiting signs of EAB infestation. EAB can colonize and kill trees with diameters as small as 2 cm (Cappeart et al. 2005), thus EAB infesting and killing black ash recruits is unsurprising. We found similar proportions of live black ash recruits exhibiting symptoms of EAB colonization in Mid- and Post-Invasion stands, but fewer dead black ash recruits in Mid-Invasion stands, signaling that EAB likely infests black ash recruits during mid to late stages of infestation. Live black ash recruits present in Post-Invasion stands likely represent saplings or smaller recruits that were not colonized by EAB and have released following the formation of canopy gaps. Interactions between EAB and the orphaned cohort of ash species are well discussed throughout the literature focusing on ash regeneration in Post-EAB forests (Wilson et al. 2025, Hoover et al. 2023, Klooster et al. 2014, Siegert et al. 2021) and demonstrate importance of EAB's persistence on the landscape.

Gallery densities and the presence of live EAB larvae feeding on black ash recruits within our study further depict interactions between black ash recruits and EAB during Post- and Mid-Invasion conditions. In Post-Invasion stands, total EAB gallery density was generally lower than stands representing Mid-Invasion conditions, a result that can be explained by reduced live ash phloem area in Post-Invasion stands. Siegert et al. (2021) observed a 29-fold reduction in live phloem area between Mid- and Post-Invasion conditions in study sites containing black and green ash, corresponding with a proportional reduction in EAB density. It is therefore unsurprising that EAB gallery density were highest in Mid-Invasion conditions where EAB population densities are presumably highest, and ample phloem still exists for larval development. Lower EAB gallery densities found on black ash recruits in Post-Invasion stands

and a slightly lower proportion of likely infested recruits in these stands reflects low residual populations of EAB following black ash overstory mortality as described by Klooster et al. (2014).

Pressure from EAB, and the presumable mortality of black ash regeneration as they release make it unlikely that regenerating trees will reach a size class where they can produce seed (Gucker 2005a). Even if black ash can release and produce seed, the low number of seeds produced by small trees and the limitations of seed viability and seedling establishment make it unlikely that black ash will remain present within the seed bank (Klooster 2014).

In Post-Invasion stands an apparent lack of seedlings supports our hypothesis that seedling establishment can be lower in Post-Invasion sites, however the exact mechanisms that lead to this are unclear. In Post-Invasion stands that lacked black ash seedlings, the absence of seed produced by overstory black ash is likely the largest contributor to reduced total seedling densities, as black ash seedlings were the dominant seedling species across Invasion Strata (Klooster et al. 2014). However, water inundation (Tardif and Bergeron 1999) and interspecific competition with herbaceous plants and shrub species are also likely to depress black ash seedling populations (Looney et al. 2017).

Although we lack direct hydrology data from our stands, the potential for hydrology changes and increasing water tables following overstory ash mortality is well known, in both upland and riparian forest systems, and in simulated black ash harvests. Robertson et al. (2018) found a significantly lower soil moisture in canopy gaps where white ash had been killed by EAB compared to undisturbed forested areas, and significantly higher daily evapotranspiration rates in forests than in canopy gaps. Krezmein et al. (2024) observed increased water table depth in riparian canopy gaps that formerly contained green and black ash. Similarly, in Minnesota

black ash forests, water table levels following the girdling and clearcutting of black ash increased and remained high (Slesak et al. 2014). In Post-Invasion sites with minimal regeneration, lower average non-ash basal area and generally high pre-EAB black ash relative basal area could foreseeably lead to more pronounced changes in hydrology, compared to what would be seen when substantial basal area of non-ash species remain after EAB.

Herbaceous plant species present in black ash stands do not appear to differ greatly across Invasion Strata, and the percent cover of graminoids and bare ground were consistent even when overstory black ash were dead. Because black ash stands often contain many canopy gaps and have diverse and well-established herbaceous plant communities in their understories (Weber et al. 2007), we are not surprised by this result. Looney et al. (2017) observed increased abundance of graminoids in black ash stands that were clearcut to resemble EAB-related mortality, however the composition of herbaceous plants in girdled tree treatments and control treatment remained the same. Overstory tree conditions in Post- and Mid-Invasion study sites are more resemblant of girdle treatments described by Looney et al. (2017), thus our results are consistent with their work. Of note, is the presence of *Typha* species (cattails) in multiple Post-Invasion stands and one Mid-Invasion stand that all had high relative dominance of ash species in the overstory prior to EAB infestation. Presence of cattails suggests an ecological regime shift and supports the hypothesis that in some cases, the loss of overstory black ash due to EAB converts forested wetlands to ecosystems that resemble wet meadows (Windmuller-Campione et al. 2021, Looney et al. 2017, Krezmien et al. 2024).

The most important community differences observed across our stands was the difference in overstory tree communities, driven by the lack of overstory black ash in Post-Invasion Stands. There were no differences in regeneration communities when ash was included or excluded in

analysis, suggesting no large shift in community composition has occurred yet, despite mortality of black ash recruits in Post-Invasion stands. We expect, that as mortality of black ash recruits continues, and saplings grow and are eventually killed by EAB, we will see a shift in Post-Invasion tree communities similar to what we observed in overstory tree species. When other tree species are present in the overstory and regeneration layers, we expect that the loss of black ash will result in a shift in species dominance, likely favoring red maple, balsam fir, and white cedar. These tree species were found throughout our study area as both overstory and regenerating trees. Furthermore, the results of our Co-Inertia analysis support the hypothesis that regenerating tree communities resemble overstory tree species, suggesting that overstory non-ash tree species will contribute to regeneration in Post-Invasion forests.

As EAB continues to spread, the opportunity to better understand and preserve black ash forests with respect to regeneration dynamics and species composition is waning. High levels of overstory and recruit mortality in Post-Invasion forests suggest that the persistence of black ash on the landscape will be limited, as recruits, saplings, and seedlings will likely be killed by EAB before they can produce seeds. Densities of all recruit species appear to be low in some Post-Invasion stands, particularly those that had high relative pre-EAB black ash basal area and lower residual basal area of non-ash. Given the cultural importance and ecological significance of this unique species, black ash conservation and preservation is a priority for forest managers and landowners, we encourage researchers to establish long term studies within black ash stands in areas where EAB has not yet arrived. These studies should look to not only assess changes in forest vegetation overtime but also assess hydrological changes to more fully understand the legacy effects of EAB on black ash forest communities.

Tables

Table 1.1 Mean (SE) relative importance values (RIVs) of the ten most important overstory tree species by Invasion Strata, with blank spaces indicating the absence of particular species within stands at each Stratum.

Species	Post-Invasion	Mid-Invasion	Pre-Invasion
Fraxinus nigra	**35.12 (20.63)**	**94.04 (21.12)**	**106.43 (14.23)**
Thuja occidentalis	58.23 (17.15)	66.3 (23.56)	25.32 (14.98)
Abies balsamea	41.57 (12.74)	41.49 (9.14)	17.4 (5.76)
Betula papyrifera	12.44 (4.09)	25.32 (11.37)	-
Acer rubrum	34.7 (11.92)	21.46 (6.91)	14.27 (5.92)
Fraxinus pennsylvanica	-	15.16 (10.83)	33.32 (13.49)
Betula alleghaniensis	-	13.68 (4.34)	11.36 (4.34)
Populus balsamifera	14.36 (9.72)	12.87 (6.94)	14.91 (14.91)
Ulmus americana	27.59 (13.22)	5.35 (3.78)	14.65 (5.65)
Populus grandidentata	-	2.43 (2.43)	-
Tilia americana	14.56 (8.57)	-	12.43 (4.54)
Picea mariana	14.02 (7.73)	-	-
Populus tremuloides	12.38 (12.38)	-	27.12 (14.37)

Table 1.2. Mean (± SE) shrub percent cover across Invasion Strata with significant differences denoted by stars (*; $P < 0.05$), densities (stems · ha^{-1}), and frequencies of the four most frequently occurring shrubs by genus or species in 24 stands grouped by Invasion Strata.

Status	Mean (SE) Total Shrub % Cover	Species	Frequency	Mean (SE) Stem Density
Post-Invasion	22.9% (4.30)	*Alnus spp.*	10	1240.24 (137.63)
		Prunus spp.	6	14.65 (7.61)
		Cornus sericea	3	2.73 (1.50)
		Ilex verticulata	3	262.87 (111.90)
Mid-Invasion	30.4% (6.70)*	*Alnus spp.*	5	1255.85 (129.70)
		Prunus spp.	3	16.4 (8.92)
		Rhamnus spp.	2	35.41 (21.71)
		Amelanchier spp.	1	3.93 (3.93)
Pre-Invasion	6.7% (5.63)	*Alnus spp.*	4	589.29 (103.05)
		Carpinus caroliniana	2	14.99 (7.75)
		Ilex verticulata	2	12.18 (7.69)
		Amelanchier spp.	1	0.94 (0.94)

Table 1.3. Mean (SE) seedling densities (seedlings · ha^{-1}) of the four most abundant seedling species by Invasion Strata. Significant differences are indicated by letters ($P < 0.05$), for comparisons of black ash seedling density and total seedling density among Invasion Strata.

Status	Species	Mean (SE) Seedling Density	Mean (SE) Total Seedling Density
Post-Invasion	***Fraxinus nigra***	**18796 (8880)^{A}**	21389 (9418)^{A}
	Acer rubrum	926 (830)	
	Populus balsamea	463 (463)	
	Ulmus americana	370 (209)	
Mid-Invasion	***Fraxinus nigra***	**30000 (24741)^{AB}**	40444 (28654)^{AB}
	Acer rubrum	4000 (3014)	
	Thuja occidentalis	3333 (2222)	
	Abies balsamea	2889 (1846)	
Pre-Invasion	***Fraxinus nigra***	**54603 (11014)^{B}**	60159 (11356)^{B}
	Ulmus americana	1746 (1411)	
	Acer rubrum	1270 (921)	
	Acer saccharum	794 (794)	

Table 1.4. Mean (SE) graminoid percent cover and bareground percent cover for auxiliary plots in stands across Invasion Strata, frequency expressed as number of stands where plants occurred, and mean (SE) percent cover of the four most frequently recorded plants by Invasion Strata.

Status	Mean (SE) Graminoid % Cover	Mean (SE) Bareground % Cover	Species	Frequency	Mean (SE)% Cover
Post-Invasion	38.1% (6.1)	30.5% (0.4)	*Asteraceae spp.*	10	5.03 (3.07)
			Equisetum spp.	7	0.78 (0.25)
			Impatiens spp.	7	3.9 (1.74)
			Galium spp.	6	0.75 (0.42)
Mid-Invasion	38.5% (9.3)	23.1% (5.5)	*Impatiens spp.*	4	7.38 (6)
			Asteraceae spp.	3	1.12 (0.5)
			Equisetum spp.	3	1.08 (0.58)
			Galium spp.	3	0.52 (0.24)
Pre-Invasion	24.1% (6.6)	41.9% (5.6)	*Impatiens spp.*	7	4.67 (1.87)
			Asteraceae spp.	6	1.21 (0.32)
			Onoclea sensibilis	6	1.89 (0.53)
			Equisetum spp.	5	2.83 (1.5)

Table 1.5. Likelihood ratio tests comparing the null models and three other negative binomial models predicting total seedling density by mean graminoid cover, mean graminoid cover and Invasion Strata as a factor, and with an interaction between mean graminoid cover and Invasion Strata.

Model	Log L	D.F.	Chisq	P
Null Model	-86.15	-	-	-
Seedling Density ~ Mean Graminoid Cover	**-84.16**	**1**	**3.98**	**0.046**
Seedling Density ~ Mean Graminoid Cover + Invasion Status	-83.9	3	0.0515	0.773
Seedling Density ~ Mean Graminoid Cover · Invasion Status	-82.25	3	2.4	0.135

Table 1.6. ANOVA table with estimated means (SE) testing for a difference in the CoIA distances between Overstory/Recruit communities and Overstory/Sapling communities. Distances were tabulated by using the coordinates of each community within the canonical CoIA plot.

Model	Overall Model			Model Estimates	
	D.F.	*F*	*P*	Status	Estimate (SE)
Co-Inertia Distances Overstory/Recruits (Including Black Ash)	2, 21	0.09	0.9	Post-Invasion	0.65 (0.12)
				Mid-Invasion	0.56 (0.16)
				Pre-Invasion	0.59 (0.15)
Co-Inertia Distances Overstory/Recruits (Excluding Black Ash)	2, 21	0.09	0.9	Post-Invasion	0.71 (0.17)
				Mid-Invasion	0.73 (0.25)
				Pre-Invasion	0.84 (0.24)
Co-Inertia Distances Overstory/Saplings (Including Black Ash)	2, 21	10.03	>0.001	Post-Invasion	1.63 (0.25)[b]
				Mid-Invasion	0.41 (0.1)[a]
				Pre-Invasion	1.43 (0.3)[b]
Co-Inertia Distances Overstory/Saplings (Excluding Black Ash)	2, 21	1.45	0.2582	Post-Invasion	1.21 (0.2)
				Mid-Invasion	0.74 (0.19)
				Pre-Invasion	1.21 (0.26)

Figures

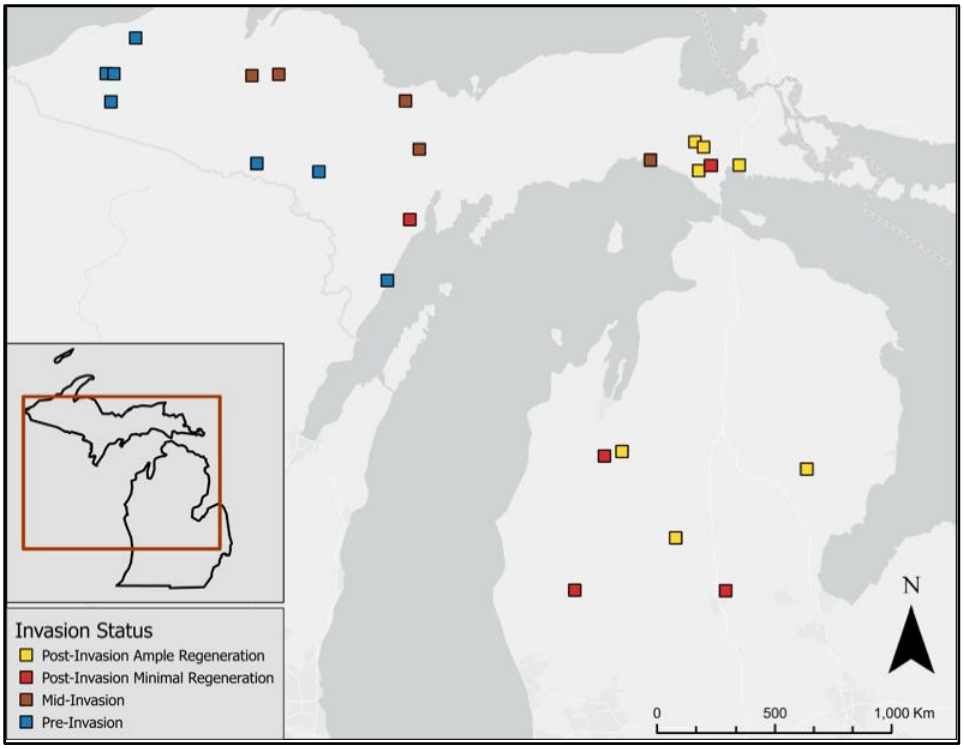

Figure 1.1. Map of 24 black ash stands assessed in Michigan representing three broad Invasion Strata (Post-, Mid-, and Pre-Invasion), and the location of Post-Invasion stands with ample and minimal regeneration.

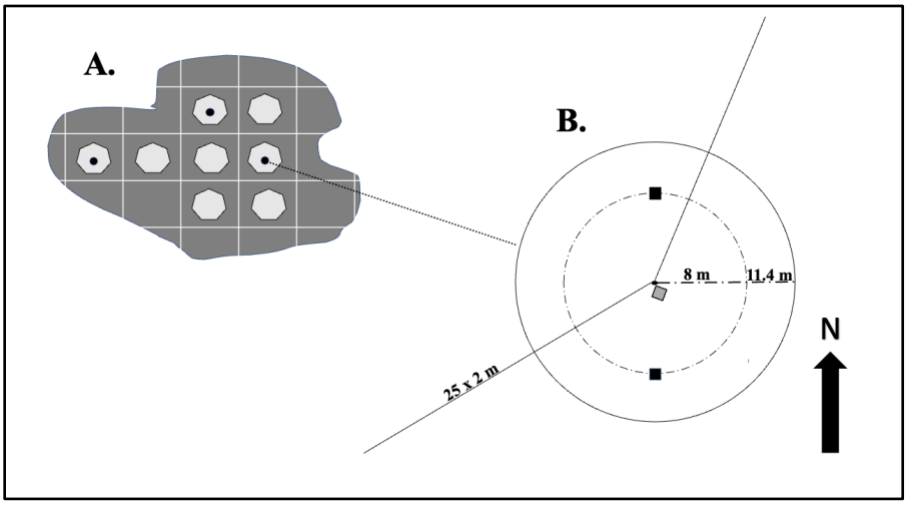

Figure 1.2. (A) Representation of grid cells overlaying a black ash stand where gray hexagons represent suitable grid cells and hexagons with black points represent three randomly selected cells where plots were centered. (B) Layout of nested fixed radius plots including a 11.4 m macroplot (solid outer circle), 8 m sublot (dashed inner circle), 1x1 m herbaceous plot oriented diagonally from the center at a random compass heading (gray square), two additional herbaceous cover plots (black squares), and two 25 x 2 m coarse woody debris transects (black solid lines).

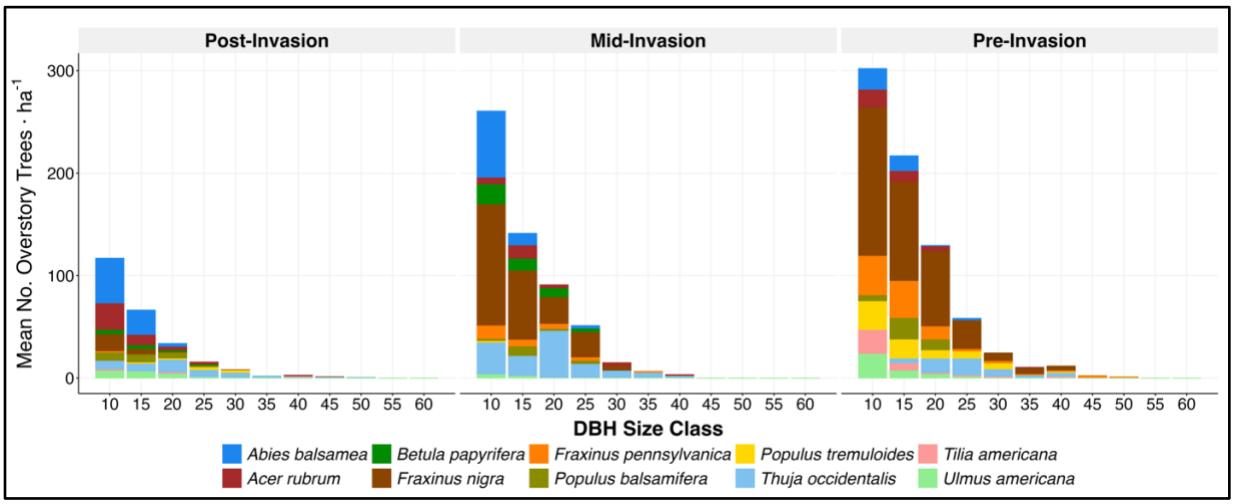

Figure 1.3. Size class distribution and density of the seven overstory species with the highest relative importance values across 24 stands. See Table S1.2, Appendix A for mean (± SE) of density by size class for all overstory species.

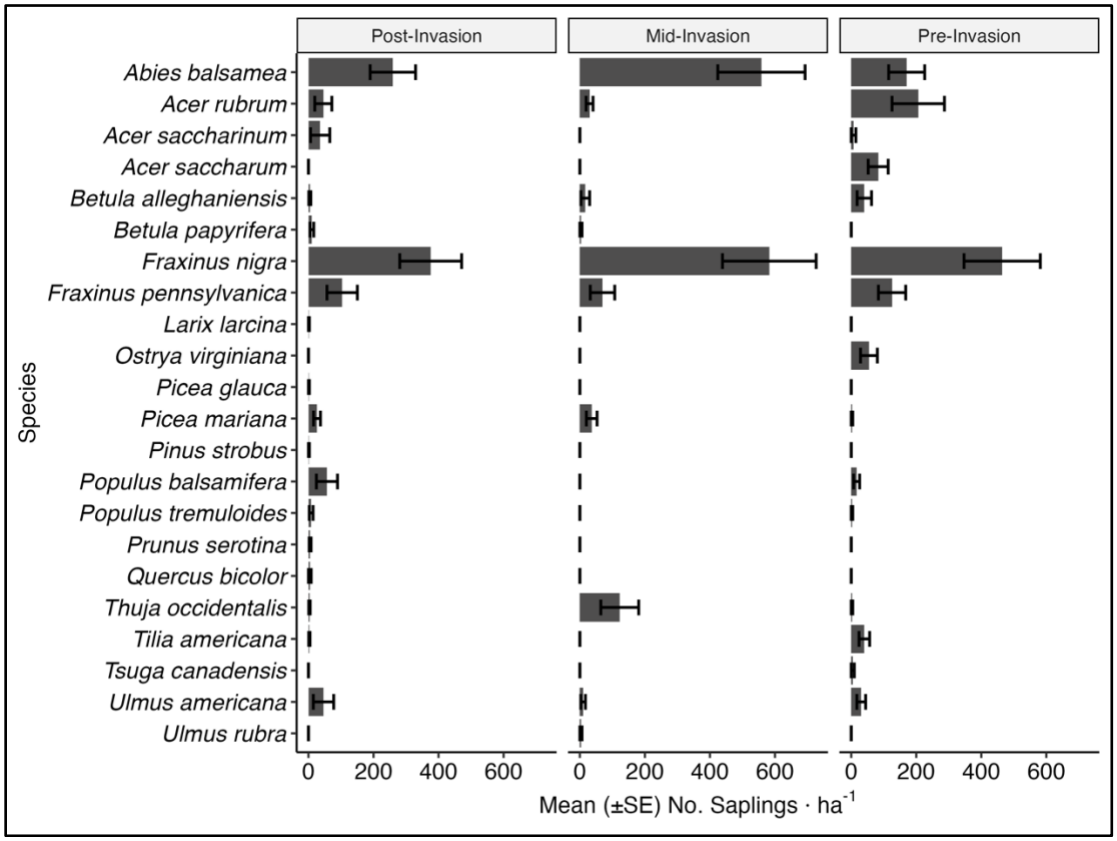

Figure 1.4. (A) Observed mean (±SE) density of recruits by species for each Invasion Strata recorded in Post-Invasion Ample Regeneration, Post-Invasion Minimal Regeneration, Mid-Invasion, and Pre-Invasion stands (24 stands total).

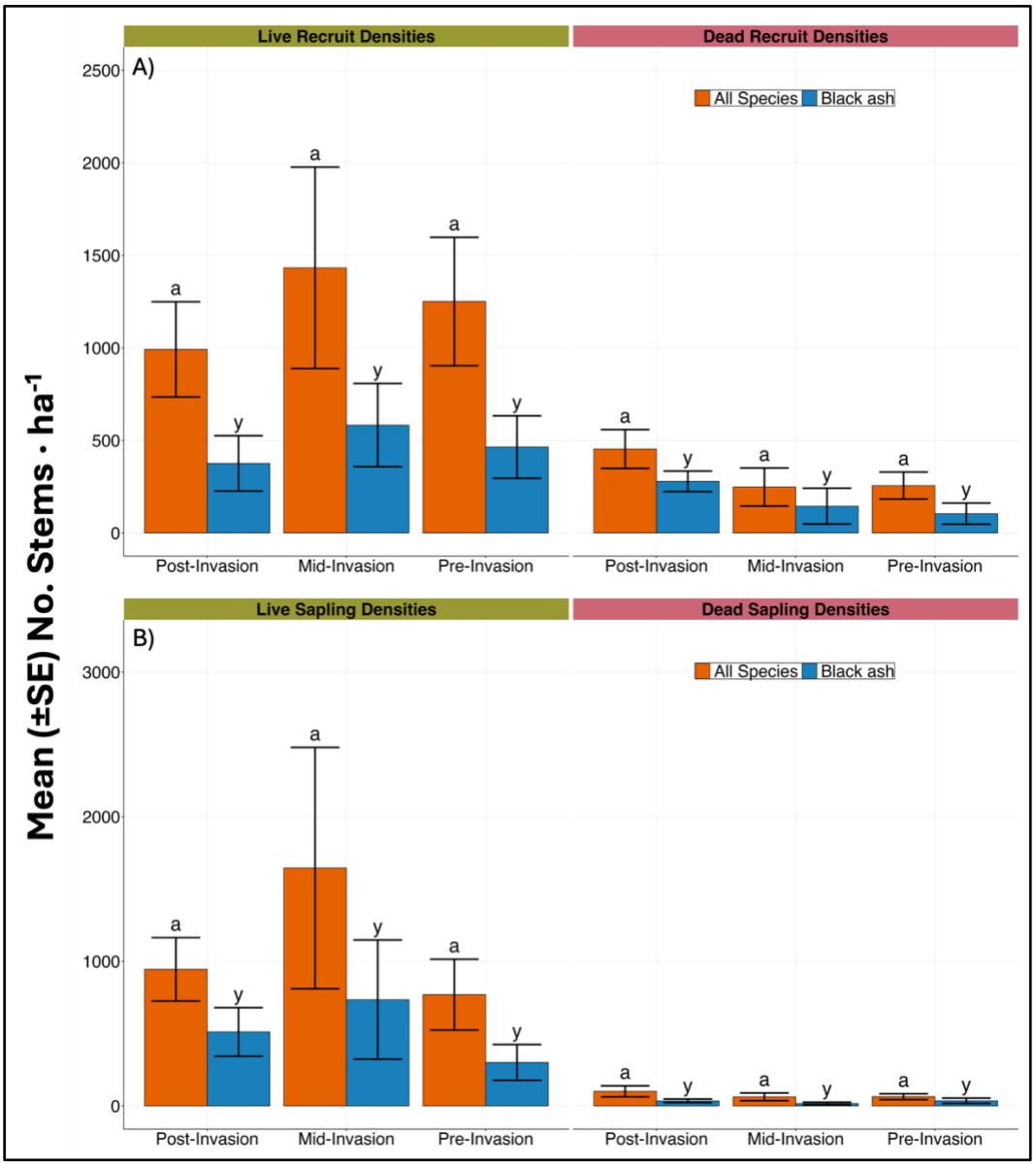

Figure 1.5. (A) Observed mean (± SE) density (stems · ha^{-1}) of live (left) and dead (right) recruits of black ash and all other species averaged by three EAB Invasion Strata (24 stands total). (B) The same plots are presented, but for sapling density data. Letters represent significant differences across Invasion Strata within species groups (all species and black ash), separately for live and dead stems.

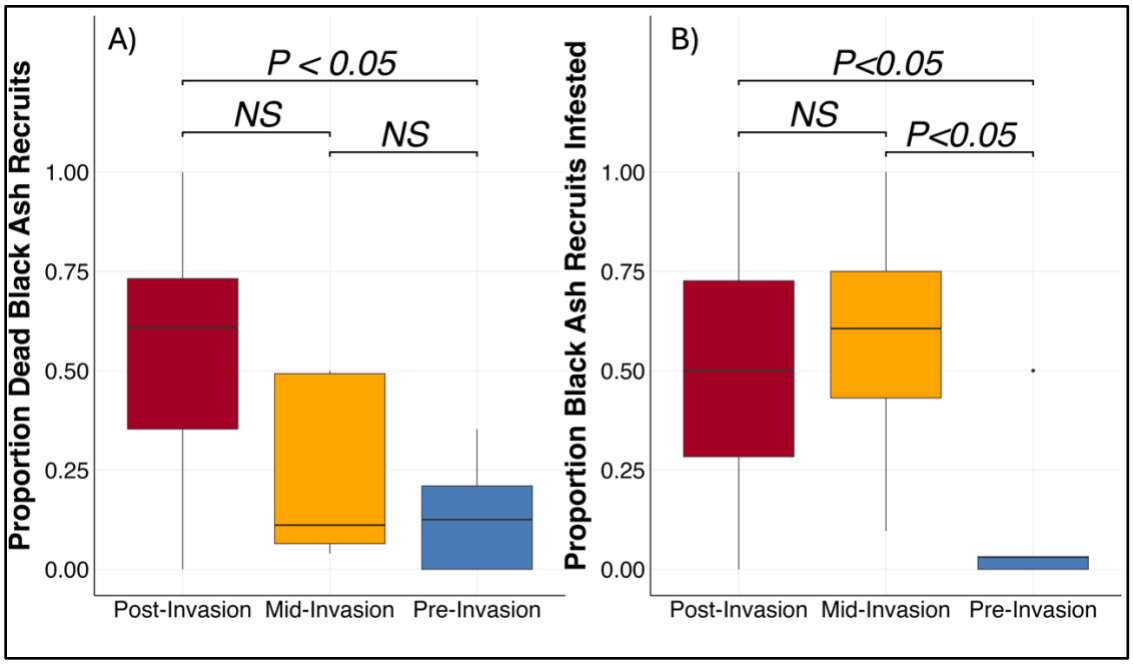

Figure 1.6. Box and whisker plot depicting mean proportions of dead black ash recruits (A) and live black ash recruits (B) infested by EAB. Center lines represent median values, boxes depict first and third quartiles, whiskers representing 1.5*inter quartile range (IQR), and points depict outliers.

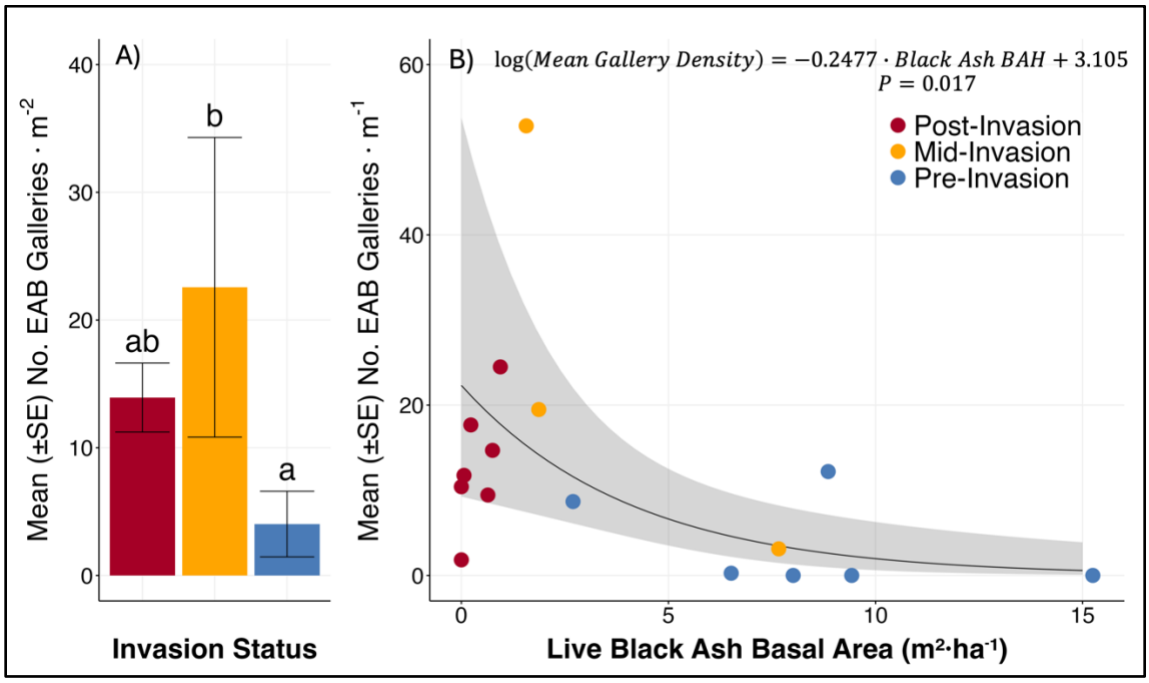

Figure 1.7. (A) Mean (±SE) density of black ash recruits across three EAB Invasion Strata with letters representing significant differences from post-hoc analysis. (B) Negative binomial relationship between density of EAB galleries and basal area of live black ash overstory trees, with 95% confidence interval (shading), and EAB Invasion Strata designated by color.

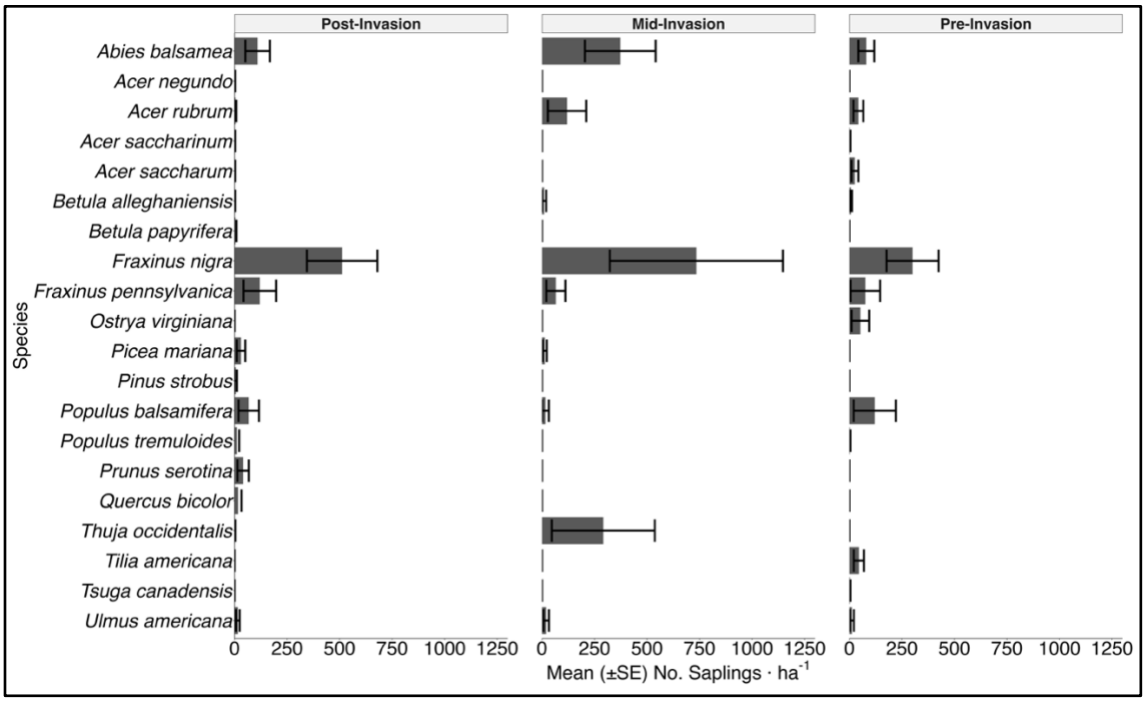

Figure 1.8. Mean (± SE) density of saplings by species tallied in stands representing Post-Invasion with Ample Regeneration, Post-Invasion with Minimal Regeneration, Mid-Invasion and Pre-Invasion (24 stands total).

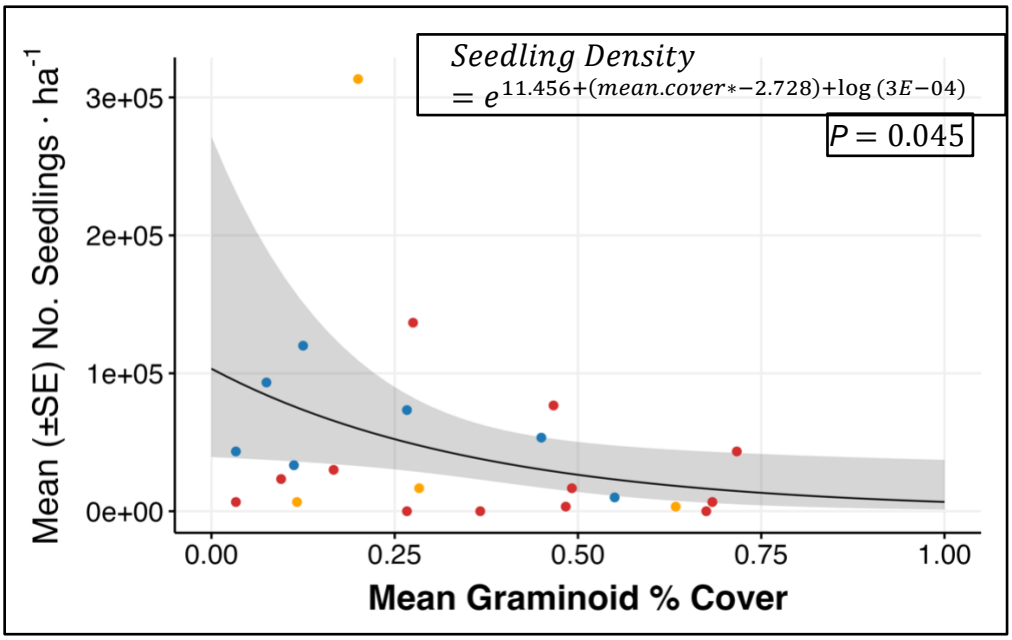

Figure 1.9. Negative binomial relationships from a GLM predicting seedling density (stems·ha^{-1}) by graminoid percent cover as a continuous variable for 24 black ash stands. Mean % cover was negatively related to seedling density. Shaded areas represent 95% confidence intervals, and points indicate mean stand values.

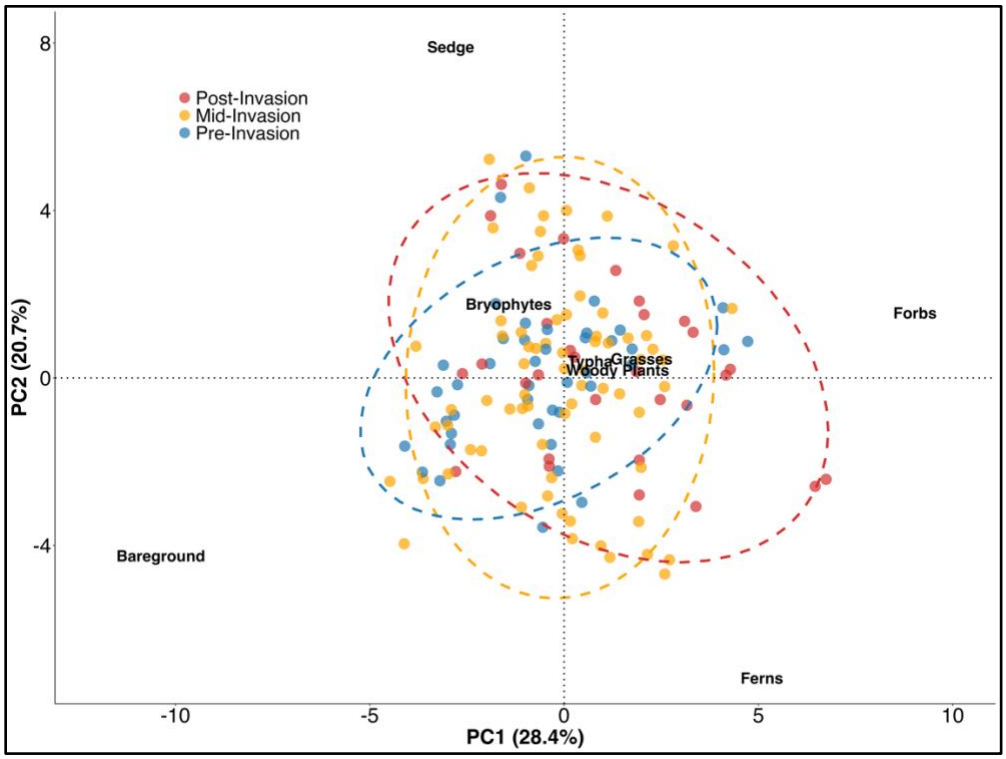

Figure 1.10. Results from principal components analysis (PCA) showing variation and similarities in percent cover of plant groups in 24 black ash stands grouped by four Invasion Strata. Variation explained by each axis is displayed, and total variation explained by the first two axes was 49.1%.

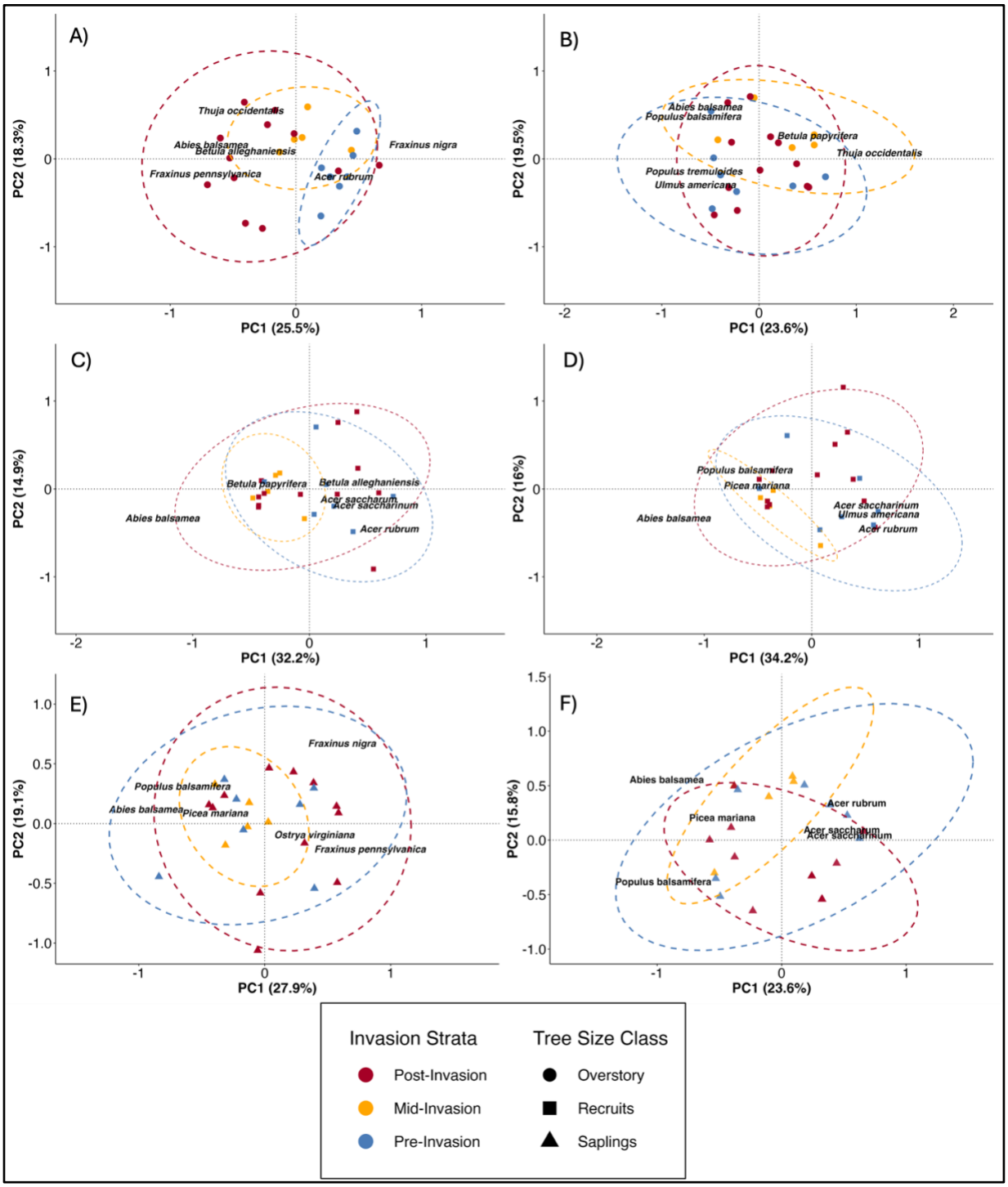

Figure 1.11. Results from PCA and RDA for overstory communities with (A) and without black ash (B), recruit communities with (C) and without black ash (D), and sapling communities with (E) and without black ash (F). Ellipses represent 95% confidence intervals.

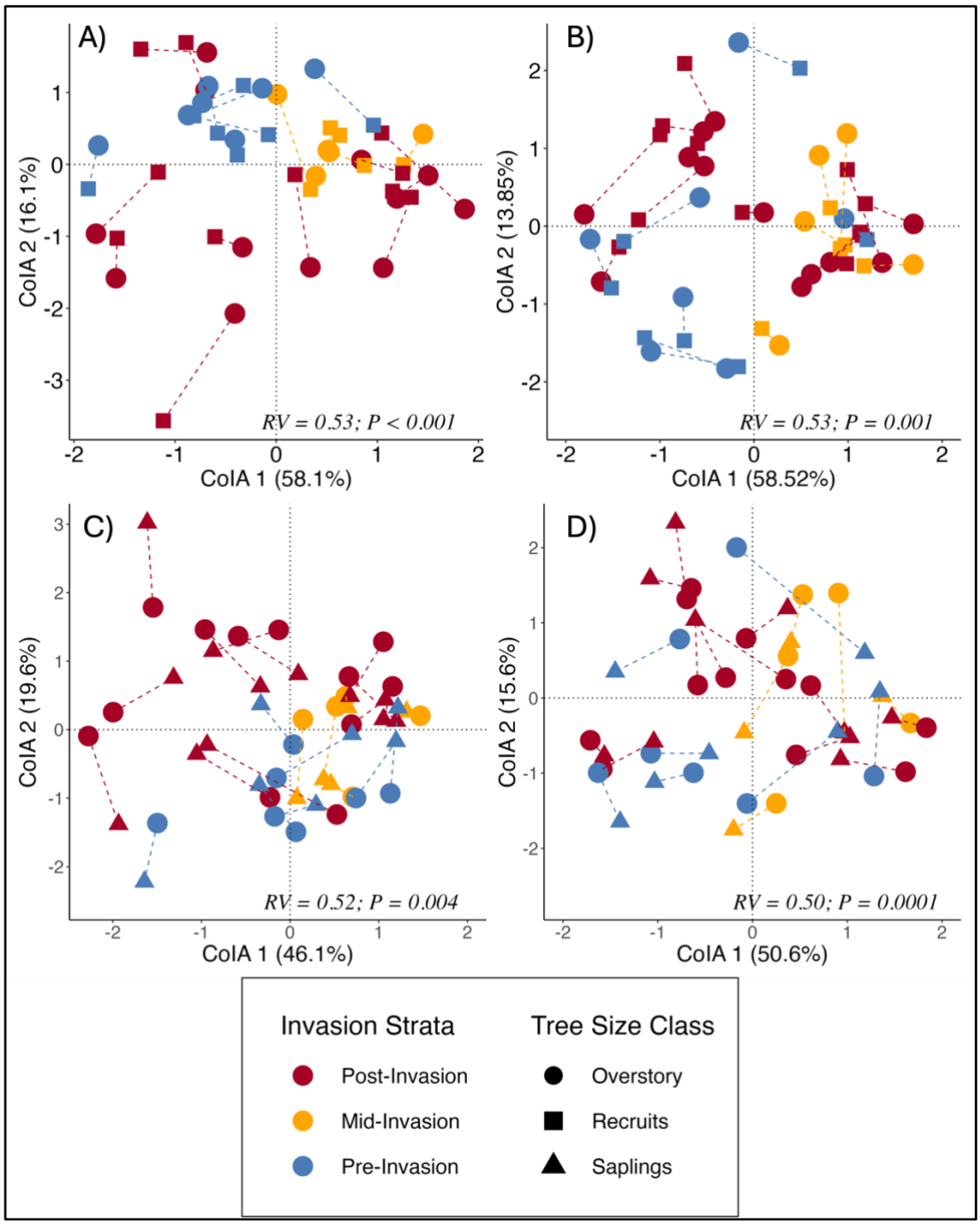

Figure 1.12. Co-Inertia Analysis (CoIA) plots representing similarities between overstory and recruit communities with ash species (A) and without ash species (B), and between overstory and sapling communities with ash (C) and without ash (D). Length of the lines represents how similar the overstory community is to the corresponding recruit or sapling community in each stand. RV values represent the overall similarity of overstory tree communities to understory communities in each case, and P-values represent the significance of this relationship.

CHAPTER TWO: DENDROECOLOGY OF BLACK ASH IN FORESTS SPANNING A RANGE OF EAB INVASION: IMPLICATIONS FOR FUTURE FOREST CONDITION AND MANAGMENT

Introduction

In eastern forests, stand-replacing disturbances, or disturbances that effectively eliminate a foundational species, are rare (Lorimer and Frelich 1994, Seymour and White 2002). A small proportion of invasive pests, however, have caused the functional loss of tree species from forest systems, substantially altering stand dynamics (Ellison et al. 2005). Historic examples include impacts of chestnut blight (*Cryphonectria parasitica* Murril M.E. Barr) and hemlock woolly adelgid (HWA) (*Adelges tsugae* Annand) in North American forests once dominated by American chestnut (*Castanea dentata*) or eastern hemlock (*Tsuga canadensis*), respectively (Ellison et al. 2005, Orwig et al. 2002). Impacts of these pests and others, have prompted efforts to reduce introductions of non-native forest insects and slow spread of established invaders (McCullough and Mercader 2011,Poland and Rassati 2019, Liebhold and Kean 2019, Lovett et al. 2016). Nevertheless, given current and projected levels of international and national trade, threats posed by invasive forest pests seem likely to continue (Aukema et al. 2010, Lovett et al. 2016). Understanding the impacts of specific invaders on structure and dynamics of vulnerable forests is therefore paramount for effectively managing affected stands.

Emerald ash borer (EAB) (*Agrilus planipennis,* Fairmaire), first detected in southeast Michigan in 2002 (Cappaert et al. 2005, Siegert et al. 2014), has caused widespread mortality of ash in forests and landscapes across much of eastern North America. Currently, EAB is established in at least 37 states and six Canadian provinces but continues to spread via natural dispersal of adult beetles and accidental human mediated transport infested material (EAB.info 2025, Herms and McCullough 2014, Siegert et al. 2014). Near complete mortality of native ash

species, particularly overstory trees, has been documented in forest stands in southern Michigan and northern Ohio invaded by EAB relatively early (Burr and McCullough 2014, Engelken et al. 2020, Flower et al. 2013, Klooster et al. 2014, Knight et al. 2013, Smith et al. 2015, Siegert et al. 2021). Similar levels of ash mortality have also been observed in more recently infested northeastern forests (Morris et al. 2023, Ward et al. 2021).

Nevertheless, intraspecific variability in EAB host preference and host vulnerability among ash species has been consistently observed in forested areas, common gardens, and landscapes. Blue ash (*Fraxinus quadrangulata*) trees are generally resistant to EAB unless they are stressed by drought or poor growing conditions, white ash (*Fraxinus americana*) is an intermediate EAB host, while green ash (*Fraxinus pennsylvanica*) and black ash *(Fraxinus nigra)* are highly preferred and vulnerable, with reported overstory mortality rates of 80% or more in forests and common garden studies (Anulewicz et al. 2007, Burr and McCullough 2014, Cippolini and Morton 2023, Engelken and McCullough 2020, Mathieu and McCullough 2025, Spei and Kashian 2017, Robinett and McCullough 2019, Tanis and McCullough 2012, 2015, Smith et al. 2015).

Black ash is considered a foundational wetland species throughout much of its range. In stands where it is dominant, the species largely controls hydrologic regime through evapotranspiration (Slesak et al. 2014), fostering habitat for a diverse range of herbaceous plants, birds, insects, and amphibians (COSEWIC 2018, Youngquist et al. 2017). EAB represents the largest threat to black ash and the ecosystem in which it thrives, with functional extirpation of black ash expected throughout its range by 2050 (Siegert et al. 2023). Concerns regarding the loss of black ash largely focus on changes in stand hydrology that are likely to cause the conversion of forests to sedge dominated wet meadows (Slesak et al. 2014, Windmuller-

Campione et al. 2021, Youngquist et al. 2017), reduced black ash seed production, resulting in decreased in seedling establishment (Klooster et al. 2014), along with the observed lack of non-ash tree species present in the regeneration layer of uninvaded stands to replace overstory trees (Palik et al. 2012). Seedling establishment and development of all species is likely to be further hampered by interspecific competition with shrubs and herbaceous plants (Engelken and McCullough 2020a, Looney et al. 2017, Windmuller-Campione et al. 2021). Concerns regarding the future of black ash are further heightened due to the species' cultural significance.

Black ash, a cultural keystone species, is used by Indigenous people throughout its native range for traditional basketry practices and is an integral aspect of the cultural identify for many tribal nations (Diamond and Emery 2011, Costanza et al. 2017, Siegert et al. 2023). Black ash is uniquely suited for the type of basketry practiced by Indigenous people, which involves peeling bark then pounding logs to separate the ring-porous growth rings. Strips of sapwood, called splints, are cut to desirable widths and lengths for weaving into utilitarian or artistic baskets (Costanza et al. 2017). Because the separation between growth rings forms the splints, annual ring width is a critical factor affecting the quality of a tree for basketry. Black ash trees with very wide annual rings yield splints too rigid for basket making, while very narrow rings yield weak splints likely to shatter (Costanza et al. 2017, Diamond and Emery 2011, Boudreault et al. 2024). Typically, ring widths between 2- and 3-mm yield optimal splints, and trees with these ring widths are deemed of basket quality (Costanza et al. 2017, Diamond and Emery 2011, Boudreault et al. 2024). As EAB spreads, Indigenous basket makers and community knowledge holders are concerned about the long-term survival of black ash, including the presence and persistence of basket quality trees on the landscape (Costanza et al. 2017).

Black ash stand dynamics in regions that have not been invaded by EAB, are characterized by small gap formation following single tree mortality and periodic flooding events (Tardif and Bergeron 1999, Fraver and White 2005, Springer and Dech 2021). When young black ash reach 30 to 40 years in age, they are capable of producing seed, with good seed crops occurring at one to eight-year intervals (Gucker 2005a; Wright and Rauscher 1990), however, black ash seed do not persist long in the seed bank, loosing viability after eight years (Gucker 2005a; Wright and Rasucher 1990). Black ash seed germination takes place after a two-to-three-year stratification period, and once germinated, seedlings grow quickly, capable of reaching 15 cm tall after one year when growing conditions are optimal (Gucker 2005a). Despite this potential for rapid growth, black ash have been observed to remain in understory for decades and, likely release following small gap formation (Springer and Dech, 2019, Tardif and Bergeron 1999). It is therefore likely that canopy gaps created by EAB caused overstory black ash mortality could facilitate the release of black ash regeneration.

To evaluate the impacts of overstory black ash mortality on stand dynamics in Michigan, we conducted dendroecological analysis of overstory black ash, black ash recruits, and balsam fir (*Abies balsamea*) recruits. Our primary objectives were to (1) quantify growth of overstory black ash and black ash recruits in Pre-Invasion stands in Michigan's Upper Peninsula, and (2) the presence of basket quality black ash in those stands. We also (3) compared radial growth of black ash recruits in stands representing Pre-, Mid-, and Post-Invasion conditions and evaluated potential release of black ash and balsam fir recruits in Post-Invasion stands. We hypothesized that (1) age class structure of overstory black ash and black ash recruits would represent uneven-aged forests in Pre- and Mid-Invasion stands, and that (2) basket quality ash would be rare across the landscape. We also predicted that (3) black ash and other prevalent tree species would release

in Post-Invasion stands, that residual tree basal area would limit the degree of release, and that live black ash recruits would be younger in Post-Invasion stands because of EAB-caused mortality of older black ash recruits.

Methods

***Stand selection*:** We selected 24 stands throughout Michigan's Lower and Upper Peninsulas where black ash occurred using forest cover maps in ArcGIS Pro (MI DNR, 2022) (ArcGIS Pro; ESRI, Redlands CA), inventory data provided by the Hiawatha National Forest, and previous observations. Stands represented a range of EAB invasion conditions, including Pre-Invasion areas with healthy ash trees and little or no evidence of EAB presence, Post-Invasion stands with extensive ash mortality, and Mid-Invasion stands where there was a mix of dead, healthy, and declining ash. We visited each stand to evaluate access and ensure stands were large enough for three non-overlapping, 400 m^2 circular plots.

We estimated and delineated the boundary of each stand using Google Earth Online (Google Inc, Mountain View, CA, 2023). To facilitate random plot location, we overlaid each stand map with a 50 x 50 m grid using the fishnet tool in ArcGIS Pro (ESRI, Redlands, CA, 2023). Grid cells where at least six black ash recruits or six overstory black ash, live or dead, were identified, of these, three grid cells were randomly selected. In the center of each grid cell, we established nested fixed radius plots comprised of a macroplot (11.4 m radius), a subplot (8 m radius) centered in the macroplot, and two 25 x 2 m linear transects arising from the center point oriented in two randomly selected compass headings.

Vegetation assessments: In each macroplot, we measured diameter at breast height (DBH) and visually estimated canopy condition, including percent transparency and dieback of live overstory trees (DBH > 10 cm) by species. For each overstory black ash tree, we recorded

the number of distinct holes left by woodpeckers preying on late-instar larvae and epicormic shoots up to 2 m high on the trunk, along with presence of basal sprouts. The proportion of dead overstory black ash stems was calculated and used to assign stands to one of three Invasion Strata. In our subplots, we measured DBH and estimated canopy condition for live and dead recruits (DBH 2.5 to 10 cm) by species. We again counted woodpecks, epicormic shoots, and basal sprouts up to 2 m high on black ash recruits. On linear transects we recorded the diameter of all coarse woody debris by species (Diameter > 4 cm) crossing transects. Diameters of fallen black ash along with the DBH of black ash snags were used to estimate Pre-EAB black ash basal area in Post- and Mid-Invasion stands. Basal area and relative basal area were calculated for live and dead overstory black ash and all non-ash trees. Densities of black ash and non-ash recruits were also calculated and averaged within stands.

***Increment core collection and processing*:** In each macroplot, we collected two increment cores at breast height, offset by 90°, from up to three randomly selected live overstory black ash trees. In stands where all overstory black ash were dead, we collected a cross section at breast height from a representative black ash snag in each plot or, when necessary, from a recently fallen ash log. In each subplot, we collected two increment cores from up to three randomly selected black ash recruits. In plots where black ash recruits were scarce, we randomly selected up to nine black ash recruits along a path between plots within the stand. Three Post-Invasion stands did not have live coreable black ash recruits. In addition to collecting cores or cross-sections from black ash, we cored up to two of the two most dominant non-black ash recruit species within each plot, resulting in up to 12 non-black ash recruits cored per stand. Balsam fir was the most frequently cored non-ash recruit across Invasion Strata and was therefore focused on for analysis.

Increment cores were dried, mounted on 5.1 mm increment core mounts (Rocky Mountain Tree Ring Research, Fort Collins, CO), and sanded using a progressive grit sequence of P80, P120, P220, and P320, following Speer et al. (2010). Cores were then scanned (Epson Perfection V850 Pro flatbed scanner; Epson America Inc., Long Beach, CA) at a resolution of 2400 DPI, and ring widths were measured to the nearest 0.001 mm using CooRecorder (v9.8.1, Cybis Elektronik & Data AB, Saltsjöbaden, Stockholm Co., Sweden). Both series, all measurements from one core, collected from individual trees were visually crossdated to one another and with then crossdated to those from other trees within the stand to check for measurement errors using CDendro (v9.8.1, Cybis Elektronik & Data AB, Saltsjöbaden, Stockholm Co., Sweden) and dplR in R (Bunn et al. 2010 v1.7.6, R Core Team 2024). Crossdating was statistically confirmed using both CDendro and dplR in R. Visual crossdating was especially useful for recruits given that the last year of growth was known for many live trees, and because statistical crossdating is generally most effective when more than 50 years of growth are present (Speer 2010).

Annual ring width was averaged for each tree using the two increment cores collected, and these averages were used in subsequent analysis. Mean ring width was calculated for each tree by averaging annual ring widths across the trees' lifespan. We standardized ring widths for each tree by dividing each annual ring width by mean ring width of all years, allowing us to understand how much radial growth each year differs from overall average radial growth. For all stands, standardized annual ring width values were used to calculate mean standard radial growth before and after 2015 (the mean year of overstory mortality in Post-Invasion stands) for black ash recruits. Subsequently, in Post-Invasion stands, we calculated mean standard radial growth of black ash recruits before and after the year of overstory mortality. We also calculated the percent

difference of mean standardized radial growth for black ash and balsam fir recruits before and after 2015 for all stands, and before and after the year when overstory mortality occurred in Post-Invasion stands.

Overstory mortality estimation: We used National Agriculture Imagery Program (NAIP) imagery (leaf-on images) obtained from USGS Earth Explorer (U.S. Geological Survey 2025) to evaluate conditions in each Post-Invasion stand from 2005 to 2020, at intervals of every 2-3 years to estimate the progression of overstory ash mortality and dieback. These data, along with cross dated overstory ash, were used to determine the most plausible year in which the majority of overstory black ash died. Cross sections collected from dead overstory trees in Post-Invasion stands were visually and statistically crossdated to one another using CooRecorder and CDendro. Following visual crossdating, chronologies from the Upper Peninsula were dated using chronologies we developed from live overstory black ash collected in Pre- and Mid-Invasion stands. Chronologies of dead black ash trees in Lower Peninsula stands were dated utilizing black ash chronologies developed by Nathan Siegert in the early 2000s from nearby stands (*NW Siegert Pers. Comm.).* Using CDendro, each series from our Post-Invasion stands was crossdated to the geographically nearest live overstory black ash master chronology visually and statistically.

***Statistical analysis*:** Following sampling, stands were assigned to three Invasion Strata based on mortality of overstory ash trees for analysis. Post-Invasion stands had greater than 80% overstory black ash mortality (n = 12 stands), Mid-Invasion had between 20 and 80% overstory black ash mortality (n = 5 stands), and Pre-Invasion stands had less than 20% mortality (n = 7 stands) (Fig. 2.1). Statistical analyses were conducted in R (R Core Team 2024; v4.4.2). Model assumptions were checked following model fitting using simulated residual plots from the

DHARMa package (Hartig 2022, v0.4.6), and all post-hoc testing was conducted using the emmeans package (Lenth 2024, v1.10.2). Likelihood ratio tests were used to test the fit of GLMs and mixed models. Fit model equations for all mixed models are displayed in Supplemental Table 2.1.

We used linear mixed effect models (LMMs) to predict how age of black ash overstory trees and recruits were related to average radial growth and DBH using the glmmTMB package in R (Brooks et al. 2017). In these models, estimated establishment age was a fixed effect, stand was a random effect, average radial growth or DBH was a response, and each tree was a sample, For both analyses, ring width and age were log transformed. We additionally assessed whether EAB caused a detectable decline in annual increment of overstory black ash trees during the five years preceding death in Post-Invasion stands by testing for differences in average ring width before and this five-year point with a one-way ANOVA using Pre/Post EAB as a fixed effect to predict log mean radial growth, with site as a random effect.

Differences in average radial growth across Invasion Strata were evaluated using a one-way ANOVA with Invasion Strata as a fixed effect predicting average annual radial growth. We tested for a difference in stand average standardized radial growth after 2015 for black ash recruits across Post-, Mid-, and Pre-Invasion stands using a one-way ANOVA, with Invasion Strata as a fixed effect. To understand if there were significant differences in radial growth after 2015 across Invasion Strata, we used one way ANOVA with Invasion Strata predicting percent difference in average annual ring width before and after 2015. Percent difference in average annual ring width before and after 2015 was then regressed against the average percent dead black ash basal area in each stand.

Following initial analysis using 2015 as the estimated mortality year, we focused more closely on Post-Invasion stands and stand level mortality of overstory black ash. A paired t-test was used to test for a significant difference in mean ring width before and after the estimated year of overstory mortality. We then calculated percent difference in ring width before and after overstory black ash mortality and used a stepwise modeling approach to understand variation in percent different at these sites with the glmulti package in R, allowing for only one term in our model due to low sample size (Calcagno 2020, v1.0.8). Variables tested in stepwise model selection included live recruit density, Pre-EAB black ash basal area, mean relative Pre-EAB black ash basal area, mean pre-EAB black ash density, mean relative Pre-EAB black ash density, mean total live overstory non-ash density, and mean total recruit density. Following stepwise model selection, all models were fit using square root transformed percent difference in radial growth as the response.

Finally, we assessed the radial growth of balsam fir recruits before and after 2015 using an LMM to predict average standard ring width. Predictors tested include pre- and post-2015 (two-level factor), Invasion Strata (three-level factor), and stand as a random effect. We then tested for differences in post- 2015 radial growth between black ash and balsam fir recruits, using an LMM to predict average standard radial growth with tree species (two-level factor), Invasion Strata (three-level factor) and stand as a random effect. All models were run using the glmmTMB package, and pairwise comparisons were obtained via the Tukey method.

Results

***Vegetation and black ash assessments*:** Overstory black ash mortality varied across stands but was highest in Post- and Mid-Invasion stands, averaging 89.2 ± 6.4% of trees in Post-Invasion and 52.4 ± 12.0% in Mid-Invasion stands compared with only 4.4 ± 1.3% in Pre-

Invasion stands. Total basal area was also lower in Post-Invasion stands, where live black ash represented a minimal portion of the live BA (Table 2.1). Prior to EAB invasion, black ash basal area varied among stands but was similar among the three Invasion strata. Densities of total recruits (all species) and black ash recruits did not differ across Invasion Strata, and black ash was a dominant recruit species in most stands (Table 2.1). When we surveyed Post-Invasion stands, however, 56 ± 7% of all black ash recruit stems were dead, compared to 24 ± 10% in Mid- and 12 ± 10% in Pre-Invasion stands. Additionally, the proportion of live black ash recruits with signs of EAB infestation was significantly higher in Post- (51.8 ± 10.0%) and Mid-Invasion stands (57.6 ± 6.9%), compared to Pre-Invasion stands (8.5 ± 7.0%) ($\chi^2 = 10.96$; d.f. = 2*; P* = 0.004).

***Overstory black ash mortality*:** We observed variable timing of overstory black ash mortality across Post-Invasion stands (Table 2.2). Dead black ash in Post-Invasion stands in the Lower Peninsula appeared to have died earlier than those from the Upper Peninsula, with mortality ranging between 2008 and 2014. In Upper Peninsula stands, overstory black ash mortality occurred between 2011 and 2018. In general, tree decline and mortality observed through aerial imagery aligned with the mortality date from cross sections, with one exception when the overstory trees we evaluated died seven years before substantial decline was visible on aerial imagery. County detection dates preceded overstory black ash mortality by one to 13 years; one stand had black ash trees that died the year before EAB was detected in the county.

***Black ash overstory radial growth and age*:** The chronology of live overstory black ash in Pre- and Mid-Invasion stands included 97 trees and spanned from 1740 to 2022 (283 years), with an average series length of 79.2 years (Fig. 2.2) (Table 2.3). Annual ring width in Pre-Invasion overstory black ash averaged 1.21 ± 0.07 mm. Fewer live overstory black ash were

available for coring in Mid-Invasion stands, but the chronology from those trees was similar to the Pre-Invasion chronology, ranging from 1847 to 2023 (176 years) with an average series length of 90 years, and average annual radial growth of 0.84 ± 0.05 mm (Table 2.3). Estimated live overstory black ash age across Pre- and Mid-Invasion stands was negatively correlated with DBH ($\chi^2 = 38.08$; d.f. = 1; $P < 0.001$) and positively correlated with average annual growth ($\chi^2 = 50.6$; d.f. = 1; $P < 0.001$) (Fig. 2.3A, B). Ages of overstory black ash varied within stands, with difference in age between youngest and oldest overstory black ash averaging 69.6 ± 16.1 years (Fig. 2.3C). Average annual ring width of overstory black ash was not correlated with average stand basal area (F = 0.075; d.f. = 1, 10; $P = 0.78$).

Radial growth of dead overstory black ash trees in Post-Invasion stands was similar to radial growth of live black ash in Pre-Invasion and Mid-Invasion stands (Fig. 2.4). In Lower Peninsula stands, the cross-section chronology spanned 1883 to 2015, with an average series length of 79 years, while the chronology from Upper Peninsula stands spanned 1858 to 2020, with an average series length of 96 years. Average annual radial growth for overstory black ash before mortality in Post- Invasion stands was 1.16 mm (± 0.147 mm). During the five years preceding death, average annual increment was 14% lower than average annual increment from the preceding 30 years, however they did not differ significantly ($\chi^2 = 1.28$; d.f. = 1; $P = 0.258$).

Increment cores were collected from six live overstory black ash in one Post-Invasion stand in the Lower Peninsula, with an average DBH of 11.5 ± 0.83 cm. The chronology developed from these trees was shorter than chronologies developed from Pre- and Mid-Invasion stands, ranging from 1996 to 2022 with an average series length of 21.83 years. Average annual ring width of these trees from 2000-2022 was 2.07 ± 0.23 mm, and ranged from 0.43 to 5.18

mm. Average annual ring width of overstory black ash during this time period in Pre- and Mid-Invasion stands was lower, averaging just 1.015 ± 0.106 mm

Basket quality trees: Annual ring width of overstory black ash during the past 25 years averaged 1.011 ± 0.104 mm and although growth varied across stands, results generally indicated a low presence of basket quality trees (Fig. 2.5). Of all the live overstory black ash cored (n = 97), 23 had an average annual radial growth in the last 25 years between 1.5 and 2.5 mm (21%). In four stands, we observed no basket quality trees based on average 25-year ring widths alone. On average, only 22 .4 ± 56.1 % of the overstory black ash across all stands had ring widths indicative of basket quality trees.

Black ash recruit radial growth and age: We cored a total of 141 black ash recruits across 21 black ash stands; three stands had no live coreable black ash recruits (Table 2.4). Similar to overstory black ash, DBH of black ash recruits was negatively related to recruit establishment year ($\chi^2 = 11.4$; d.f. = 2; $P < 0.001$) and positively related to recruit average radial growth ($\chi^2 = 200.9$; d.f. = 1; $P < 0.001$) (Fig. 2.6). Black ash recruit age was highly variable, ranging from 98 to 11 years old across all stands, and 10% were over 75 years old. Average annual ring width of black ash recruits across entire chronologies was generally small and did not differ significantly among Invasion Strata (F = 23.382; d.f. = 2, 18; $P = 0.057$), but were slightly higher in Post-Invasion (1.03 ± 0.144 mm) stands than Mid- (0.643 ± 0.093 mm) and Pre-Invasion stands (0.829 ± 0.058 mm).

Average annual ring width from 2015 (the average year of overstory mortality in Post-Invasion stands) to 2022 differed across Invasion Strata (F = 35.2; d.f. = 2,18; $P = 0.0015$), and was greatest in Post-Invasion stands (Fig. 2.7A). Before 2015, trends in standardized ring width appear similar across Invasion Strata, but clearly increased during the 2010s within Post-

Invasion stands (Fig. 2.8). Average standardized ring width of black ash recruits from 2015 to 2022 differed significantly by Invasion strata ($F = 7.93$; d.f. = 2, 18; $P = 0.003$) and was 1.5 times greater in Post-Invasion stands than in Pre-Invasion stands. There were no significant differences in standardized ring widths between Mid-Invasion stands and all other strata from 2015 to 2022 (Fig. 2.7B). Percent difference between average historic black ash annual ring width and average ring width after 2015 varied among Invasion Strata and was highest in Post-Invasion stands followed by Mid-, and Pre-Invasion stands (Fig. 2.9A). Furthermore, percent differences in black ash recruit annual ring width before and after 2015 was strongly correlated with percent dead black ash basal area ($F = 15.6$; d.f. = 1, 19; $P < 0.001$; Adj $R^2 = 0.42$), increasing by 9.6 ± 0.24 % with each 10% increase in black ash basal area lost (Fig. 2.9B).

We observed clear signs of black ash recruit release when Post-Invasion stand ring widths were observed separately using the year of overstory mortality to facilitate analysis. In Post-Invasion stands, average annual ring width of recruits after overstory black ash mortality died was greater than before mortality ($t = 3.1$; d.f. = 8; $P = 0.01$) (Fig. 2.10A), increasing by 95 ± 34 % on average. Variability in the release of black ash following overstory mortality was apparent, with recruits in some sites releasing more than others. Regression analysis yielded no significant relationships between radial growth percent difference before and after mortality. Upon inspecting these models, we noticed one outlier stand. This stand had few regenerating trees of all species and only one live coreable black ash recruit that had sever canopy dieback and noticeable EAB galleries, which did not experience release following overstory mortality. When this stand was dropped from analysis, we observed significant relationships between radial growth percent difference and mean live overstory tree density, relative Pre-EAB black ash density, and relative Pre-EAB black ash basal area (Table 2.5). Total live overstory tree basal

area was the best predictor of percent difference in recruit radial growth before and after overstory mortality (Fig. 2.10B), and average recruit density was not related to percent difference in mean ring widths (F = 2.286; d.f = 1, 6; $P > 0.1$).

In addition to differences in radial growth, we observed differences in the age class structure of black ash recruits across Invasion Strata (F = 4.807; d.f. = 2, 18; $P = 0.021$). The age of black ash recruits was greatest in Mid-Invasions stands (55.9 years, 95% CI [43.4,70.4]), which were on average 23.5 (± 7.7) years older than recruits in Post-Invasion stands (33.4 years, 95% CI [24.4,42.4]) (T ratio = -3.051; d.f. = 18; $P = 0.018$), and 13.1 (±7.86) years older than Pre-Invasion recruits (33.4 years, 95% CI [24.4,42.4]) (T ratio= 1.668; d.f. = 18; $P = 0.244$). Recruits in Pre-Invasion stands were on average 10.4 (± 6.2) years older than recruits in Post-Invasion stands but the difference was not significant (T ratio = -1.671; d.f. = 18; $P = 0.243$) (Fig. 2.11). Most black ash recruits in Post-Invasion stands established after 1990, and this trend was less pronounced in Pre- and Mid-Invasion stands, however proportion of black ash recruits establishing after 1990 did not differ across Invasion Strata ($\chi^2 = 4.4929$; d.f. = 2; $P = 0.1058$) (Fig. 2.10). On average, 56% ± 15% of recruits in Post-Invasion stands established after 1990, compared to 17 ± 13% in Mid- and 20 ± 9.7% in Pre-Invasion stands. Post-Invasion stands where > 50% of black ash recruits established before 1990 were only present in the Upper Peninsula, whereas recruits in the Lower Peninsula stands mostly established after 1990 (Table 2.4). On average, black ash recruits in the Upper Peninsula 1.6 times older than those in the Lower Peninsula (F = 5.9; d.f. = 1,7; $P = 0.046$), and we observed a marginally insignificant negative relationship average age of black ash recruits in Post-Invasion stands and the timing of overstory mortality (F= 5.35; d.f. = 1, 7; $P = 0.053$).

***Balsam fir radial growth*:** Balsam fir was the most commonly occurring non-ash recruit species, and we cored a total of 53 across 12 stands. Average annual ring width of balsam fir was similar across Invasion Strata although mean values were slightly higher in Pre- (1.09 ± 0.15 mm) and Post-Invasion (1.06 ± 0.34 mm) stands than in Mid-Invasion stands (0.72 ± 0.21 mm). Average ring width from 2015 to 2022 did not differ across Invasion Strata ($F = 0.622$; d.f. = 2, 9; $P = 0.552$) but was lower from 2015 to 2022 than historical growth rates regardless of Invasion Strata ($\chi^2 = 12.763$; d.f. = 3; $P = 0.005$) (Fig 2.12). Furthermore, average annual ring width differed between black ash and balsam fir recruits ($\chi^2 = 26.26$; d.f. = 1; $P < 0.001$) and the interaction between species and Invasion Status was significant ($\chi^2 = 13.66$; d.f. = 2; $P = 0.001$). Annual ring width of balsam fir recruits was lower than that of black ash recruits in Post- (T ratio = -5.088; d.f. = 16; $P = 0.001$), while growth of balsam fir and black ash were similar in Mid-(T ratio = -3.089; d.f. = 16; $P = 0.063$), Pre-Invasion stands Mid-Invasion stands where both species co-occurred (T ratio = -3.089; d.f. = 16; $P = 0.063$) (Fig. 2.13).

Discussion

Our work contributes to the literature on black ash stand dynamics under Pre-Invasion conditions and is the first to quantify changes in stand dynamics following the decline and loss of overstory black ash in Post- and Mid-Invasion stands. We observed old overstory black ash trees in Pre- and Mid-Invasion stands in Michigan's Upper Peninsula, and an age class distribution of live overstory trees that clearly represented uneven aged forests with multiple cohorts in the overstory. We also observed old black ash recruits across our stands, and the release of black ash recruits in Post-Invasion stands, suggesting that regenerating black ash respond to the formation of canopy gaps following EAB caused black ash mortality. Together, these results provide

insight into the growth conditions that characterize black ash stands before EAB, and how stand dynamics change following EAB invasion.

The oldest live black ash tree observed in our study was 283 years old, dating back to 1742, and there were multiple other overstory black ash over 100 years old. The presence of old black ash on the landscape is not in itself a phenomenon, as live black ash dating back to the 1600s have been observed in Minnesota and northern Quebec (Fraver et al. 2022, Tardiff and Bergeron 1999). The presence of trees that predate the late 1800s is still astonishing given the land use history of Michigan's Upper Peninsula, where extensive logging occurred between the mid-1850s and early-1990s (Schulte et al. 2007; Williams 1998; Karamanski 1989). The oldest tree in our study pre-dated widespread logging by over 100 years, meaning it had likely reached the overstory size class and should have been cut by loggers, as even small diameter hardwoods were harvested during the early 1900s (Whitney 1987). Combined with the presence of overstory black ash at multiple age class, and old recruits in this stand, it seems likely that this particular black ash stand was spared during the logging era of the Upper Great Lakes and represents old growth conditions. Stands in our study with trees that established during the late 1800s and early 1900s, are likely trees that were recruited either after logging events or natural overstory mortality that occurred during this time period.

Overstory black ash trees in Pre- and Mid-Invasion stands had narrow average ring widths, indicative of the species slow growth consistently observed across the literature. Comparable annual ring widths to those observed in our study for overstory black ash have been observed in Michigan and Minnesota, with ring widths in a Michigan black ash stand averaging 1.68 ± 0.08 mm (Seigert et al. 2021), and average ring widths in Minnesota black ash stands ranging from 0.68 to 1.085 mm (Bendict and Frelich 2008). In our study, annual ring width of

overstory black ash was positively associated with tree age, suggesting that black ash growth rate slows as they become older. It is important to note, however that some younger overstory trees in our study still had slow annual radial growth, and the oldest tree in our study did not have the lowest average annual ring width. Variation in black ash radial growth across our study area is likely linked to variable site conditions, and we would expect differences in total tree basal area and stand hydrology to impact radial growth. We observed no relationship between black ash annual ring width and stand basal area, although Indigenous basket makers consistently note that basket quality trees with larger rings widths are typically more open grown (Costanza et al. 2017). The lack of a relationship between stand basal area and black ash annual ring width suggests that other environmental factors may impact black ash radial growth more than competition. Frelich and Benedict (2008) also found no relationship between stand basal area and overstory black ash 5-year ring widths but observed significant differences in ring widths based on stand hydrology, with narrower ring widths observed in ephemerally wet stands compared to lowland and upland stands. Furthermore, historic structure and hydrology for our stands are unknown, and changing conditions throughout the lifetime of a tree would likely impact average ring widths.

In Pre- and Mid-Invasion stands, age class distribution of overstory black ash and recruits in our study are consistent with previous studies on black ash stand dynamics. Black ash overstory trees in our study clearly represent an uneven age distribution across the landscape, with few old trees and more young trees present across stands. Within stands we observed differences in tree age, likely indicating different cohorts of black ash present in the overstory. Black ash forests in Minnesota and Ontario followed similar age class distributions to the stands in our study, with different cohorts clearly represented in the overstory size class (Springer and

Dech, 2021, Fraver et al. 2022). Our work therefore supports the hypothesis that overstory trees remain on the landscape while younger cohorts remain in the understory until they are released.

Losing overstory black ash following EAB invasion ash will result in significant reductions in seed production, hampering the ability for black ash to remain on the landscape following EAB (Klooster et al. 2014). Furthermore, vegetative sprouting is unlikely to facilitate the replacement of overstory black ash as sprouts on stump black ash exhibit high mortality rates in Post-EAB and natural conditions (Siegert et al. 2021, Tardif and Bergeron 1999). The future of black ash, therefore, depends on the ability of established black ash regeneration to release once overstory trees are killed by EAB. Studies have demonstrated that in the wake of EAB, ash regeneration is typically abundant in stands across a variety of ecosystems (Engelken and McCullough 2020, Kashian 2016, Wilson et al. 2025). Black ash recruits and saplings were generally common across Invasion Strata, and were present in most Post-Invasion stands despite black ash recruit mortality and clear signs of EAB infestation on recruits.

We expected black ash recruits to release in Post-Invasion stands following overstory black ash mortality and expected annual ring widths of recruits Pre- and Mid-Invasion stands to remain relatively unchanged over the past 20 years. Black ash recruits released in all, but one Post-Invasion stands, and radial growth of black ash recruits in Pre-Invasion stands remained consistent over time. The strong negative relationship between the proportion of dead black ash basal area and percent difference in mean annual ring width before and after 2015 indicates that recruits in Mid-Invasion stands are beginning to release as overstory black ash succumb to EAB.

Slow radial growth of black ash recruits in our study and the ages of recruits supports the growing body of literature suggesting that black ash can be shade tolerant. Black ash is widely considered a moderately shade tolerant species when young (Wright and Rauscher 1990),

however discourse in the past two decades has challenged this. Springer and Dech (2021) and Tardif and Bergeron (1999), conducted extensive dendrochronological sampling of black ash in Ontario and Quebec, where they observed black ash (DBH 2.5-10 cm) approaching 100 years of age. Recruits in our study were comparable, as we observed 16 black ash recruits over 75 years in age, and one recruit that was 98 years old. Age class distribution of our recruits across our study area also suggests that there are multiple cohorts present in the 2-10 cm size class, a trend observed by both Springer and Dech (2021), and Tardif and Bergeron (1999). Furthermore, Tardif and Bergeron (1999) observed constant recruitment of trees that were seedling germinates across black ash chronologies in Quebec, suggesting that black ash can be recruited under natural condition even when they are old. Old black ash recruits in our study were present at all Invasion Strata, suggesting that, even in the wake of EAB, some old black ash recruits remain present in Post-Invasion conditions, and appear to be exhibiting signs of release.

Particularly old recruits in Post-Invasion stands were only represented the Upper Peninsula, where EAB mortality occurred later than in Lower Peninsula stands. In the Lower-Peninsula we noted younger black ash recruits averaging 25 ± 3.72 years old, whereas recruits in the Upper Peninsula Post-Invasion stands were older, averaging 40.6 ± 5.6 years old. We would expect the ages of recruits in Post-Invasion stands in the Upper and Lower Peninsula to be similar, and the mismatch in ages suggests the older cohort of black ash recruits is missing from our Lower Peninsula stands. Given the high mortality rates of black ash recruits across Post-Invasion stands, and high proportions of EAB infested recruits in Post- and Mid-Invasion stands, we expect that EAB killed older black ash recruits in the Lower Peninsula during initial invasion and in the years following overstory black ash mortality.

Although we are the first to explicitly measure the release of black ash regeneration in Post-Invasion conditions, similar work has been published on regenerating non-ash species in forests where ash mortality occurred (Costilow et al. 2017, Hoven et al. 2020). Costilow et al (2017) observed a 72% increase in radial growth of red maples during ash canopy decline onset and mortality, and release of red maple recruits in their study was also correlated with dead relative ash basal area (Costilow et al. 2017). In our study, annual ring widths of black ash recruits in Post-Invasion stands increased by 95 ± 34 % on average after overstory mortality. Hoven et al. (2020) also observed the release of maple species in ash forests where ash were dead or in poor condition. Similar to black ash, maple species are generally considered mildly shade tolerant to shade tolerant and respond readily to the formation of canopy gaps (Walters and Yawney 1990, Godman et al. 1990), therefore it is unsurprising that our results mirror these studies.

We expected non-ash species of recruits would be released following overstory black ash mortality, much like black ash recruits. Balsam fir, the most common non-ash recruit species across our stands, however, did not exhibit an observable growth response in Post- or Mid-Invasion stands where black ash recruits were released. Balsam fir is a shade tolerant, late successional species (Uchytil 1991) that can thrive in canopy gaps in many forest types throughout its range (Kneeshaw and Bergeron 1998, Battles and Fahey 2000, Dumais and Prévost 2014). We expected the increased availability of light would stimulate balsam fir radial growth as trees released and fill gaps created by dead overstory black ash or other disturbances. It is unclear as to why black ash recruits were released in these stands, but balsam fir recruits remained suppressed following overstory black ash mortality. One potential explanation is that balsam fir, has not yet responded to the increased light available after the loss of overstory black

ash. Increases in balsam fir radial growth may become more apparent over time, depending on survival of the more rapidly growing black ash recruits.

Increased water table height in Post- and even Mid-Invasion stands could also contribute to the lack of a growth response in balsam fir recruits. Balsam fir is generally tolerant of ephemeral flooding, but water tables that remain high throughout the growing season could negatively impact radial growth. Bolton et al. (2018) observed very little height or radial growth of balsam fir seedlings planted in stands where black ash trees were felled in an effort to simulate EAB impacts treatments. Although Bolton et al. (2018) focused only on seedlings, similar patterns could occur with established recruits.

As EAB continues to spread, the impending mortality of overstory black ash in Michigan's Upper Peninsula will cause the loss of forests that are likely unchanged since the 1700 and 1800s, as well as the loss of a significant cultural resource. In Pre- and Mid-Invasion stands, we observed low proportions basket quality black ash trees based on ring widths, consistent with that of other studies (Benedict and Frelich 2008), and the traditional ecological knowledge held by Indigenous basket makers (Costanza et al. 2017, Diamond and Emery 2011). Without intervention, these basket quality trees and all overstory black ash will be lost from the landscape, and our study suggests that regenerating black ash will not replace overstory trees, despite their ability to release in the wake of EAB. Recruitment of black ash into the overstory will likely be limited by EAB infestation, killing trees before they are able to bear seed. In one Post-Invasion stand, we did however, observe black ash (DBH 11-15 cm) that released; however this trend was not observed in plots of any other Post-Invasion stand, suggesting its occurrence to be rare. Furthermore, some of these trees were exhibiting signs of EAB infestation.

Given the seemingly low chance that black ash regeneration will reach seed producing size and age in Post-Invasion stands, preservation of black ash seed trees is imperative for retaining black ash on the landscape. Treatment of overstory black ash with systemic insecticide, such as emamectin benzoate, can provide protection from EAB for 2-3 years (McCullough 2020), and is a viable method for retaining selected black ash trees. Furthermore, silvicultural techniques that emulate the natural disturbance regime of black ash forests could foster more advanced black ash tree regeneration in the understory, potentially increasing stand resiliency as pressures from EAB mount. Although we expect non-black ash overstory trees to release, our study demonstrates that one species, balsam fir, may not release immediately following overstory mortality. Other species in black ash stands, like red maple may release more readily, as suggested by Costilow et al. (2017) and Hoven et al. (2020), however more research is needed to understand how overstory black ash mortality effects regeneration dynamics of non-ash species.

Tables

Table 2.1. Mean (SE) ash basal area ($m^2 \cdot ha^{-1}$), Pre-EAB black ash basal area ($m^2 \cdot ha^{-1}$), associated species basal area ($m^2 \cdot ha^{-1}$), overstory black ash age, black ash recruit density ($m^2 \cdot ha^{-1}$), associated species recruit density ($m^2 \cdot ha^{-1}$), and recruit age for 24 stands.

Invasion Status	Stand	Live Black Ash BA	Estimated Pre-EAB Black Ash BA	Mean Non-ash BA	Mean Overstory Black Ash Age	Black Ash Recruit Density	Non-Ash Recruit Density	Mean Black Ash Recruit Age
Post Invasion	FIC*	0 (0)	10.87 (1.42)	2.41 (0.69)	-	33.16 (33.16)	182.37 (72.27)	45 (NA)
	MAN	0 (0)	15.39 (0.62)	3.63 (0.82)	-	16.58 (16.58)	66.32 (43.86)	18.2 (2.8)
	NCK	0 (0)	2.11 (0.35)	15.12 (7.66)	-	132.63 (16.58)	1475.51 (880.55)	36.5 (6.74)
	ORC*	0.75 (0.4)	5.85 (1.49)	12.42 (0.54)	-	348.15 (159.88)	994.73 (75.97)	51.8 (10.64)
	RIF	0.64 (0.33)	1.8 (0.89)	8.78 (1.86)	-	1591.56 (388.45)	944.99 (131.59)	24.44 (0.71)
	SIL	0.06 (0.06)	7.42 (1.86)	5.16 (1.88)	-	663.15 (387.75)	381.31 (43.86)	24.56 (1.07)
	SIR*	1.38 (0.2)	9.93 (0.4)	8.18 (2.68)	-	232.1 (43.86)	613.42 (207.73)	48.67 (4.5)
	TRT*	0.23 (0.12)	6.16 (0.49)	10.35 (3.33)	-	266.08 (40.93)	1555.53 (347.95)	32.57 (2.94)
	WOR*	0 (0)	7.31 (1.12)	13.96 (3.5)	-	1193.67 (287.15)	928.41 (507.48)	27.78 (1.61)
	ELR*	1.33 (0.7)	11.74 (1.66)	0.17 (0.17)	-	16.58 (16.58)	49.74 (49.74)	-
	ISA	0 (0)	3.04 (1.46)	2.36 (1.11)	-	16.58 (16.58)	165.79 (87.73)	-
	MOL	0 (0)	4.04 (0.8)	13.69 (1.77)	-	0 (0)	33.16 (33.16)	-
Mid Invasion	CFR	1.87 (1.14)	5.3 (0.32)	16.49 (2.52)	93 (1.87)	961.57 (315)	1757.35 (230.32)	38.57 (7.45)
	HIR	2.31 (0.4)	4.6 (1.64)	6.62 (4.59)	77.25 (10.93)	61.4 (61.4)	122.8 (61.4)	54.5 (11.99)
	M28	15.47 (2.86)	5.03 (0.7)	5.58 (2.17)	102.3 (9.62)	132.63 (43.86)	182.37 (43.86)	64.5 (14.5)
	NRR	1.57 (0.05)	5.58 (0.76)	11.08 (7)	94.67 (4.33)	547.1 (282.81)	762.62 (414.47)	68.56 (8.09)
	RUL	7.66 (3.1)	3.09 (0.57)	10.65 (2.51)	116.1 (11.46)	1210.25 (186.83)	1425.78 (168.26)	74.12 (6.38)
Pre Invasion	CMT	21.8 (2.61)	-	8.8 (1.35)	100.89 (7.88)	33.16 (16.58)	198.95 (151.95)	37.67 (0.88)
	CZL	8.86 (0.81)	-	23.95 (1.22)	101.25 (5.43)	82.89 (16.58)	248.68 (75.97)	57.25 (6.15)
	DCR	2.83 (0.16)	-	15.21 (0.38)	66.12 (7.7)	33.16 (16.58)	1475.51 (141.65)	34.17 (2.89)
	ESR	6.52 (0.71)	-	13.63 (2.37)	46.5 (3.45)	1027.89 (258.97)	1724.2 (408.46)	37.67 (2.24)
	GCP	15.25 (2.8)	-	11.9 (2.07)	139.67 (25.17)	464.21 (191.2)	99.47 (57.43)	44.44 (2.75)
	SML	8.01 (2.81)	-	9.95 (2.87)	81.57 (5.17)	1061.04 (473.88)	580.26 (119.55)	30.67 (3.24)
	WSR	9.43 (1.14)	-	13.69 (1.2)	75.22 (11.46)	547.1 (188.3)	1177.09 (182.37)	48.12 (3.55)

[1]* Indicate Post-Invasion stands in the Upper Peninsula.

Table 2.2. Estimated year of overstory black ash mortality for Post-Invasion stands in Michigan's Lower and Upper Peninsula, informed by tree ring dates from overstory black ash, aerial imagery, and EAB county detections.[1] Aerial imagery time ranges represent the period when canopy dieback became evident and then ceased to progress further. Tree ring mortality represents the range of years of the most recent dated ring of the three trees sampled per stand.[2]

Stand	County	County Detection Year	Aerial Imagery Decline	Tree Ring Mortality Date(s)	**Estimated Mortality Year**
			Lower Peninsula		
MAN	Wexford	2011	2012-2014	2010-2012	**2012**
RIF	Ogemaw	2004	2011-2014	2008-2011	**2010**
SIL	Wexford	2011	2012-2014	2013	**2013**
MOL	Newaygo	2010	2012-2014	-	**2013**
NCK	Clare	2006	2012-2014	2009-2013	**2012**
ISA	Isabella	2005	2012-2016	2008-2014	**2014**
			Upper Peninsula		
TRT	Chippewa	2005	2016-2020	2017	**2018**
ORC	Chippewa	2005	2016-2020	2018	**2018**
ELR	Mackinac	2007	2016-2020	2011	**2018**
SIR	Mackinac	2007	2016-2020	2020	**2018**
WOR	Mackinac	2007	2016-2020	2015-2016	**2018**
FIC	Delta	2008	2018-2022	2018-2019	**2020**

[1]Years of county detections were obtained from EAB.Info.
[2]Cross sections collected from stand MOL were decayed and cross dating was not possible. Overstory mortality was estimated using aerial imagery only.

Table 2.3. Summary of radial growth for overstory black ash trees (DBH > 10 cm) grouped by Invasion Strata. Standard errors and standard deviations are in parentheses. For Post-Invasion stands, values are from cross sections rather than increment cores.

Status	Site	Mean Ring Width (mm) (SE)	No. series	Span	Range (Years)	Mean Series Length (Years)	Mean Series Intercorrelation (SD)	Mean AR1 (SD)
Post Invasion	ELR	1.05 (0.04)	6	1923 - 2011	88	87.67	0.66 (0.1)	0.65 (0.11)
	FIC	1.56 (0.2)	6	1934 - 2019	85	75.67	0.59 (0.17)	0.61 (0.07)
	ISA	1.19 (0.05)	6	1952 - 2014	62	57.33	0.48 (0.14)	0.78 (0.07)
	MAN	2.71 (0.56)	6	1883 - 2015	132	76.17	0.51 (0.15)	0.71 (0.08)
	NCK	2.42 (0.46)	6	1910 - 2013	103	60.33	0.56 (0.22)	0.41 (0.28)
	ORC	0.59 (0.02)	4	1910 - 2018	108	105.75	0.32 (0.2)	0.67 (0.08)
	RIF	1.19 (0.31)	6	1915 - 2011	96	82.67	0.58 (0.11)	0.7 (0.04)
	SIL	0.89 (0.07)	2	1922 - 2013	91	90	0.77 (0)	0.84 (0.03)
	SIR	0.69 (0.08)	6	1858 - 2020	162	124	0.31 (0.23)	0.74 (0.08)
	TRT	0.8 (0.07)	6	1925 - 2017	92	88	0.33 (0.14)	0.72 (0.17)
	WOR	1.07 (0.13)	4	1903 - 2017	114	102.75	0.65 (0.1)	0.83 (0.03)
Mid Invasion	CFR	0.87 (0.04)	9	1919 - 2021	102	89.33	0.53 (0.26)	0.76 (0.04)
	HIR	1.05 (0.14)	16	1916 - 2022	106	73.19	0.37 (0.12)	0.54 (0.2)
	M28	0.82 (0.05)	20	1892 - 2023	131	93.3	0.51 (0.12)	0.61 (0.09)
	NRR	0.81 (0.02)	6	1923 - 2020	97	89.83	0.63 (0.03)	0.66 (0.15)
	RUL	0.71 (0.04)	17	1847 - 2022	175	105.59	0.35 (0.27)	0.67 (0.13)
Pre Invasion	CMT	1.21 (0.13)	17	1905 - 2022	117	92	0.47 (0.1)	0.72 (0.13)
	CZL	0.96 (0.04)	18	1891 - 2022	131	96.44	0.63 (0.08)	0.74 (0.12)
	DCR	1.2 (0.1)	13	1940 - 2022	82	65.15	0.59 (0.2)	0.59 (0.22)
	ESR	1.46 (0.1)	16	1963 - 2022	59	42.25	0.56 (0.17)	0.41 (0.16)
	GCP	1.03 (0.12)	17	1747 - 2022	275	126.35	0.44 (0.14)	0.73 (0.11)
	SML	1.44 (0.1)	18	1920 - 2022	102	61.89	0.68 (0.08)	0.64 (0.15)
	WSR	1.28 (0.11)	18	1901 - 2022	121	65.94	0.52 (0.16)	0.62 (0.19)
Overall		1.15 (0.04)	243	1747 - 2023	276	83.84	0.29 (0.18)	0.65 (0.17)

Table 2.4. Summary statistics for black ash recruits across all stands where coreable recruits (DBH 5-10 cm) were present, grouped by Invasion Strata. Standard errors and standard deviations are shown in parentheses.

Status	Site	Mean Ring Width (mm) (SE)	No. series	Span	Range (Years)	Mean Series Length (Years)	Mean Series Intercorrelation (SD)	Mean AR1 (SD)
Post Invasion	FIC	0.8 (0.08)	2	1980 - 2022	42	40	0.31 (0)	0.53 (0.14)
	MAN	2 (0.21)	12	1995 - 2022	27	14.08	0.31 (0.42)	0.42 (0.33)
	NCK	0.78 (0.13)	8	1977 - 2022	45	34.12	0.49 (0.08)	0.62 (0.1)
	ORC	0.69 (0.08)	8	1931 - 2023	92	48.38	0.51 (0.09)	0.56 (0.18)
	RIF	1.42 (0.06)	18	1998 - 2022	24	21	0.56 (0.16)	0.69 (0.11)
	SIL	1.37 (0.12)	18	1997 - 2022	25	20.22	0.62 (0.18)	0.58 (0.22)
	SIR	0.69 (0.06)	17	1945 - 2023	78	44.47	0.45 (0.17)	0.67 (0.14)
	TRT	0.81 (0.06)	14	1982 - 2022	40	28.43	0.47 (0.15)	0.37 (0.3)
	WOR	1 (0.04)	18	1990 - 2023	33	26	0.21 (0.15)	0.54 (0.18)
Mid Invasion	CFR	0.98 (0.06)	15	1957 - 2022	65	31.13	0.55 (0.23)	0.63 (0.1)
	HIR	0.78 (0.1)	8	1925 - 2022	97	50.75	0.17 (0.26)	0.44 (0.1)
	M28	0.46 (0.13)	4	1946 - 2023	77	52.25	0.05 (0.26)	0.53 (0.08)
	NRR	0.54 (0.06)	18	1926 - 2023	97	64.17	0.46 (0.15)	0.58 (0.16)
	RUL	0.46 (0.05)	16	1939 - 2022	83	70.44	0.37 (0.14)	0.66 (0.14)
Pre Invasion	CMT	0.8 (0.08)	6	1986 - 2022	36	35.17	0.56 (0.12)	0.48 (0.24)
	CZL	0.62 (0.06)	16	1939 - 2022	83	48.62	0.27 (0.19)	0.51 (0.18)
	DCR	0.94 (0.04)	12	1982 - 2022	40	31.17	0.4 (0.15)	0.52 (0.25)
	ESR	0.9 (0.09)	18	1977 - 2022	45	32.39	0.46 (0.23)	0.39 (0.24)
	GCP	0.73 (0.05)	18	1966 - 2022	56	39.78	0.36 (0.22)	0.51 (0.24)
	SML	1.09 (0.07)	18	1976 - 2022	46	27.72	0.37 (0.2)	0.54 (0.25)
	WSR	0.8 (0.03)	16	1965 - 2022	57	42.88	0.53 (0.17)	0.59 (0.15)
Overall		0.92 (0.03)	280	1925 - 2023	98	37.44	0.25 (0.22)	0.55 (0.21)

Table 2.5. Model estimates for seven separate linear regression models fit to understand variability in release of black ash recruits across Post-Invasion stands. All models were fit to predict square root transformed percent difference in radial growth before and after overstory black ash mortality occurred.

Predictor	Model Estimate	D.F.	*P*	R^2
Total Live Basal Area	-0.099	1,6	0.000	0.921
Total Live Density	-0.003	1,6	0.000	0.894
Pre-EAB Black Ash Relative Density	4.888	1,6	0.005	0.764
Pre-EAB Black Ash Relative Basal Area	1.804	1,6	0.008	0.720
Pre-EAB Black Ash Basal Area	0.071	1,6	0.049	0.502
Total Live Recruit Density	0.000	1,6	0.081	0.424
Mean Pre-EAB Black Ash Density	0.003	1,6	0.196	0.260

Figures

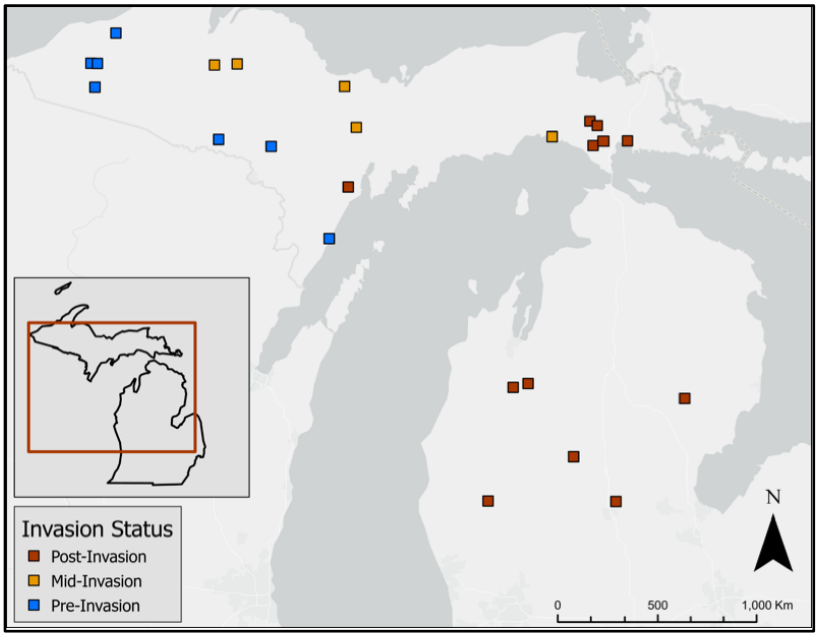

Figure 2.1. Map of black ash stands where dendrochronology work was conducted throughout Michigan across three different EAB Invasion Strata.

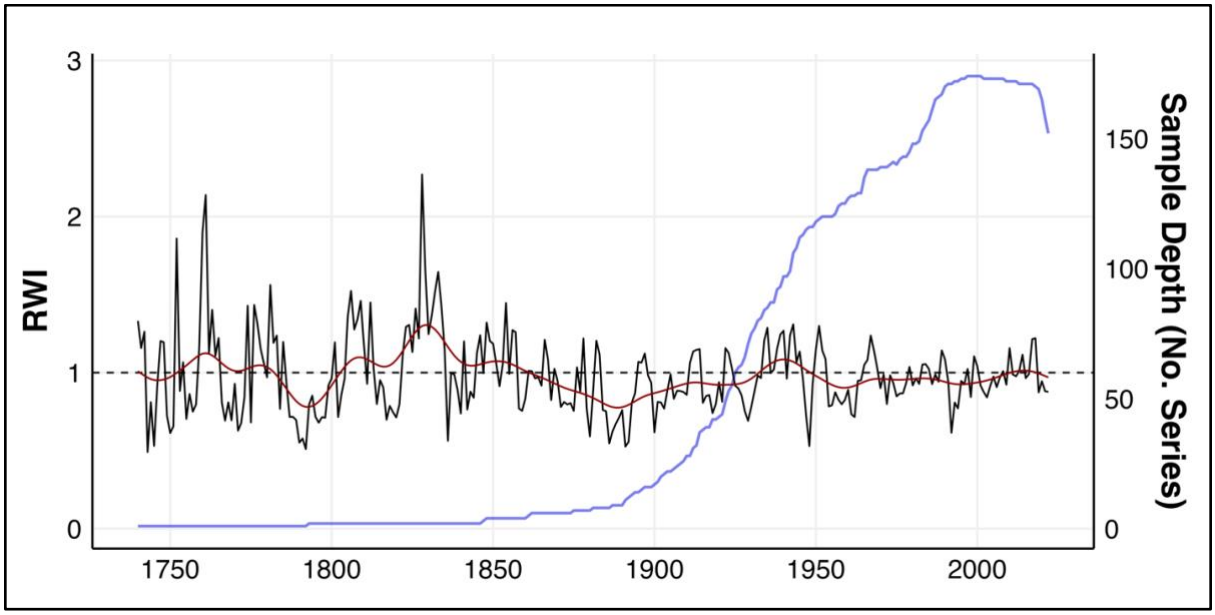

Figure 2.2. Standardized chronology (black line) of 97 overstory black ash trees from Pre- and Mid-Invasion stands with a 30-year spline (red line). Sample depth representing the number of cores contributing toward the standard chronology each year (blue line). The chronology spanned 283 years with an average series length of 84 years and a mean series intercorrelation of 0.32 (± 0.16).

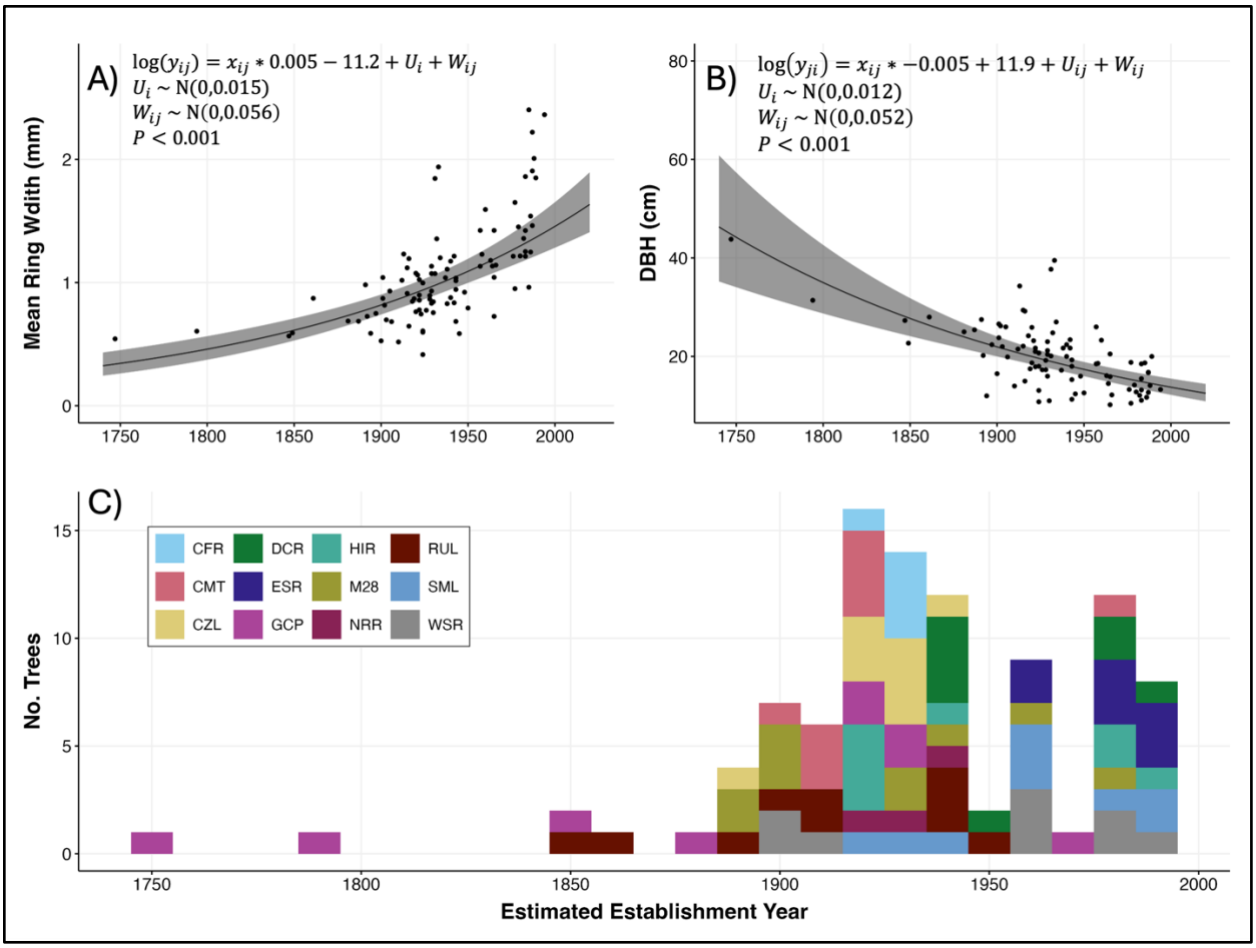

Figure 2.3. Relationships between estimated establishment year and mean annual ring width (A), and DBH (B) for overstory black ash, with generalized linear mixed models (GLMMs) shown as black lines and 95% confidence intervals represented by shading. Individual tree observations are represented by points. Distribution of estimated overstory ash establishment dates for Mid- and Pre-Invasion stands, with individual stands represented by separate colors (C).

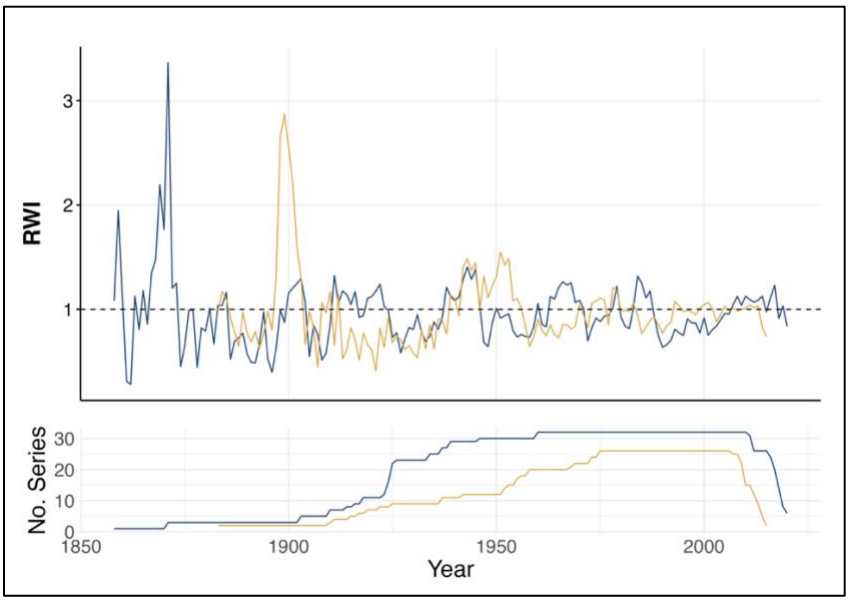

Figure 2.4. Standardized chronology (black line) of dead overstory black ash trees in Post-Invasion stands (top) developed from cross sections collected from the Upper Peninsula (blue line) and the Lower Peninsula (yellow line). Sample depth representing the number of cores contributing toward the standard chronology each year (bottom).

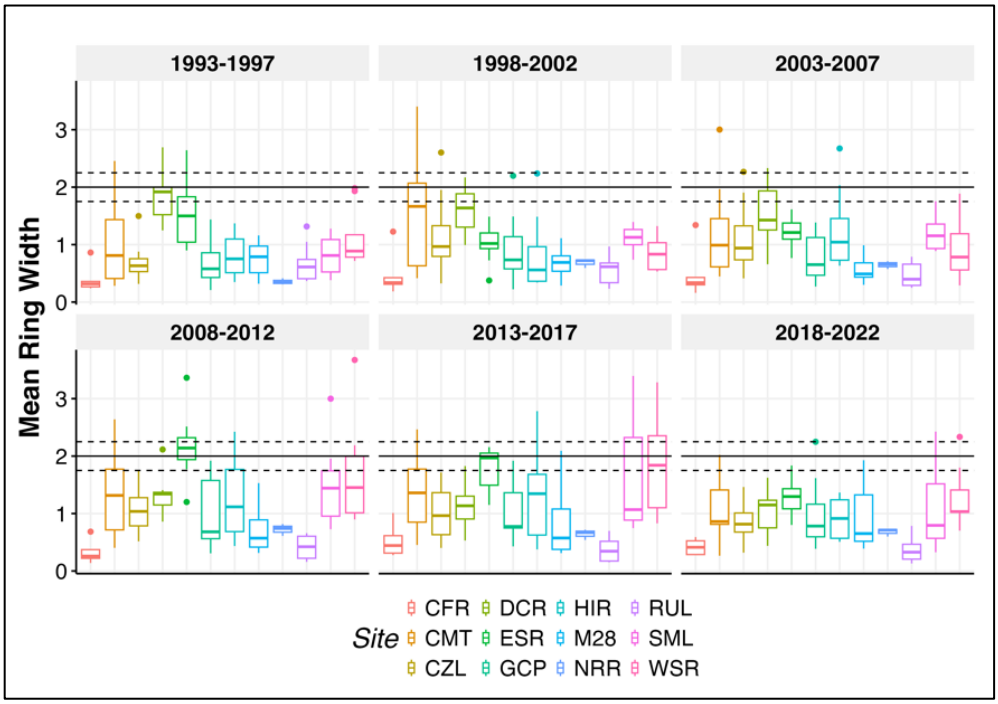

Figure 2.5. Distribution of average 5-year ring widths from 1993-2022 for overstory black ash trees cored across Pre- and Mid-Invasion stands. Optimal ring width for basket quality (2 mm) is denoted by the black solid line, with range of acceptable ring widths (1.75-2.25 mm) denoted by dashed black lines.

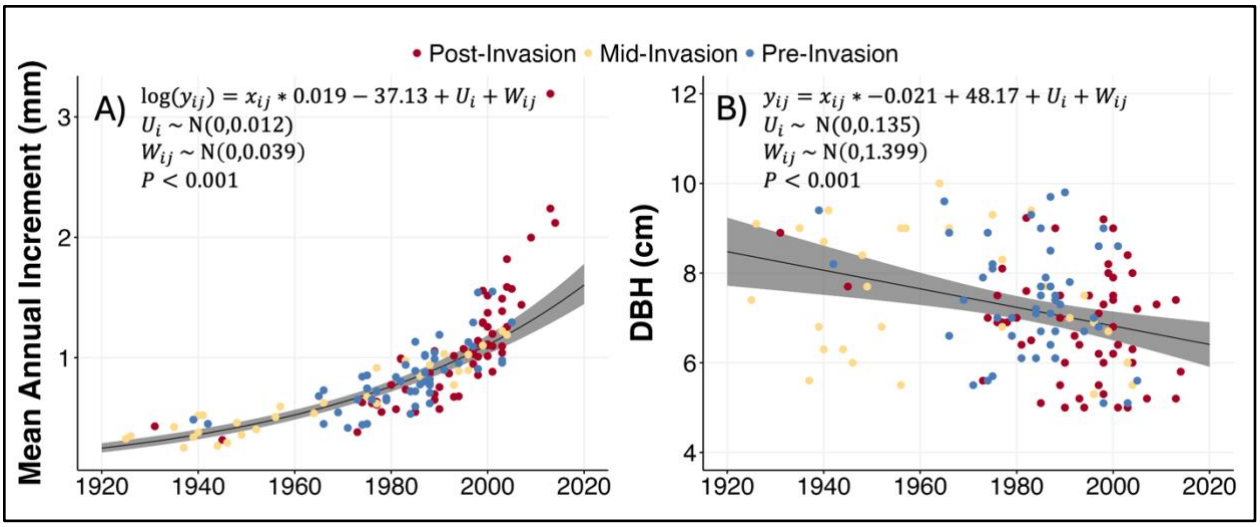

Figure 2.6. The relationships between estimated establishment year and mean annual increment (A), and DBH (B) for black ash recruits across all stands, with generalized linear mixed models (GLMMs) shown as black lines and 95% confidence intervals represented by shading. Colors indicate Invasion Strata. Model equations and variance of random intercepts and residuals are displayed.

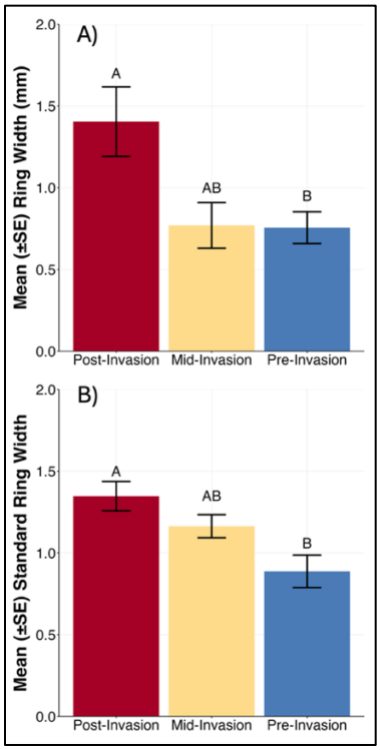

Figure 2.7. Mean (±SE) ring width (A) and mean (±SE) standard ring width (B) for black ash recruits between the years 2015 (the average year of overstory mortality across Post-Invasion stands) and 2022 for all Invasion Strata. Letter codes indicate significant differences.

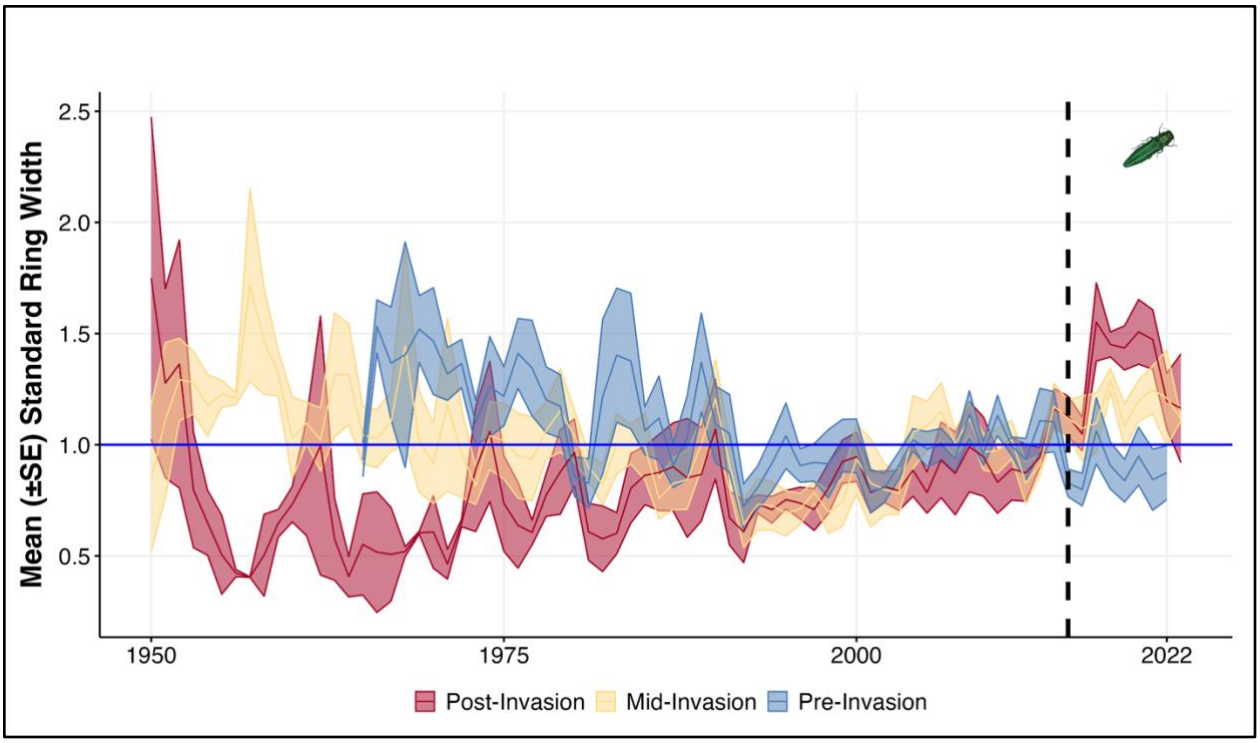

Figure 2.8. Mean (± SE indicated by shading) standard ring width of black ash recruits from 1950 to 2022 in Post-Invasion (red), Mid-Invasion (yellow), and Pre-Invasion sites (blue) (141 trees cored). Black vertical dashed line represents the average year of overstory black ash mortality for Post-Invasion stands.

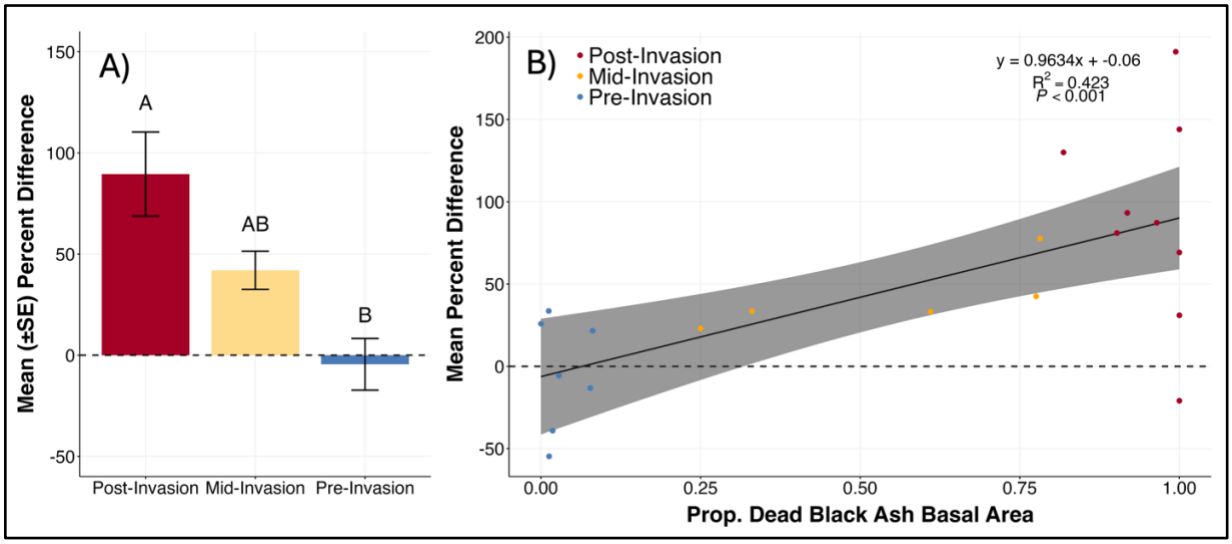

Figure 2.9. (A) Mean (± SE) percent difference in annual ring width before and after 2015 for black ash recruits across Invasion Strata, with letter codes to indicate significant differences. (B) Relationship between percent difference in radial growth before and after 2015 for black ash recruits (black line) and 95% confidence interval (shaded area). Horizontal dashed lines at zero display a point of comparison that would represent no change in average annual ring width before and after 2015.

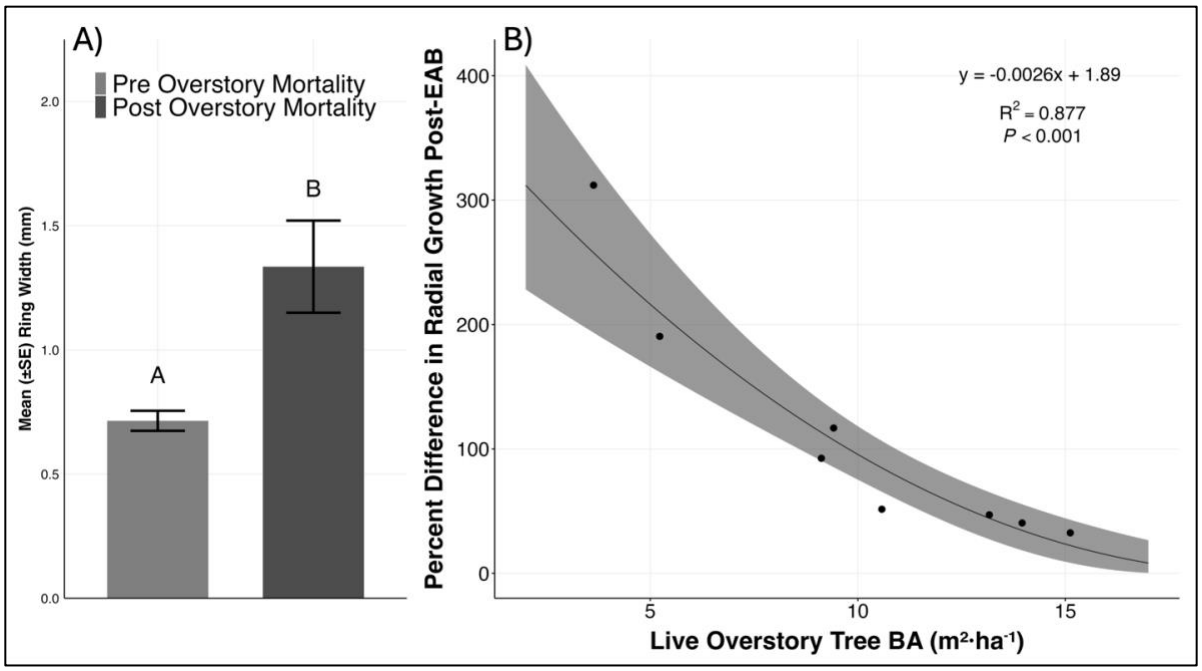

Figure 2.10. (A) Mean (±SE) annual ring width of black ash recruits in Post-Invasion stands before and after the year of overstory black ash mortality. (B) The relationship between percent difference in mean annual ring width before and after the year of overstory mortality and the average basal area ($m^2 \cdot ha^{-1}$) of all live overstory trees in each stand. Shading represents 95% confidence intervals.

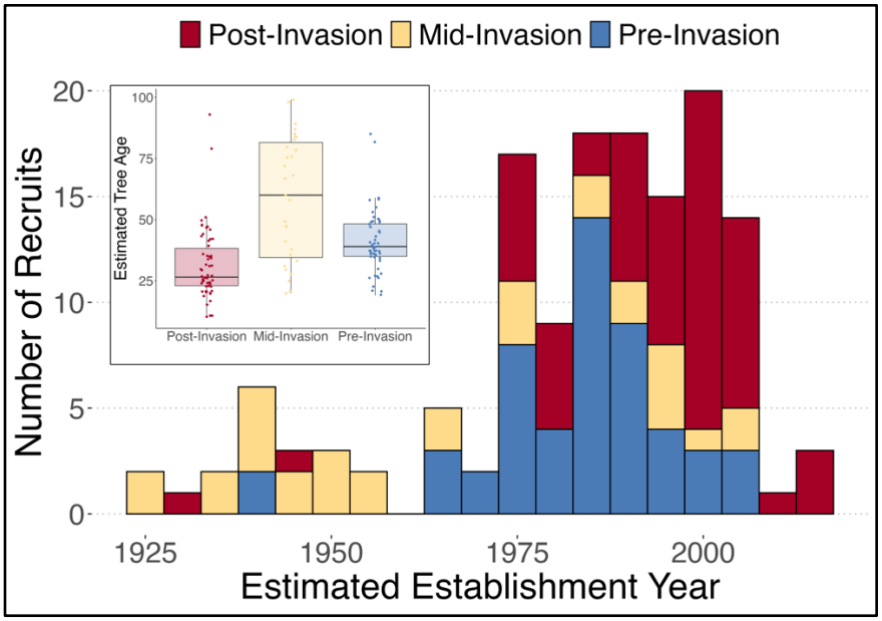

Figure 2.11. Histogram depicting age distribution of black ash recruits across Invasion Strata. Bars represent the number of recruits whose earliest dated ring falls into 5-year age intervals. Boxplot representing median and distribution of black ash recruit age across Invasion Strata (Inset).

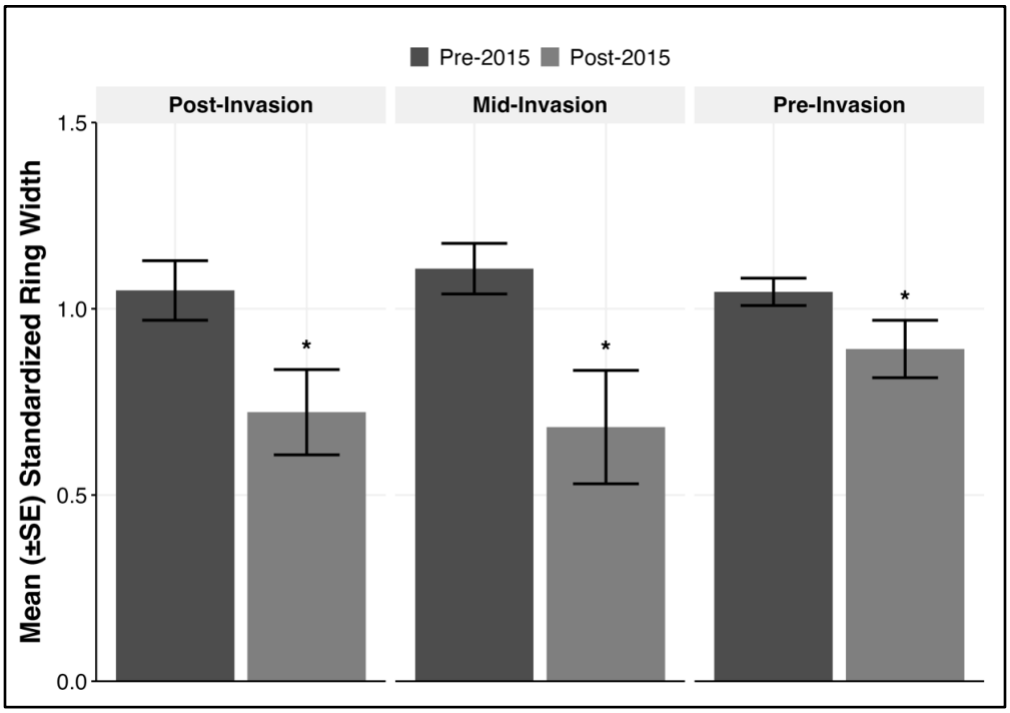

Figure 2.12. Mean (±SE) standardized ring width of balsam fir recruits before (dark grey) and after (grey) 2015 across three Invasion strata. Asterisks represent significant differences between standardized radial growth within Invasion Strata.

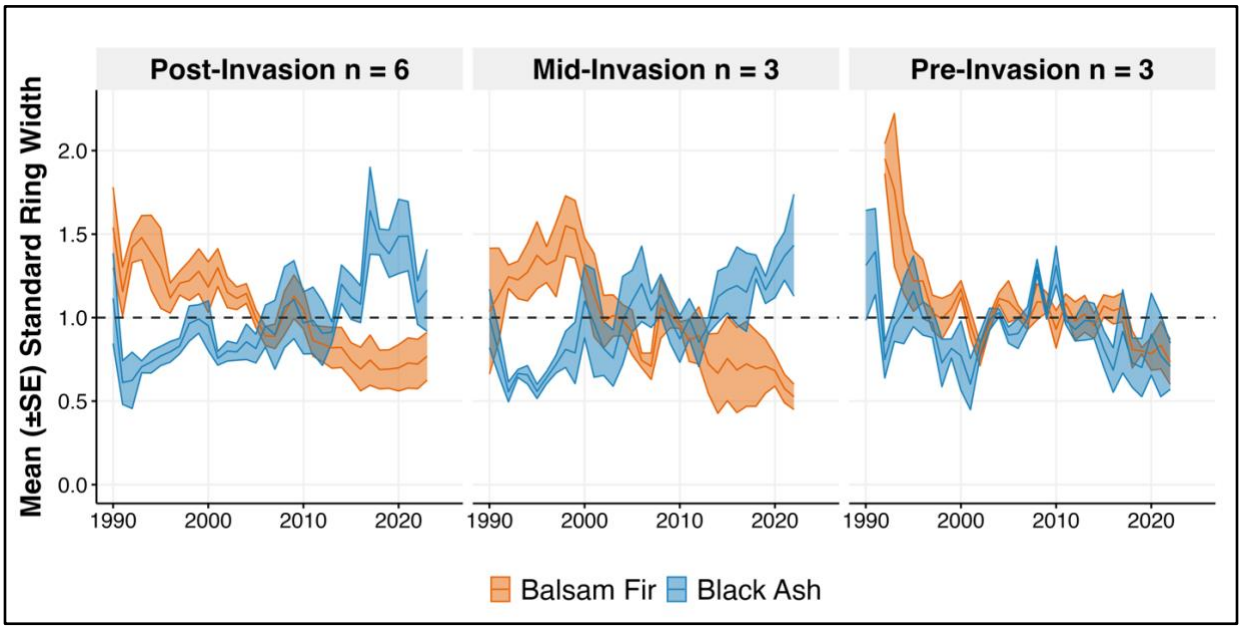

Figure 2.13. Mean (±SE, shading) standardized radial growth of balsam fir (orange) and black ash (blue) recruits stands where both species co-occurred, grouped by Invasion Strata.

CHAPTER THREE: CERAMBYCIDAE IN BLACK ASH FORESTS OF MICHIGAN'S UPPER PENINSULA

Introduction

Black ash (*Fraxinus nigra*) is frequently present in hardwood and mixed conifer swamps in Michigan's Upper Peninsula, often occurring as dominant or co-dominant species (Gucker 2005a). Historically overlooked by western science, black ash stands often include diverse flora and fauna that thrive on nutrient rich, poorly drained soils where hydrology is largely controlled by overstory black ash trees (Telander et al. 2015, Diamond et al. 2018, Looney et al. 2018). These forests, and the unique ecosystem they support, are imperiled by the emerald ash borer (*Agrilus planipennis* Fairmaire) (EAB), an invasive beetle that has killed hundreds of millions of ash trees. Since EAB was introduced from its native range in Asia in the mid-1990s, populations have become established in at least 37 US States and six Canadian Provinces (Herms and McCullough 2014, Siegert et al. 2014, USDA Aphis 2025). Black ash is the most preferred and vulnerable ash species EAB has encountered to date (Herms and McCullough 2014, Tanis and McCullough 2015, Seigert et al. 2021, Mathieu and McCullough 2025). Recent models indicate that of 90% of black ash basal area will be dead by 2040 and this unique species will be functionally extirpated from its range by 2050 (Siegert et al. 2023). Understanding biodiversity within black ash forests and assessing EAB-related changes in tree demography are crucial for understanding the extent of the indirect impacts of invasion.

Native longhorned beetles in the Cerambycidae family (Coleoptera: Cerambycidae), are important components of forest ecosystems, including those likely to be invaded by EAB. Typically secondary pests, native cerambycids colonize trees that are severely declining or have recently died, been felled, or broken (Linsley 1959, Hanks 1999, Evans et al. 2007, Haack 2017). Early-stage larvae feed in phloem while later stages feed in galleries in the sapwood,

contributing to decomposition and nutrient cycling of dead trees (Ulyshen 2016, Haack 2017, Haack et al. 2017). Abundance and species assemblages of cerambycids are driven by the abundance of dead and dying trees and availability of relatively fresh coarse woody debris (CWD). Cerambycids may colonize dead trees or fallen logs after a disturbance but species assemblages can change as wood decomposition progresses (Langor et al. 2008, Hammond et al. 2017, Ulyshen et al. 2020). In Michigan, Engelken and McCullough (2020b) observed that assemblages of cerambycid species captured in baited traps varied among stands with different EAB invasion histories where the availability of standing dead ash and ash CWD varied.

Given the important roles of cerambycids in forest ecosystems and the potential for disturbances such as EAB invasion to alter cerambycid species assemblages and abundance, there is a need to further understand their ecology and distribution. Cerambycid host range in literature can be vague, at times citing broad groups of trees in which larvae develop, like "hardwoods" or "conifers" (Yanega 1996, Lingafelter 2007). Furthermore, many historic records of cerambycids in Michigan represent researchers actively collecting and incidentally observing beetles (Adams et al. 1909, Andrews 1916, Gosling 1973, 1983, 1986, Gosling and Gosling 1976), a labor intensive process that can only be accomplished in limited areas. Over the past 25 years, research on chemical ecology of cerambycids, largely motivated by a need to detect non-native species, has identified broadly attractant pheromones or kairomones that are attractive to a variety of cerambycid species across multiple subfamilies (Miller 2006, Lacey et al. 2007, 2009, Graham et al. 2012, Hanks et al. 2012). Traps baited with broadly attractive semiochemicals can be used to assess species assemblages of native cerambycids across broader spatial scales or to compare species found in tree canopies with those captured in traps near the ground (Graham et al. 2012, Dodds et al. 2010).

To our knowledge, there have been no previous attempts to characterize cerambycid species assemblages in black ash forests, particularly in the Upper Peninsula of Michigan, where 85% of the 4.25 million ha area is forested (Cook 2014). Green ash (*Fraxinus pennsylvanica*), white cedar (*Thuja occidentalis*), balsam fir (*Abies balsamea*) and red maple (*Acer rubrum*) commonly co-occur with black ash, while alder (*Alnus spp.*) and Michigan holly (*Ilex verticulata*) comprise much of the understory (Gucker 2005a, Weber et al. 2007). Generally, there are low amounts of dead woody material, including snags and CWD in black ash stands (Woodall et al. 2011). Much like northern hardwood stands, black ash forests are characterized by single tree mortality and small-scale disturbances (Springer and Dech 2021, Tardif and Bergeron 1999). Following EAB invasion, however, snag density and CWD volume typically increase in stands where either green ash or black ash or both species occur (Engelken and McCullough 2020a, 2020b, Siegert et al. 2021).

In the Upper Peninsula, EAB was first detected in Chippewa County in 2005, followed by detections of several satellite populations throughout much of the Upper Peninsula (EAB.info 2025, USDA APHIS 2025). As of early 2025, extensive ash mortality has occurred in the eastern Upper Peninsula, while ash mortality in the central Upper Peninsula varies considerably. Forests in the western Upper Peninsula were more recently invaded and as of 2024, overstory ash mortality was low in most black ash forests in this region. Given the continuing spread of EAB, the last vestiges of healthy black ash forests in Michigan are found in the western and central Upper Peninsula, providing a time-limited opportunity to evaluate indirect impacts of EAB.

The primary objective of our study was to identify species assemblages of native cerambycids in black ash stands of Michigan's Upper Peninsula, contributing to the literature on native biodiversity in these unique forest ecosystems. We further sought to assess how EAB

invasion may impact cerambycid species abundance and diversity. We predicted that stands impacted by EAB would have a higher density of snags and more volume of relatively fresh CWD, both of which represent suitable brood material for cerambycid larval development, compared to stands not yet affected by EAB. Increased snag and CWD in stands would presumably result in changes to cerambycid beetle species assemblages and abundance, with higher abundances in stands with more brood material. Additionally, we deployed baited traps in overstory tree canopies and near the ground across all stands to determine if species assemblages varied by trap position.

Methods

Study Design: Eight black ash stands in the Upper Peninsula were systematically selected based on previous and related field research (Fig. 3.1). Four stands had been invaded by EAB and represented Mid-Invasion conditions with a mix of healthy, declining and dead overstory ash trees. The other four stands represented Pre-Invasion stands where there were no signs of ash tree decline, or mortality attributed to EAB was observed in 2022 and 2023. Stand boundaries were delineated using Google Earth imagery (Google Inc, Mountain View, CA, 2023) and ArcGIS Pro (ESRI, Redlands, CA, 2023). We overlaid a 50x50m grid on each stand and selected grid cells that contained at least six overstory black ash near the center point. We randomly selected three of these grid cells for sampling. At the center of each chosen grid cell, we established a 11.4 m fixed radius plot and two 25x2 m linear transects leading away from the center of each plot in random compass headings.

Overstory trees and coarse woody debris: Overstory tree assessments were conducted in seven of the eight stands where traps were deployed in 2023, and all eight stands were assessed in 2024 (one Mid-Invasion stand was surveyed in only 2024). In fixed radius plots, we measured

DBH of live and dead overstory trees (DBH > 10 cm) by species, and estimated percent canopy dieback and transparency of live trees. For ash trees, we tallied the number of holes left by woodpeckers feeding on late instar EAB larvae and the number of epicormic shoots on stems up to 2 m high. We also recorded the number of live basal sprouts, if present, on ash trees. Total basal area of live black ash, non-ash, dead black ash, and total snag basal area was calculated for each plot and averaged for each stand.

In linear transects, we measured the diameter at the center of each piece of coarse woody debris intercepted and estimated the length of the piece within the transect, determining species when possible. Decay was ranked on a qualitative scale ranging from 1 to 4 where (1) indicated bark was present, mostly present and firm with few areas of solid wood exposed; (2) bark was present but loose and sloughing off in multiple spots while exposed wood was mostly firm with some soft areas; (3) bark was absent or loose in some areas, exposed wood was firm but soft in some areas; (4) bark was absent, exposed wood was soft and spongy (Engelken and McCullough 2020). Average total CWD volume · ha^{-1} was calculated , and average volume of CWD · ha^{-1} in decay classes one and two combined was calculated to quantify the volume of suitable cerambycid brood material (Engelken and McCullough 2020b).

***Beetle collection*:** In June 2023 and again in June 2024, we deployed two cross-vane panel traps (1.2 m height by 0.3 m width) (Contech Enterprises Inc., Victoria, British Columbia, Canada) on the edge of a canopy gap within each stand. Traps were deployed before vegetation plots were established in 2023 and were located no more than 100 m from at least one of the plots in each stand. Surfaces of traps were coated with Fluon® (Fisher Scientific, Pittsburg, PA) to create slippery conditions to reduce the ability of insects landing on the traps to escape (Graham et al. 2010). Each trap was baited with a bubble cap lure containing 3-hydroxy-2-

hexanon, hereafter refenced as 3R* (release rate 3-4 mg/day at 25 C; Synergy Semiochemicals Corp., Burnaby BC, Canada) and an ultra-high release (UHR) ethanol polyethylene pouch (release rate 200-400 mg/day at 25 C; Synergy Semiochemicals Corp., Burnaby BC, Canada). The 3R* lure is a sex-aggregation pheromone produced by *Neoclytus mucronatus* but is broadly attractive to numerous cerambycid species, particularly in the Cerambycinae, Lamiinae, and Spondylidinae subfamilies (Lacey et al. 2007, Graham et al. 2010, Hanks and Millar 2013, Engelken and McCullough 2020b).

In each site, we hung a ground trap, approximately 1.5 m high, from a bent length of rebar embedded in the ground. A canopy trap was suspended from a lower canopy branch of a live black ash tree, 5-10 m high and directly above the ground trap. We recorded GPS coordinates for each pair of traps. In two stands, there were no ash trees with live canopy branches near the plots. Therefore, to avoid the risk of traps falling because of dead branches breaking, canopy traps were suspended from branches of red maple (*Acer rubrum*) trees. Traps were deployed in 2023 and 2024 in the same tree, with the exception of one site where the original trap tree died, prompting selection of an adjacent live black ash tree.

Collection cups affixed to the bottom of traps contained non-ethanol propylene glycol (RV and Marine Anti-Freeze −50°F Burst Proof, National Automotive Parts Association, NAPA, Atlanta, GA) to preserve captured insects. Traps were checked to collect captured insects at approximately 28-day intervals following deployment in early June until early August (total deployment = 56 days). Lures were replaced on the first trap check (approx. 28 days after deployment).

***Beetle identification*:** Captured insects were stored in a freezer (-20 C) until they were sorted. Cerambycids were placed into 5-dram vials with 70% ethanol until identification. We

identified cerambycids to species using two keys and reference samples from a pinned type collection curated and maintained by the MSU Forest Entomology Lab (Lingafelter 2007, Yanega 1996). Pinned voucher specimens were submitted to the A. J. Cooke Arthropod Collection at MSU.

Statistical analysis: Data analysis and management was conducted were using R (R Core Team, 2024; Version 4.3.2). *S*pecies composition, size and basal area of live and dead overstory trees in stands were averaged using data from the three plots and compared between Mid-Invasion and Pre-Invasion stands. Using a Hellinger transformed distance matrix of species abundances at each site (Legendre and Gallagher 2001), we conducted principal components analysis (PCA) and subsequent redundancy analysis (RDA) to test for divergence in overstory tree species composition between Mid and Pre-Invasion stands. We tested for significant differences in plot total basal area of dead black ash using linear mixed effect models with EAB invasion class as a fixed effect and stands as a random effect with the glmmTMB package (Brooks et al. 2017) (Table S3.1), and then utilized a quasi-binomial GLM, accounting for zero inflated proportion data, to predict differences in the stand average proportion of dead black ash basal area within Invasion Strata as a two level factor.

To evaluate differences in dead woody material between Mid- and Pre-invasion stands, we compared total CWD volume with a two-sample T-test. Differences in plot total volume of coarse woody debris volume by decay class between Mid- and Pre-Invasion stands were examined using a linear model with decay class (4 level factor) and Invasion Strata (2 level factor) as interacting fixed effects, with stand as a random effect (Table S3.1). We then tested for significant differences in the mean volume of ash CWD between Strata using a two-sample T-test. Differences in total snag basal area (all species) and basal area of black ash snags between

Invasion Strata were tested in separate mixed models predicting plot total snag basal area of all species or plot snag basal area of black ash by Invasion Status with stand as a random effect (Table S3.1).

Alpha diversity of cerambycids was assessed by testing for differences in captures of beetles between Mid- and Pre-invasion stands and ground vs. canopy traps using two separate mixed effects models where species richness at each stand each year was predicted by EAB invasion class or trap position as fixed effects and stand and year as random effects (Table S3.1). Differences in total beetles caught between Mid- and Pre-invasion stands and canopy vs ground traps were examined using separate mixed effect models were total individuals caught at each site each years was predicted by Invasion Status or trap placement as fixed effects and stand and year as random effects (Table S3.1). Chao2 species estimates and species accumulation curves with individual-based rarefaction were calculated for Mid- and Pre-Invasion stands and trap position separately for 2023 and 2024 and with both years combined. Individual based rarefaction curves were developed for separate years and for both years using individual beetle counts by species for by Invasion Strata and by trap placement. Beta diversity of cerambycids was assessed using principal coordinates analysis (PCoA) on a Bray-Curtis dissimilarity matrix derived from species abundance data. We utilized permutational analysis of variance (PERMANOVA) to test for differences in Bray Curtis dissimilarity of beetle captures for Mid- and Pre-Invasion stands and between trap positions and tested the explanatory power of multiple site-related variables including mean values for volume of ash CWD and total CWD, fresh ash CWD and total fresh CWD, basal area of all snags and ash snags only, and basal area of live trees. Chao2 estimates, species accumulation curves, and beta diversity analyses were all conducted using the vegan package in R (Oksanen et al. 2024, v2.6.6).

Results

Overstory trees: Overstory tree communities in Mid-Invasion and Pre-Invasion stands were similar (Fig. 3.2) ($F = 1.889$; d.f. = 1, 22; $P = 0.657$). In addition to black ash, we recorded balsam fir, red maple and to lesser extent sugar maple, white cedar, and balsam poplar across stands. Stands represented a range of EAB invasion conditions with varying levels of live, dead and declining black ash trees (Table 3.1). In Mid-Invasion stands, basal area of dead black ash, killed by EAB, was higher than in Pre-Invasion stands ($\chi^2 = 127.26$; d.f. = 1; $P < 0.001$), and the proportion of dead black ash basal area in Mid-Invasion stands was 40% greater than in Pre-Invasion stands ($\chi^2 = 25.6$, d.f. = 1; $P < 0.001$). In Mid-Invasion stands, mean basal area of live black ash ranged from 1.86 ± 1.1 to 15.4 ± 2 $m^2 \cdot ha^{-1}$, and canopy dieback averaged 94.7 ± 1%, indicating nearly all trees were heavily infested by EAB and declining. In contrast, average basal area of live black ash ranged from 8.01 ± 2.8 to 21.79 ± 2.60 $m^2 \cdot ha^{-1}$in Pre-Invasion stands, and black ash trees appeared much healthier with estimated canopy dieback averaging 35.1 ± 5.9%.

Between 2023 and 2024, black ash condition deteriorated, and mortality increased in most resurveyed stands (Table 3.2). In 2024, mortality of black ash increased from an average of 70.5 ± 7.0% to 92.6 ± 7.3% in Mid-Invasion stands and from 4.4 ± 2.2% to 11.2 ± 6.5% in Pre-Invasion stands. In two Pre-Invasion stands, black ash mortality had increased notably when we re-surveyed the plots (Table 3.2), and differences in percent canopy dieback increased markedly from 2023 to 2024, presumably indicative of increasing EAB density in these stands (Table 3.2).

***Coarse woody debris and snags*:** Overall, CWD in black ash stands was variable, and generally more abundant in Mid-Invasion stands. Total volume of CWD, including all species, did not differ between Mid- and Pre-Invasion stands ($F = 0.314$; d.f. = 1, 6; $P = 0.595$), nor did Invasion Status affect CWD volume by decay class ($\chi^2 = 4.4$, d.f. = 3; $P = 0.224$) (Fig. 3.3A). On

average, most CWD observed in Mid-Invasion stands was comprised of black ash (50.1 ± 12.0%) followed by balsam fir (23.2 ± 9.2), while in Pre-Invasion stands, CWD was mainly white cedar (53.9 ± 1.4%), followed by black ash (21.4 ± 8.5). Mean volume of total black ash CWD did not differ between Mid- and Pre-Invasion stands (F = 5.27; d.f. = 1, 6; $P = 0.061$), nor did volume of fresh black ash CWD (decay class one and two) (F= 3.076; d.f. = 1,6; $P = 0.13$). On average, the majority of black ash CWD across our study sites were classified as decay class two (23.7 ± 10.2 %) and three (63.6 ± 14%), with decay classes one (12.5) and four (0.1 ± 0.1%) represented less often across all stands.

Basal area and species composition of snags (standing dead trees) was variable across Mid- and Pre-Invasion stands, and ash snag basal area was generally higher in Mid-Invasion stands (Fig. 3.3B). Basal area of all snags was similar across Invasion Strata ($\chi^2 = 3.57$; d.f. = 1; $P = 0.0587$) largely due to variability and the abundance of large dead white cedars in one Pre-Invasion stand. Basal area of black ash snags, however, was higher in Mid-Invasion than in Pre-Invasion stands ($\chi^2 = 92.37$; d.f. = 1; $P < 0.001$) (Fig. 3.3B). Black ash comprised 71.7 ± 15.3% of snag basal area in Mid-Invasion stands, while balsam fir and white cedar comprised 26.7 ± 12.5% and 19.9 ± 15%, respectively of the basal area of snags in Pre-Invasion stands.

Cerambycid beetle captures: We captured a total of 705 cerambycid beetles, representing three subfamilies and 28 species, with the 16 traps deployed during the 2023 and 2024 field seasons in eight black ash stands in Upper Michigan (Table 3.3). Over both years, the most captured species belonged to the subfamily Cerambycinae, which represented 87.6% of total beetle captures. Within Cerambycinae, *Clytus ruricola* (Olivier) and *Xylotrechus colonus* (Fabricius) were captured most frequently, accounting for 45.7% and 34% of total beetles, respectively. The third most captured species was *Crytophorus verrucosus* (Olivier) (subfamily

Anglyptini), representing 4.7% of all captured beetles. Of the 28 species captured, 22 were represented by less than 10 individuals, and seven species were represented by just one individual.

Beetle species assemblages across all stands in 2023 and 2024 were different ($F = 2.7$; d.f. = 1, 30; $P = 0.026$), likely driven by reduced captures in 2024. In 2023, we captured 462 beetles across all stands compared to 243 in 2024. In 2023, a total of 24 cerambycid species were captured, 88.1% of which belonged to the subfamily Cerambycinae, with beetles in the subfamily Lamiinae and Lepturinae only accounting for 3% and 8.9% of captures, respectively. In 2024, we captured 19 cerambycid species, with 87.6% of beetles belonging to the subfamily Cerambycinae, 2% belonging to the subfamily Lamiinae, and 10% belonging to Lepturinae. Of the total species caught across all years, 34.4% were only captured in 2023, and 7.3% were only captured in 2024.

Cerambycid traps were located in eight counties across Michigan's Upper Peninsula, and based on our extensive review of literature, our captures represent 43 new county records for 22 cerambycid species (Table S3.2). This included 9 species in the subfamily Cerambycinae (25 new county records), five species in the subfamily Lamiinae (8 new county records), and eight species in the subfamily Lepturinae (10 new county records) (Figures 3.4-3.6, Table S1).

Overall, the numbers of beetles captured, beetle species richness, and Chao 2 estimates of species richness were similar between Mid- and Pre-invasion stands and between canopy and ground traps (Table 3.4). Differences in number of beetles captured did not differ between Mid- and Pre-invasion stands ($\chi^2 = 1.1$; d.f. = 1; $P = 0.295$) nor did species richness ($\chi^2 = 0.039$; d.f. = 1; $P = 0.842$) (Table 3.). Likewise, canopy and ground traps captured similar numbers of beetles ($\chi^2 = 1.16$; d.f. = 1; $P = 0.0.28$) and species richness did not differ between canopy traps and

ground traps ($\chi^2 = 3.39$, d.f. = 1; $P = 0.065$). Rarefaction curves indicate that we had varying degrees of sample coverage across trap year and trap placement, however overall rarefaction curves do not appear to be approaching asymptotes, suggesting low sample coverage (Fig 3.7).

Species assemblages of beetle were similar across all stands regardless of EAB invasion status (Fig 3.8A, Table 3.5). *C. ruricola* and *X. colonus,* the most captured beetles in our study, were caught evenly across all stands. In one outlier stand, the species assemblage was largely driven by the presence of *Stictoleptura canadensis* (Olivier) in a single trap (Fig. 3.8A). Other species driving variation within stands included *Trigonarthris proxima* (Say) and *Anthophylax attenuatus* (Haldeman), which represented 0.6 % and 0.1% of total captures, respectively. Total volume of CWD, volume of CWD in decay class two and three, and basal area of all snags were not significant predictors of beetle species assemblages (Table 3.5). Consistent with the lack of differences in beta diversity of captured species, there were no indicator species of EAB invasion status.

We observed no significant differences in species assemblages captured in canopy and ground traps (F = 1.1; d.f. = 1, 15; $P = 0.31$) (Fig. 3.8B, Table 3.5), and there were no significant indicators of trap placement. Across all years we captured 409 cerambycids in canopy traps, and 296 in ground traps. Beetle captures decreased from 2023 to 2024, with 65.0% and 66.5% fewer beetles captured in 2024 in canopy and ground traps, respectively. Of the total number of species caught (28) 34.5% were observed in canopy traps only, 20.7% were observed in only ground traps, and 41.3% were captured in both trap types.

Discussion

Although research on native cerambycids in North America has increased over the past two decades, information on geographic and host range remains limited for many species.

Effects of invasive pests set against a backdrop of climate change are altering many eastern forests in North America and will likely affect woodboring cerambycids. Stands where we deployed our traps represent the early to mid-stages of EAB invasion in black ash forests, and overstory ash mortality will lead to the presence of black ash snags and eventually an influx of dead woody material. Our results contribute generally to information related to native cerambycid species present in black ash stands, a relatively understudied ecosystem and provide baseline information for further studies as EAB-related impacts progress in these unique forests.

Of the 28 species captured in our traps, all except *Xylotrechus integer* (Fabricius) were previously reported to be present in Michigan, and all but two species (*X. integer* and *Stenochorus schaumii* (LeConte) species were previously collected in the Upper Peninsula. Overall, our trapping yielded a relatively high number of new county records for both rare and common species. *C. ruricola and X. colonus* for example, are widely distributed, but had not been previously reported in five counties in the western Upper Peninsula. We expect that most new county records reflect low sampling efforts in western counties of the Upper Peninsula, relative to other regions of Michigan. Moreover, county records from Andrews (1916), Gosling (1973, 1983, 1986), and Gosling and Gosling (1976) predate use of broadly attractive semiochemical baited traps. County records from Andrews (1916) are paired with detailed descriptions of observation methods, ranging from incidental observances to active searching, to reared beetle observations. County records detailed by Gosling (1973, 1983, 1986), and Gosling and Gosling (1976) were obtained through analysis of specimens in the University of Michigan Museum of Zoology, and collection methods are not detailed. The first cerambycid pheromones were identified in the 1980s, and the use of semiochemicals in trapping efforts was not widely used until the 2000s (Iwabuchi 1982, Dodds et al. 2010, Curkovic et al. 2022). While historic

methodologies for observing beetles remain valuable, the use of semeiochemicals as lures affixed to traps, including cross-vane panel trap baited with 3R* and ethanol, has increased the effectiveness of cerambycid surveys, resulting in broader sample coverage (Dodds et al. 2010, Graham et al. 2012, Hanks et al. 2012, Lacey et al. 2009, Miller 2006).

The three most commonly captured beetles in our traps belonged to the subfamily Cerambycinae, which is consistent with literature utilizing the same traps and lure combinations (Graham et al. 2012, Handley et al. 2015, Engelken et al. 2020b). *C. ruricola,* the most common beetle captured in our study, feeds on a variety of tree species across multiple families and genera, with a preference toward *Acer* spp. (Gosling 1973, Lingafelter, 2007). *C. ruricola* has also been reared from white ash (*Fraxinus americana*) logs (Maier 2018). In riparian forests where green and black ash had been killed by EAB, Engelken and McCullough (2020b) observed a relatively high proportion of *C. ruricola* (20%) in southeast Michigan riparian forests where overstory ash mortality was caused by 2006, compared to previous studies in which *C. ruricola* consistently comprised less than 1% of total captures (Graham et al. 2012, Hanks and Millar 2013, Hanks et al. 2014, Handley et al. 2015, Schmeelk et al. 2016). In our study, *C. ruricola* represented 45.7% of total captures, regardless of Invasion Strata, further adding to the evidence that this species develops in ash species. Contrary to Engelken and Mccullough (2020b), we observed high proportions of *C. ruricola* in both Mid- (47.5%) and Pre-Invasion stands (43.8%), suggesting that the presence of dead ash trees in our stands may not be related to increased *C. ruricola* abundance.

Xylotrechus colonus, the second most captured species, is similarly present throughout Michigan, feeds on multiple hardwoods (Gosling 1973, Lingafelter, 2007) and was also abundant in riparian forests where ash killed by EAB provided ample brood material (Engelken et al.

2020). *Crytophorus verrucosus*, the third most commonly caught species, feeds on several genera of hardwoods including *Acer, Betula,* and *Ulmus* species (Lingafelter, 2007), all of which can occur in black ash forests and were present in the stands we trapped.

Most species that were rarely captured in our traps represented new county records. *Xylotrechus integer*, has no published records in Michigan, and was captured by our traps in a stand in Marquette County, reportedly develops in balsam fir (*Abies balsamea*), which was common in our stands, along with eastern hemlock (*Tsuga canadensis*) (Yanega 1996), which was rarely present. Little information about the host range of *Stenocorus schaumii* is available although Yanega (1996) noted its ability to develop in multiple hardwood species.

Overall, nearly all species captured were previously captured in traps baited with 3R* and UHR ethanol lures (Lacey et al. 2007, Dodds et al. 2010, Graham et al. 2012, Engelken and McCullough 2020). Many cerambycids that develop in dying, newly dead or recently felled or broken hardwood trees are attracted to ethanol (Miller 2006), while the chemical structure of sex pheromones is similar across several cerambycid genera and species (Hanks et al. 2012). We expect that additional cerambycid species could be captured in black ash stands if traps were also baited with lures such as alpha pinene, which commonly produced by conifers (Miller 2006, Graham et al. 2012). Recent research indicates a multicomponent lure, often consisting of various combinations of pheromones from different cerambycid species and tree kairomones, can attract a diverse assemblage of cerambycid species and is particularly useful for detection of non-native cerambycid species at ports-of-entry, land.f.ills and other high sites (Hanks et al. 2012, Fan et al. 2018, Roques et al. 2023)

Despite differences between Mid- and Pre-Invasion stands in availability of brood material, such as ash snags and recently fallen CWD, cerambycid species richness, abundance

and species assemblages were similar across stands. Generally low numbers of cerambycid captures, with the exception of *Clytus ruricola* and *Xylotrechus colonus*, presumably contributed to the lack of significant differences. Past studies have linked differences in cerambycid species assemblages to the abundance of suitable brood material, e.g., dead and dying trees following disturbance. In some cases, species assemblages responded relatively quickly to the disturbance (Hammond et al. 2017, Ulyshen et al. 2020). Engelken and McCullough (2020b), however, observed a temporal lag before cerambycid species assemblages in riparian forests were affected by EAB invasion. In their study, species assemblages of cerambycids differed between stands where EAB-related mortality preceded trapping by at least ten years versus stands where overstory trees were killed up to five years before trapping. We expect, therefore, that cerambycid species assemblages in the black ash stands may eventually shift as EAB increases availability of brood material.

The rate of decline of overstory black ash trees between 2023 and 2024, particularly in the stands that appeared to be ahead of the EAB invasion in early 2023, was unanticipated. Average canopy dieback in Pre-Invasion stands increased from 36.2 ± 4.8% in 2023 to 82.0 ± 3.2% in 2024, and some trees were dead in two of these stands by late summer in 2024. Multiple years of trapping in these sites will likely be necessary to document changes in cerambycid abundance and species composition as trees succumb to EAB, break and fall. Complete or nearly complete mortality of overstory black ash caused by EAB invasion (Engelken and McCullough 2020a, Siegert et al. 2021, 2023) should provide ample brood material for cerambycids for a number of years. This contrasts sharply with the typical small scale or single-tree mortality common in black ash forests before EAB arrived (Fraver et al. 2022, Springer and Dech 2021). Documenting the response of cerambycid communities to EAB invasion in black ash forest will

be essential both for understanding cascading effects of EAB and dynamics of native cerambycids.

Similarity of cerambycid numbers and species assemblages captured in canopy versus ground traps was also unexpected. In multiple studies, different cerambycid species were captured in canopy versus ground traps and individual species indicative of trap placement were often identified (Dodds et al. 2010, Graham et al. 2012, Schmeelk et al. 2016, Engelken and McCullough 2020b). Differences in the species or general abundance of captured cerambycids may be driven in part by the type of brood material where the captured beetles developed, whether that was CWD or standing dead trees (Graham et al. 2012, Engelken and McCullough 2020b). *Xylotrechus colonus* and *Clytus ruricola* are commonly caught in ground traps, suggesting that they primarily develop in CWD (Graham et al. 2012, Engelken and McCullough 2020b). In our stands, similar proportions of both species captured in canopy and ground traps suggest beetles are colonizing dead snags, which were generally more abundant than high volumes of CWD.

It is unclear as to why beetle species assemblages and beetle abundances differed between 2023 and 2024, with beetle captures in 2024 being significantly reduced compared to 2023. Natural variations in beetle abundances have been noted to occur from year to year in other studies (Graham et al. 2012, Handley et al. 2015, Engelken and McCullough 2020b). It is possible that emergence and flight period of beetle species differed between the two year (Handley et al. 2015), but only if substantial differences in spring and summer temperatures occurred. Traps were deployed during the early weeks of June each year, and accumulation of growing degree days was similar during the month of June in 2023 and 2024. In 2023, 291 degree days$_{10}$ had accumulated in Escanaba, Michigan (the most central weather station where

accurate growing degree day data is available). In 2024, 280-degree days$_{10}$ had accumulated. By the end of June, 654 and 6411degree days$_{10}$ had accumulated in 2023 and 2024 respectively. We therefore have no reason to expect differences in beetle emergence and flight periods in our study.

Understanding species assemblages of cerambycids in black ash stands before emerald ash borer is important for understanding how these ecosystems may change following disturbance. While our results have value, we are aware that other cerambycid species likely occur in black ash forests in northern Michigan and the Lake States region. Increased sampling effort over multiple years and lures with other semiochemicals would presumably yield additional records. Use of an effective trap design and the ability to bait traps with attractive semeiochemicals have facilitated substantial progress in research related to distribution, abundance and assemblages of cerambycids over the past 20 years. (Allison et al. 2004, Miller 2006, Lacey et al. 2007, Dodds et al. 2010). Moreover, relatively little information is available for other groups of subcortical insects such as Siricidae (Hymenoptera) and Buprestidae (Coleoptera) in black ash stands, and likely, other overlooked forest types. Further research to assess native insect diversity and ecology in severely affected forests will be needed to fully catalog the indirect impacts of EAB invasion has on native subcortical insects in North American forests.

Tables

Table 3.1. Mean (SE) basal area ($m^2 \cdot ha^{-1}$) of live and dead black ash, live non-ash trees and estimated canopy dieback of live black ash trees in three Mid-Invasion and five Pre-Invasion stands in the Upper Peninsula of Michigan. The top four most important species and their mean (SE) relative importance values (RIV) are also displayed.

Status	Live Black Ash BA (SE)	Dead Black Ash BA (SE)	Live Non-Black Ash BA (SE)	Mean Black Ash Canopy Dieback (SE)	Species	Mean RIV (SE)
Mid Invasion	6.55 (0.73)	4.98 (0.39)	9.56 (0.76)	94.7% (1.6%)	*Fraxinus nigra*	98.9 (36.33)
					Abies balsamea	52.37 (11.04)
					Thuja occidentalis	39.65 (27.09)
					Acer rubrum	29.26 (9.12)
Pre Invasion	12.09 (0.49)	0.33 (0.06)	13.64 (0.31)	35.2% (5.9%)	*Fraxinus nigra*	119.5 (13.81)
					Thuja occidentalis	34.05 (20.08)
					Fraxinus pennsylvanica	28.74 (18.96)
					Abies balsamea	21.3 (7.5)

Table 3.2. Mean (SE) percent mortality and percent canopy dieback of overstory black ash trees for stands surveyed in 2023 and in 2023.[1]

Invasion Status	Stand Name	Year	Mean % Mortality (SE)	Mean % Canopy Dieback (SE)
EAB Impacted	CFR	2023	77.53 (9.84)	92.06 (3.84)
	CFR	2024	85.24 (0.99)	100 (0)
	HIR	2023	63.44 (13.58)	95.24 (4.76)
	HIR	2024	100 (0)	NA (NA)
EAB Unimpacted	CMT	2023	3.14 (1.6)	33.4 (3.89)
	CMT	2024	3.34 (1.68)	75.31 (10.58)
	CZL	2023	10.83 (5.83)	56.11 (2.55)
	CZL	2024	34.26 (5.63)	89.07 (4.49)
	ESR	2023	1.85 (1.85)	26.99 (1.76)
	ESR	2024	0 (0)	86.58 (2.2)
	GCP	2023	4.55 (2.62)	26.49 (7.09)
	GCP	2024	0 (0)	71.77 (10.58)
	SML	2023	0 (0)	38 (4.67)
	SML	2024	16.67 (9.62)	81.19 (10.21)

[1]Seven of the eight stands were surveyed in 2023 and 2024, while one Mid-Invasion stand was only surveyed in 2024 due to time and logistical constraints.

Table 3.3. Number of adult cerambycids captured by subfamily, tribe, and species from canopy and ground traps in 2023 and 2024.

Subfamily	Tribe	Species	Canopy	Ground	Total
Cerambycinae	Anaglyptini	*Crytophorus verrucosus* (Olivier)	23	10	33
	Callidiini	*Phymatodes aereus* (Newman)	6	6	12
		Phymatodes testaceus (Linnaeus)	5	0	5
	Clytini	*Clytus ruricola* (Olivier)	192	130	322
		Glycobius speciosus (Say)	3	0	3
		Neoclytus acuminatus (Fabricius)	0	2	2
		Sarosesthes fulminans (Fabricius)	0	1	1
		Xylotrechus colonus (Fabricius)	116	124	240
		Xylotrechus interger (Fabricius)	1	0	1
	Trachyderini	*Purpuricenus humeralis* (Fabricius)	0	1	1
Lamiinae	Acanthocinini	*Astylopsis macula* (Say)	3	0	3
		Astylopsis sexguttata (Say)	2	0	2
		Urgleptes querci (Fitch)	0	2	2
	Acanthoderini	*Aegomorphus modestus* (Gyllenhal)	3	2	5
	Monochamini	*Microgoes oculatus* (LeConte)	2	1	3
		Monochamus scutellatus (French)	1	3	4
Lepturinae	Lepturini	*Bellamira scalaris* (Say)	3	0	3
		Etorofus subhamatus (Randall)	0	1	1
		Phygoleptura nigrella (Say)	1	0	1
		Stictoleptura canadensis (Olivier)	22	2	24
		Strangalepta abbreviata (Germar)	0	1	1
		Trachysida mutabilis (Newman)	11	6	17
		Trigonarthris minnesota (Casey)	2	1	3
		Trigonarthris proxima (Say)	3	1	4
	Oxymirini	*Anthophylax attenuatus* (Halderman)	1	0	1
	Rhagiini	*Centrodera decolorata* (Harris)	2	0	2
		Gaurotes cyanipennis (Say)	3	1	4
		Stenocorus schaumii (LeConte)	4	1	5
	Total	**28**	**409**	**296**	**705**

Table 3.4. Mean (SE) number of beetles caught, species richness, and Chao Species Estimates for cerambycid beetles in Mid- and Pre-Invasion stands, canopy and ground traps, across each trapping year. Standard errors are displayed in parentheses.

Status	Year	Mean Beetles Caught (SE)	Mean Species Richness (SE)	Chao Species Estimate
Mid Invasion	2023	69 (29.09)	13.33 (1.45)	18.2
	2024	38.33 (21.36)	10.33 (1.86)	15.2
Pre Invasion	2023	51 (11.61)	11.4 (0.98)	28.0
	2024	25.6 (6.27)	11.4 (2.16)	19.5
Canopy	2023	33.5 (9.95)	6.25 (0.65)	23.4
	2024	18 (6.05)	7 (0.8)	24.4
Ground	2023	24.38 (5)	5.88 (0.77)	26.1
	2024	12.38 (3.6)	4 (0.85)	9.5

Table 3.5. PERMANOVA model outputs for individual variables (bold text), grouped by variable type (row subheadings), used to predict differences in longhorn beetle communities between Mid- and Pre-Invasion stands.

Model	Degrees of Freedom	Sum of Squares	R^2	F Statistic	*P*
Invasion Status	1	0.07	0.03	0.48	0.83
Residual	14	2.07	0.97		
Total	15	2.14	1.00		
Trap Placement	1	0.16	0.07	1.11	0.31
Residual	14	1.99	0.93		
Total	15	2.14	1.00		
CWD Volume					
Total (Black Ash)	1	0.09	0.04	0.58	0.70
Residual	14	2.06	0.96		
Total	15	2.14	1.00		
Fresh (Black Ash)	1	0.09	0.04	0.61	0.72
Residual	14	2.05	0.96		
Total	15	2.14	1.00		
Total (All Species	1	0.18	0.08	1.27	0.27
Residual	14	1.96	0.92		
Total	15	2.14	1.00		
Fresh (All Species)	1	0.11	0.05	0.74	0.58
Residual	14	2.04	0.95		
Total	15	2.14	1.00		
Basal Area					
Snags (All Species)	1	0.08	0.04	0.52	0.77
Residual	14	2.07	0.96		
Total	15	2.14	1.00		
Pre-EAB Black Ash	1	0.06	0.03	0.43	0.87
Residual	14	2.08	0.97		
Total	15	2.14	1.00		
Live (All Species)	1	0.13	0.06	0.90	0.49
Residual	14	2.01	0.94		
Total	15	2.14	1.00		

Figures

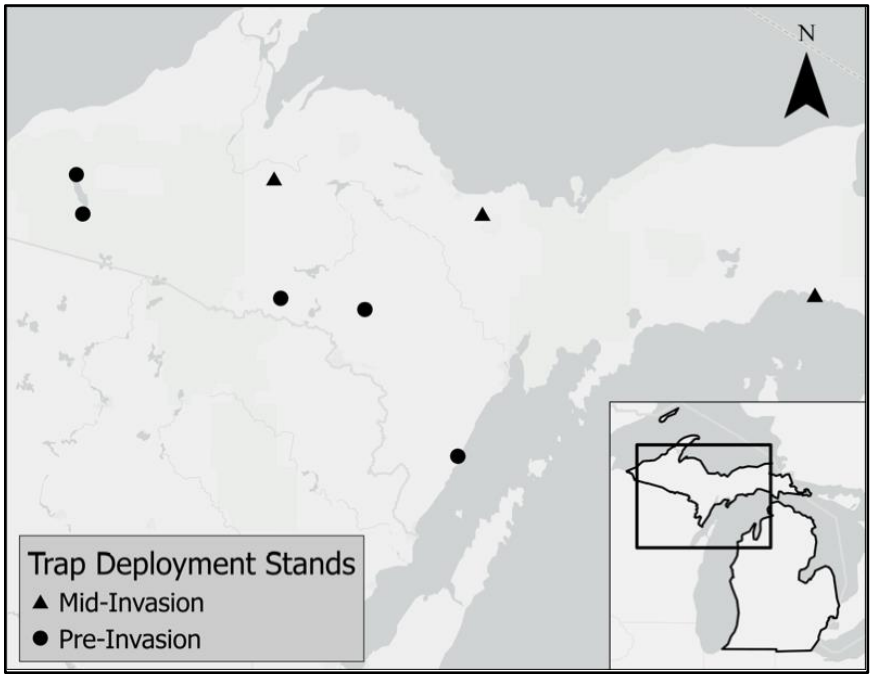

Figure 3.1. Locations of three Mid-Invasion and five Pre-Invasion stands in Michigan's Upper Peninsula where baited cross-vane panel traps were deployed from June to August in 2023 and 2024.

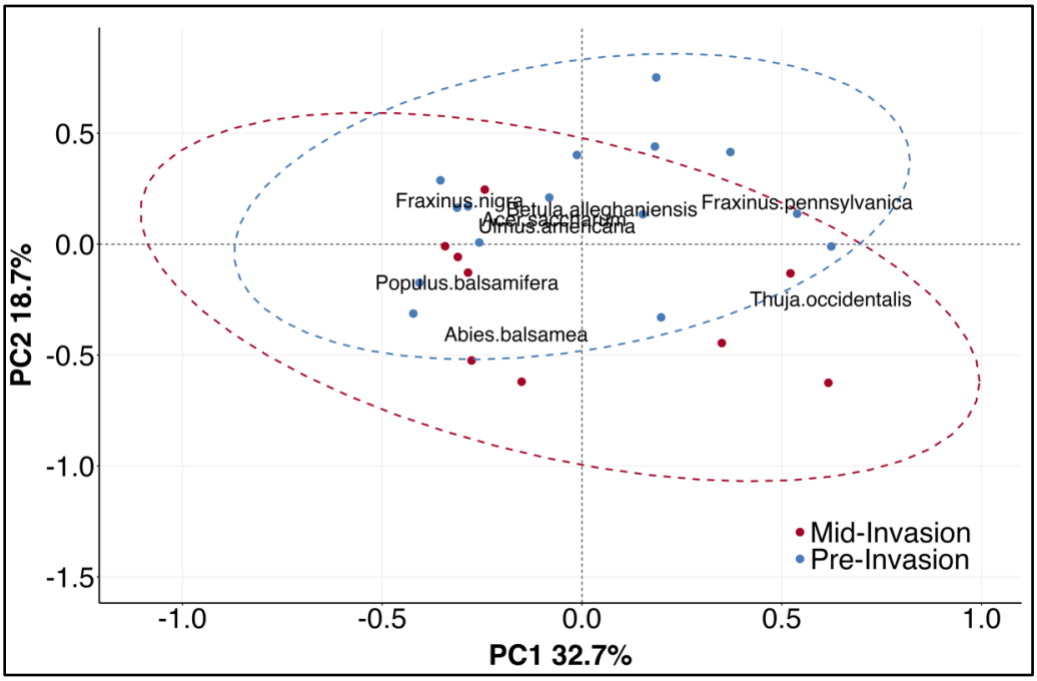

Figure 3.2. Principle components analysis of overstory tree communities in Mid- (red dots) and Pre-Invasion (blue dots) stands in the Upper Peninsula, with the eight most influential species plotted. Ellipses represent 95% confidence intervals for each Invasion Stratum. Total variation explained by two axes: 52.4%.

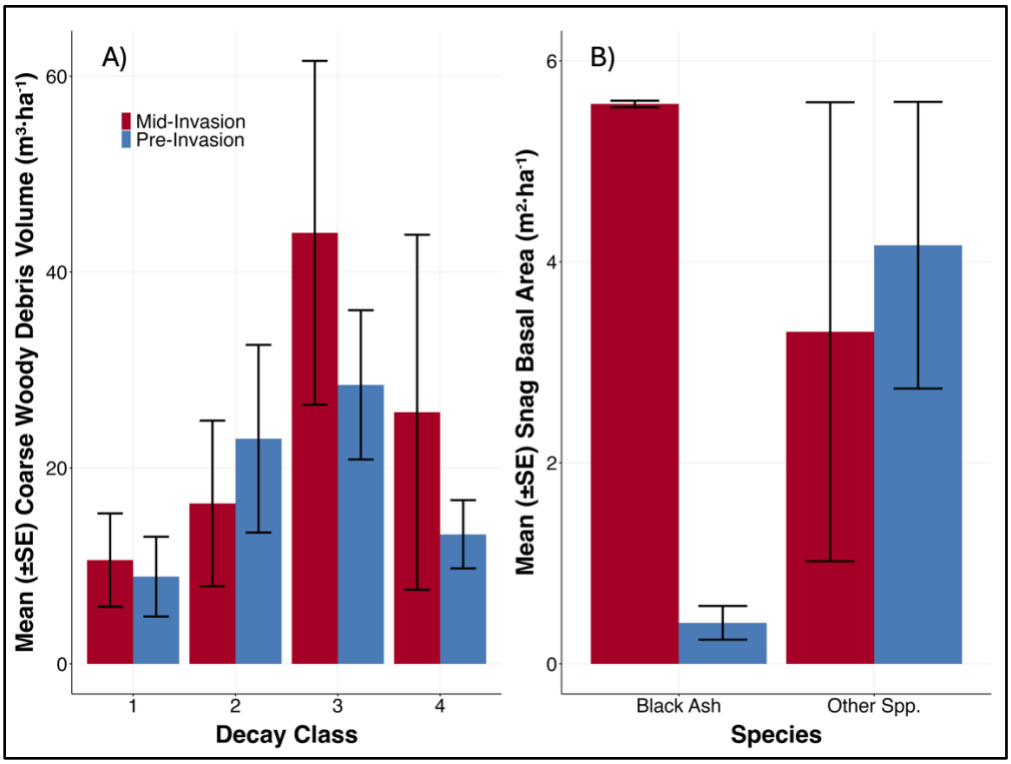

Figure 3.3. (A) Mean (±SE) volume of coarse woody debris by decay class in Mid-Invasion (n = 3) and Pre-Invasion (n = 5) stands. (B) Mean (± SE) basal area of black ash and non-ash snags in Mid- and Pre-Invasion stands.

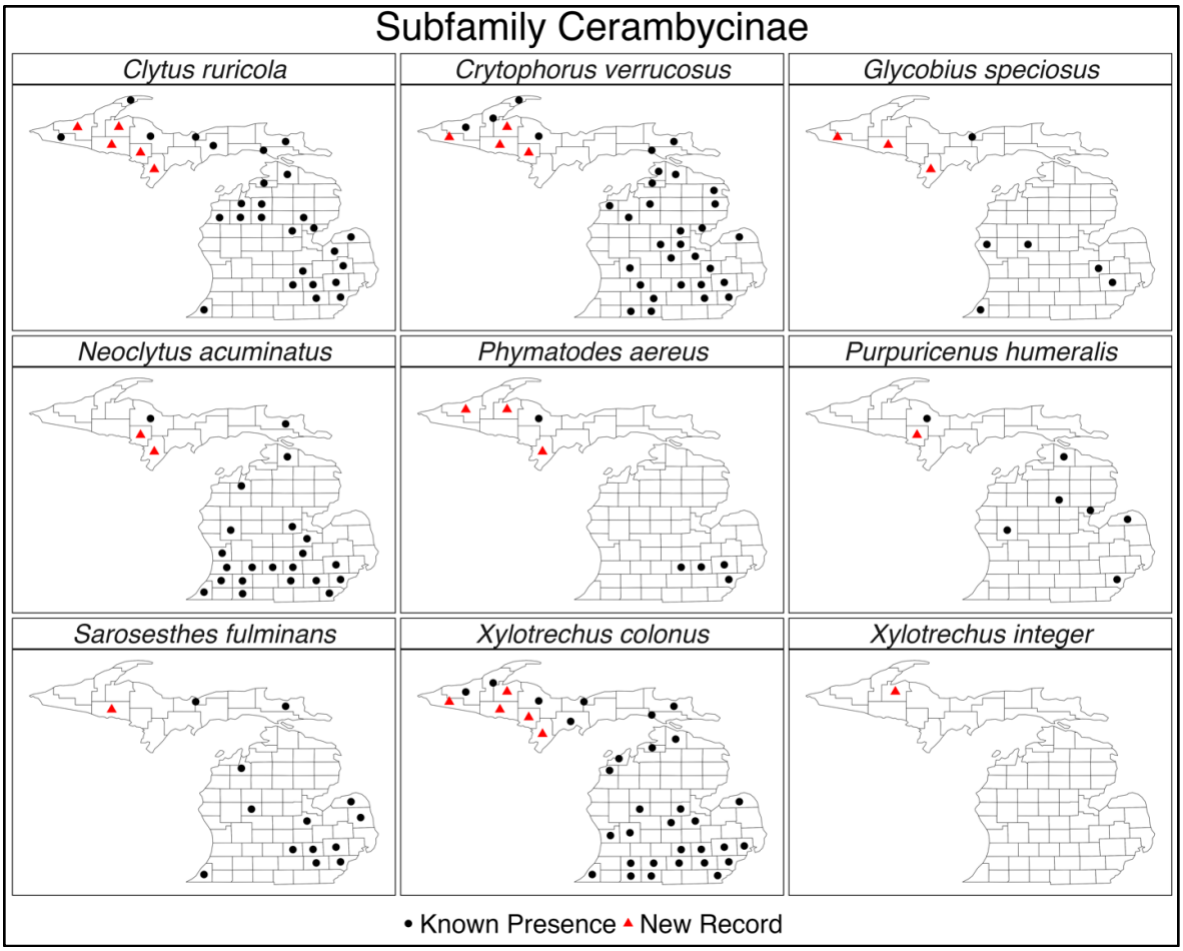

Figure 3.4. Known county records (black dots) and new county records (red triangles) for 9 species in the subfamily Cerambycinae.

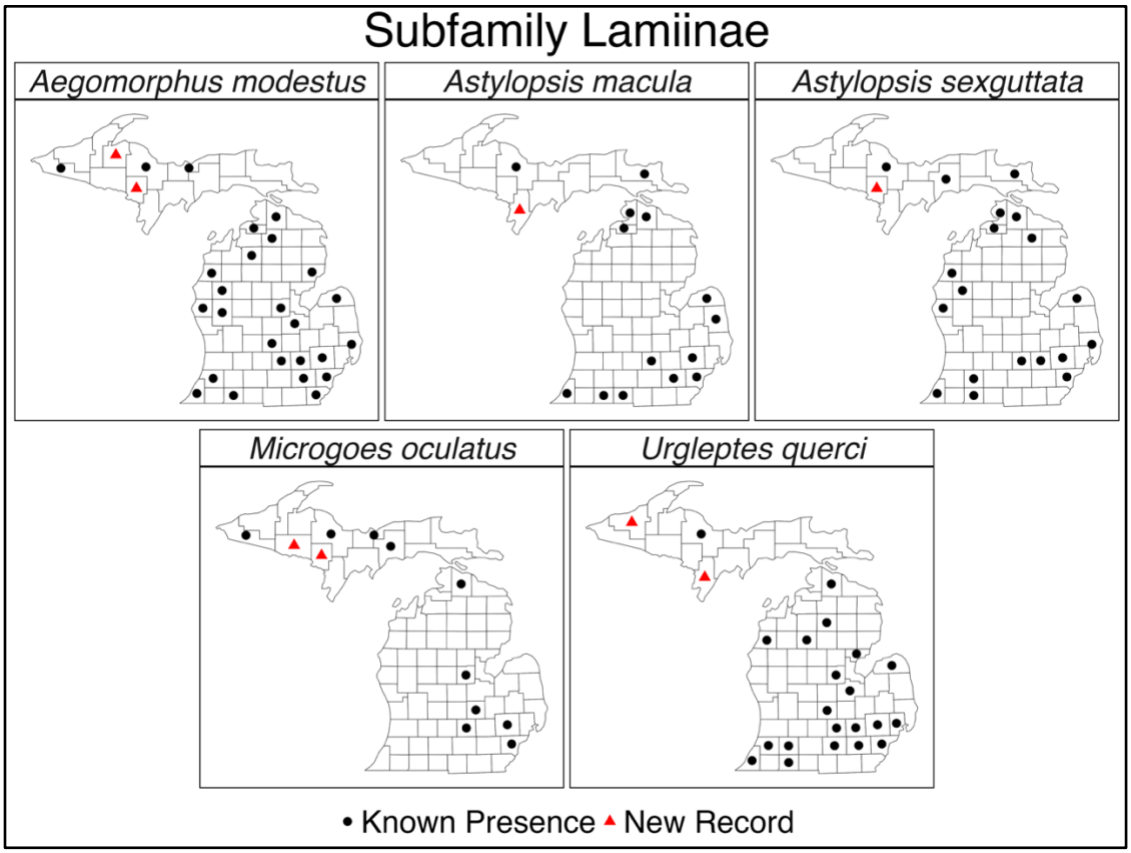

Figure 3.5. Known county records (black dots) and new county records (red triangles) for 5 species in the subfamily Lamiinae.

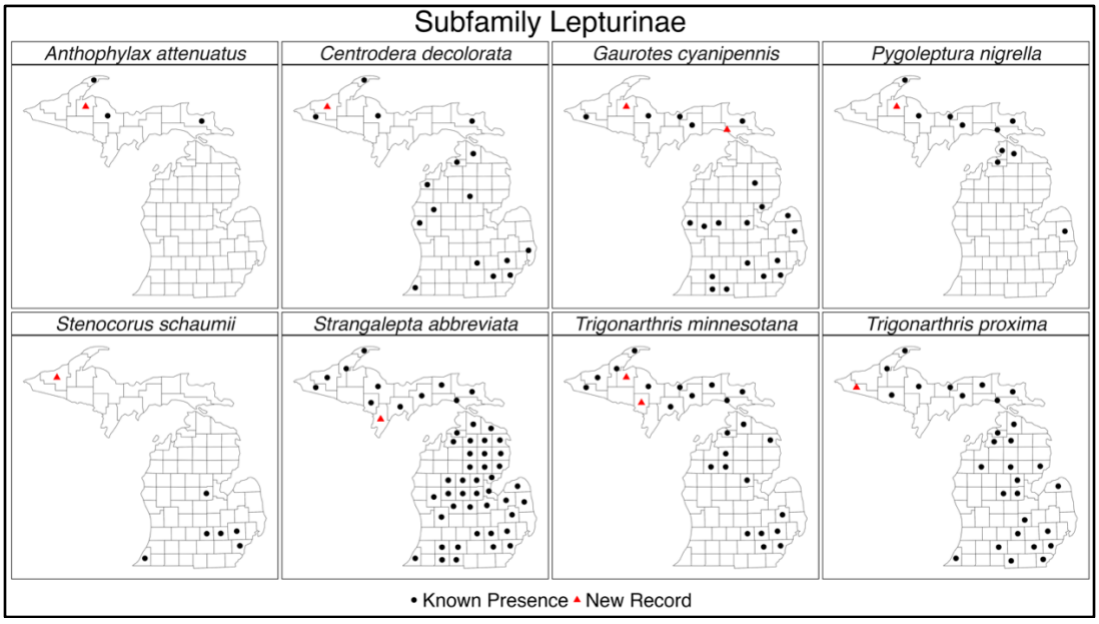

Figure 3.6. Known county records (black dots) and new county records (red triangles) for 8 species in the subfamily Lepturinae.

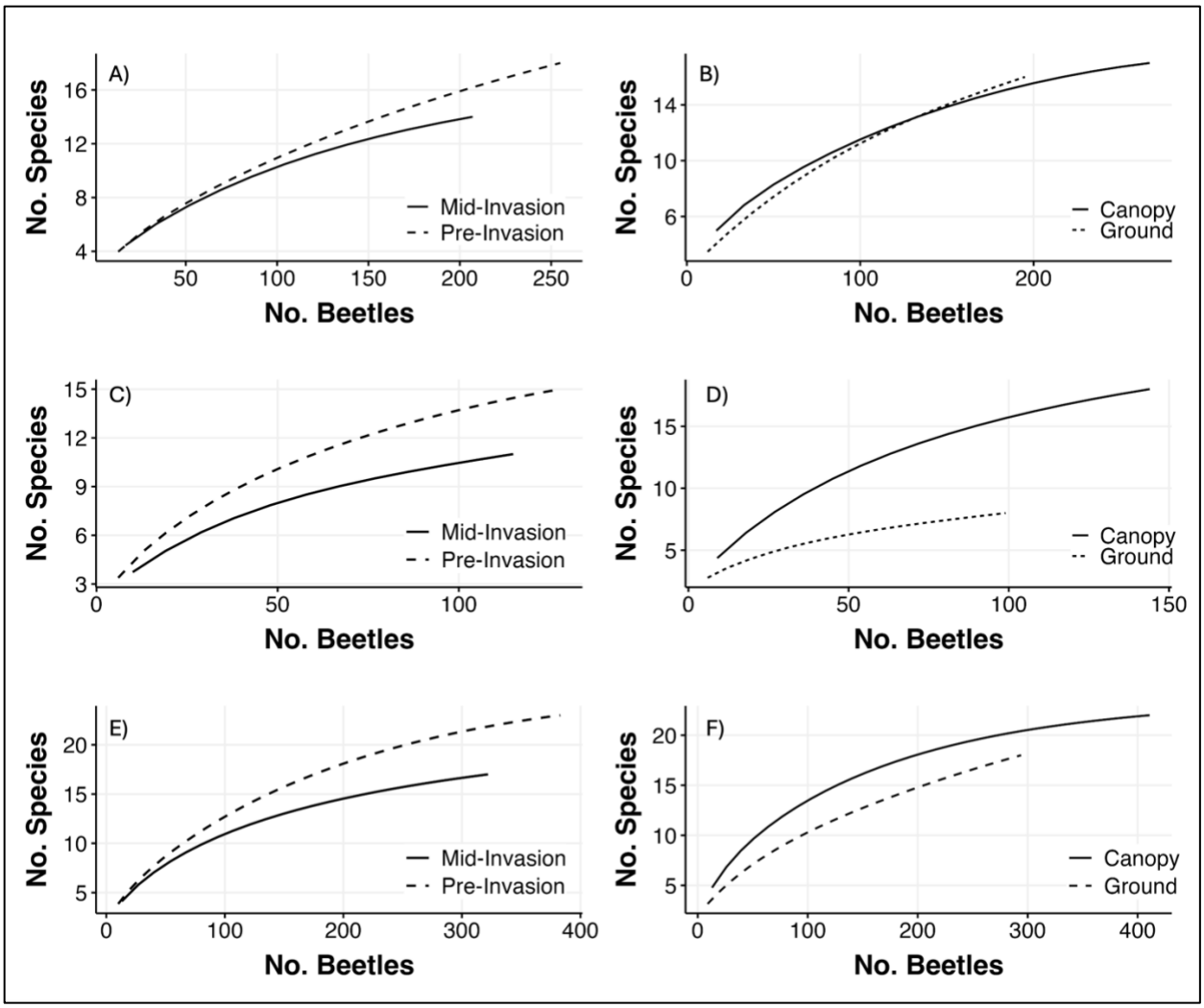

Figure 3.7. Individual based rarefaction curves showing species accumulation of cerambycids by Invasion Strata for 2023 (A), 2024 (C), all years (E), and accumulation of cerambycid species in Canopy and Ground traps for 2023 (B), 2024 (D), and all year (F).

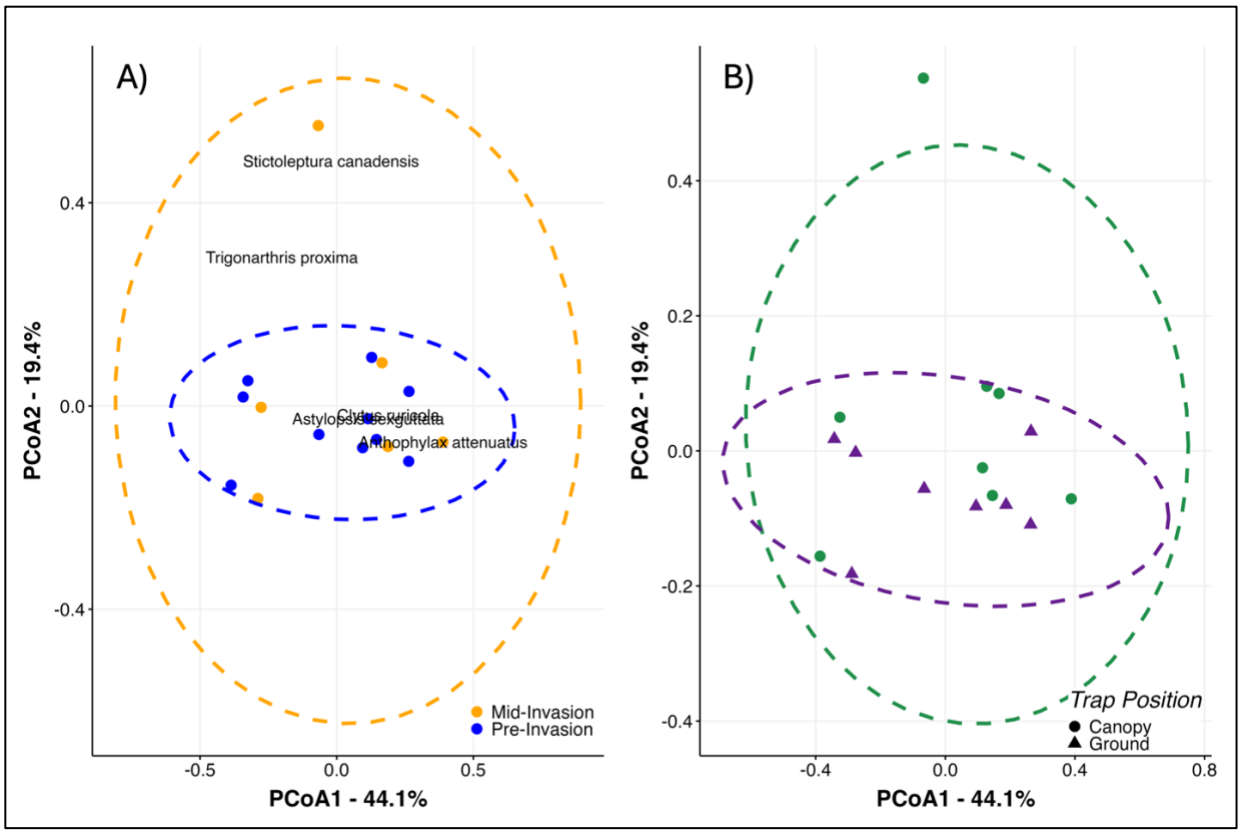

Figure 3.8. Principle coordinate analysis (PCoA) of cerambycid species assemblages grouped by (A) Invasion Strata, and (B) trap position, with ellipses representing 95% confidence intervals. Total variation explained by both axes: 63.5%.

CHAPTER FOUR: LONG-TERM SURVIVAL AND RADIAL GROWTH OF FOUR NORTH AMERICAN AND TWO ASIAN ASH SPECIES IN A COMMON GARDEN EXPOSED TO EMERALD ASH BORER INVASION

Introduction

Emerald ash borer (EAB) (*Agrilus planipennis* Fairmaire) (Coleoptera: Buprestidae) is the most destructive forest insect pest to ever invade North America, killing hundreds of millions of ash trees since its introduction from Asia into Detroit, Michigan in the mid-1990s (Herms and McCullough 2014, Siegert et al. 2014, McCullough 2020). Currently, EAB is known to be established in 37 states and 6 Canadian provinces (EAB.info 2025), reflecting both accidental transport of infested ash material such as nursery trees, logs, and firewood (Cappaert et al. 2005, Siegert et al. 2010, 2014), along with dispersal of adult beetles (Mercader et al. 2011, 2012). Regulatory efforts and public outreach have slowed new EAB introductions, although firewood movement is notoriously difficult to monitor or control (Haack et al. 2010, USDA APHIS 2011, EAB.info 2025). Emerald ash borer has also invaded and killed North American ash trees planted in landscapes in Moscow, Russia and continues to spread, threatening indigenous ash in much of Europe (Baranchikov et al. 2008, Orlova-Bienkowskaja and Volkovitsh 2018, Schrader et al. 2021, Gosner et al. 2023).

All North American ash species encountered by EAB to date appear susceptible to colonization and high rates of ash mortality have been reported in many forests (Tanis and McCullough 2012, Knight et al. 2013, Herms and McCullough 2014, Klooster et al. 2014, 2018, Smith et al. 2015, Engelken et al. 2020, Siegert et al. 2023). In forests with a substantial ash component, effects of EAB-caused mortality can cascade through ecosystems, affecting vegetation, nutrient cycles, hydrology, wildlife, and water quality (Ulyshen et al. 2011, Flower et al. 2013, Knight et al. 2013, Gandhi et al. 2014, Klooster et al 2014, 2018, Smith

et al. 2015, Engelken and McCullough 2020, Engelken et al. 2020, Larson et al. 2023, Krzemien et al. 2024). Estimates of the economic impacts of EAB in North America are staggering, reflecting the abundance of ash trees in landscapes, parks and along boulevards (Poland and McCullough 2006, Kovacs et al. 2010, 2011, 2014, Aukema et al. 2011, McKenney et al. 2012, Hauer and Peterson 2017). Costs of treating or replacing amenity ash trees, which amount to billions of USD annually, are largely borne by municipalities and private landowners (Aukema et al. 2011, Hauer and Peterson 2017, Sadof et al. 2023).

Despite widespread mortality of North American ash species, interspecific variation in EAB host preference and host vulnerability has been previously observed in areas where 2 or more ash species occur (Tanis and McCullough, 2012, 2015, Rebek et al. 2008, Robinett and McCullough 2019, Engelken and McCullough 2020). Black ash (*Fraxinus nigra*), primarily found in forested wetlands in the northeastern and Lake States regions of the US and eastern Canada (Gucker 2005a), appears to be highly vulnerable to EAB (Tanis and McCullough 2015, Engelken and McCullough 2020, Siegert et al. 2023). Green ash (*F. pennsylvanica*), which is broadly distributed across much of North America (Gucker 2005b), is also a vulnerable and preferred EAB host (Engelken and McCullough 2020, Engelken et al. 2020, Siegert et al. 2021). White ash (*F. americana*), another widely distributed species (Griffith 1991), is an intermediate host that has survived EAB invasion in some forests (Robinett and McCullough 2019), while sustaining nearly complete mortality in others (Tanis and McCullough 2012, Knight et al. 2013, Klooster et al. 2014, Smith et al. 2015). Blue ash (*F. quadrangulata*), which extends from southern Michigan and Ontario south to Arkansas, Missouri, and Tennessee (COSEWIC 2014, Peters et al. 2020), appears to be the least preferred ash species encountered by EAB in North America to date (Tanis and McCullough 2012, 2015, Cipollini and Morton 2023).

Asian ash species, which share a co-evolutionary history with EAB, are presumably more resistant to EAB than North American ash species, which have no native congener similar to EAB. In its native range, which encompasses areas of China, the Russian Far East, South Korea, Mongolia, and Japan, EAB functions as a secondary pest, colonizing, and killing severely stressed or dying ash trees, but causing minimal injury to healthy native ash (Liu et al 2003, 2007, Wei et al. 2004, Wang et al. 2010, Duan et al. 2012, Orlova-Bienkowskaja and Volkovitsh 2018). In North America, adult beetles preferentially oviposit on stressed ash trees when available, but can colonize healthy ash as well (McCullough et al. 2009a, 2009b, Siegert et al. 2010, 2014, Tluczek et al. 2011).Both Manchurian ash (*F. mandshurica*) and Chinese ash (*F. chinensis*) are relatively abundant in the native range of EAB in Asia (Wang et al. 2010, Orlova-Bienkowskaja and Volkovitsh 2018). Manchurian ash is predominantly found in southeastern Russia and northern China, while the range of Chinese ash extends from northern to southern China, where it is an important timber species and ornamental tree (Wang et al. 2010). Both species also occur on the Korean Peninsula (Orlova-Bienkowskaja and Volkovitsh 2018).

Specific mechanisms linked to variability in EAB host preference or ash resistance are unknown but likely include combinations of visual cues, host volatiles, and phloem chemistry (Eyles et al. 2007, Bartels et al. 2008, Cipollini et al. 2011, Poland and McCullough 2014, Villari et al. 2016, Kelly et al. 2020). Variation in EAB host preference and vulnerability among ash species native to North America has been previously studied (Anulewicz et al. 2007, Tanis and McCullough 2012, 2015, Rebek et al. 2008, Robinett and McCullough 2019), typically in settings were 2 ash species co-occurred. The extent of variability in EAB host preference among multiple native ash species, including Asian ash species planted in North America, is largely unknown.

Here, we report results from a relatively long-term common garden study that included 4 North American and 2 Asian ash species exposed to local EAB populations. We qualitatively assessed canopy condition and evaluated annual radial growth as trees were colonized, declined, or died. This long-running study provided an opportunity to assess interspecific differences in tree growth and EAB colonization rates, eg host preference of ovipositing adult EAB females, when trees of the same age experienced the same site and weather conditions. We expected both Chinese ash and Manchurian ash would survive longer than North American ash species, given their co-evolutionary history with EAB. Based on previous studies, we further anticipated black ash and green ash would be heavily colonized and rapidly succumb to EAB. The persistence of white ash and blue ash trees in this plantation was of particular interest given that these trees were exposed to high densities of EAB adults emerging annually from the black ash and green ash trees. Moreover, our plantation represented a highly apparent and relatively abundant source of potential host trees for adult EAB beetles emerging from unmanaged ash trees in the vicinity of the study site.

Methods

***Study site*:** We established Plantation A in April 2007 at the Michigan State University Tree Research Center, Ingham Co., Lansing, MI. Four North American ash species and one Asian ash species acquired from J. Frank Schmidt (Boring, OR) and Lawyer Nursery (Plains, MT) were planted at 2.2 × 3.0 m spacing in 30 completely randomized blocks (total of 150 trees; 15 rows, each with ten trees). Species included black ash, blue ash, green ash, white ash, and Chinese ash, all planted as bare root whips (small saplings), 0.8 to 1.2 m tall. Drip irrigation was installed and trees were watered weekly or as needed for 4 yr. Irrigation frequency of the established trees was then reduced to 1 to 2 times per month as needed, until it was discontinued

in 2015. Fertilizer (19-5-10; Harrell's Pro-Blend with Micros, Livonia, MI) was applied around the base of each tree in May 2007 and April 2008 following label rates. Herbaceous vegetation between rows of trees and grass in the surrounding 4 to 6 m wide lanes was mowed weekly or as needed each growing season. Between 2007 and 2010, ice or high winds broke a total of ten ash saplings (< 1.0 cm diam), including 4 blue ash, 1 Chinese ash, and 5 white ash. These were excluded from further sampling or analysis.

As trees in Plantation A became large enough to be colonized by EAB (DBH ≥ 2.5 cm), the trunks and large branches were wrapped with cardboard tree wrap or layers of cotton fabric each spring to protect them from EAB oviposition during the summer, as described in Tanis and McCullough (2015). Wrapping was discontinued and trees were exposed to potential EAB colonization beginning in the spring 2012. Spacing between trees was adequate to minimize potential light competition or other interactions among canopies.

Plantation B, immediately north of Plantation A, was established in April 2010 when 8 to 30 trees representing various ash species native to eastern, western, or southern North America, Europe, or Asia, were acquired as bare root stock (grown from seed) (2.0 to 3.5 cm DBH) (Anulewicz and McCullough 2012). A total of 21 green ash and 15 Manchurian ash were purchased from Bailey's Nurseries (St. Paul, MN) and Poplar Farms Nurseries (Watertman, IL), respectively. Trees were planted in 12 rows with 8 trees per row, at 2.2 × 3.0 m spacing, which minimized potential light competition among trees. Fertilizer was applied as described above in late April 2010 and 2011. Water was applied via drip irrigation weekly for 2 yr, then as needed until spring 2015 when it was discontinued. Trees in Plantation B were wrapped to protect them from EAB until spring 2012, as described above. Numerous trees failed to establish or survive winter temperatures (Anulewicz and McCullough 2012). Original stems of some trees produced

one or more basal sprouts in 2011 or 2012, typically following dieback of the original stem. When multiple sprouts were produced, all but one or occasionally two of the largest sprouts were pruned off in summer 2012 to facilitate the growth of the dominant stem(s).

By 2022, 15 green ash and 15 Manchurian ash in Plantation B were alive. In August 2022, we selected 12 pairs of live green ash and live Manchurian ash that were growing in the same or adjacent rows of the plantation (12 trees per species; 24 trees total). Paired trees were growing adjacent to each other in the same row or in the facing row. The condition of trees was visually evaluated and cores were extracted for radial growth analysis.

Ash Mortality and Condition: In Plantation A, we evaluated trees and measured diameter at breast height (DBH; 1.3 m high) of the main stem in August annually from 2017 to 2022. When live trees had basal sprouts, DBH of the main trunk and up to 2 sprouts (> 2.5 cm) were measured and summed. Trees were recorded as dead when the original stem had no live foliage. Live stump sprouts on dead trees were noted when present but were excluded from analysis. From 2017 to 2021, we tallied current-year holes left by woodpeckers preying on late-stage EAB larvae and small, D-shaped holes left by emerged EAB adults between ground level and a height of 2 m in mid-August. Holes were marked annually with large staples to prevent double-counting EAB exits or woodpecker holes. Counts were standardized by area (m^2) of bark visually examined on each tree. Current-year woodpecks and exit holes could not be accurately counted in 2022 due to extensive bark cracks, splits, and sloughing bark or wound periderm (e.g. callus tissue) on many trees.

In Plantation B, we measured DBH in August 2022 and qualitatively ranked canopy condition of the paired green ash and Manchurian ash. Trees were classed as 1 if the canopy was healthy with few or no woodpecks or epicormic sprouts, 2 if ≤ 49% of the canopy was dead and

at least a few woodpecks or epicormic sprouts were present, 3 if 50% to 89% of the canopy was dead and multiple woodpecks or sprouts were present, or 4 if the tree had at least one live branch but ≥ 90% of canopy was dead. Abundance of woodpecks and epicormic sprouts on the lower 2 m of trees were also ranked (separately) as 0 if none were visible, 1 if up to 3 woodpecks or epicormic sprouts were observed, 2 if 4 to 6 woodpecks or epicormic sprouts were present, or 3 if > 7 woodpecks or epicormic shoots were visible.

Ash Radial Growth: To assess annual radial growth, we collected 2 increment cores offset by 90° at breast height (1.3 m high) from each live tree in Plantation A and from the 24 live trees in Plantation B in August 2022. When trees had multiple stems, primarily the green ash in Plantation B, we cored the largest stem (> 5 cm DBH). Increment cores were mounted on 5.1 mm increment core mounts (Rocky Mountain Tree Ring Research, Fort Collins, CO) and sanded using a progressive grit sequence of P80, P120, P220, and P320 sandpaper. Dead trees in Plantation A were felled in August 2023 and a cross-section was collected from the trunk, 1.3 m aboveground. Cross-sections were sanded using the same grit sequence as above. After sanding, cores and cross-sections were scanned using an Epson Perfection V850 Pro flatbed scanner at a resolution of 2400 digital pixels per inch (Epson America Inc., Long Beach, CA) to facilitate ring width measurement to the nearest 0.001 mm using CooRecorder (Cybis Elektronik &Data AB, Saltsjöbaden, Stockholm Co., Sweden). Samples were visually cross-dated using Microsoft Excel™ (Microsoft Corporation, Redmond, WA) CooRecorder, CDendro (Cybis Elektronik &Data AB, Saltsjöbaden, Stockholm Co., Sweden), and dplR in R (Bunn et al. 2010, R Core Team 2024).

Mean annual increment, ie the width of each annual ring from 2007 to 2021, the last year a complete ring was formed, and total radial growth were calculated for each tree in Plantation A

and averaged by species. For dead green ash and Chinese ash in Plantation A, we calculated the difference in ring widths between the last full measurable ring and the mean width of the 3 preceding years to determine if radial growth gradually declined or dropped abruptly the year preceding mortality. We similarly calculated the mean annual increment and total radial growth from 2011 to 2021 for the live green ash and Manchurian ash trees in Plantation B.

In addition to EAB-related variables, we noted that fall webworm (*Hyphantria cunea* (Drury) (Lepidoptera: Erebidae), a generalist defoliator native to North America, had infested several trees in Plantation B. We therefore recorded the presence of fall webworm larvae and webs as we evaluated trees in Plantation B in August 2022.

***Statistical analysis*:** The mortality of trees in Plantation A was recorded annually by species from 2017 to 2022. Survival analysis for trees in Plantation A was conducted using Cox regression models for the 5 ash species and subsequently for each individual species with the survival package in R (v3.5-5, Therneau and Grambush 2000, v4.3.1, R Core Team 2024). Negative binomial models with repeated measures were used to evaluate differences in mean density of woodpecker holes and EAB adult exit holes across species (fixed effect) and by block (random effect) from 2017 to 2021 using the glmmTMB package in R (Brooks et al. 2017, v4.3.1, R Core Team 2024). When differences were significant, species contrasts were assessed with Tukey tests via the emmeans package in R (Lenth 2023, R Core Team 2024). Differences in mean annual increment from 2007 to 2021 and total radial growth from 2017 to 2021 among ash species in Plantation A were evaluated with 1-way ANOVAs followed by Tukey's HSD multiple comparison tests if ANOVA results were significant.

To assess potential differences between green ash and Manchurian ash trees in Plantation B, we used Mann–Whitney *U* tests (v4.3.1 R Core Team 2024) to compare qualitative estimates

of canopy condition, along with ranked abundance of woodpeck holes and epicormic sprouts. Differences in mean annual increment between green ash and Manchurian ash from 2010 to 2021 were assessed using a 1-way ANOVA and Tukey's HSD post-hoc test if ANOVA results were significant (v0.4.6, Hartig 2022) (v4.3.1, R Core Team 2024).

Results

Plantation A

Ash Mortality and Survivorship: Mortality caused by EAB varied substantially among ash species over the course of the study (Fig. 4.1). None of the blue ash trees were killed by EAB in any year (Fig. 4.1), although 4 saplings were broken near the ground during storms or because of ice accumulation by 2010. In August 2022, all 26 of the remaining blue ash were alive and appeared healthy. In contrast, every black ash tree had been killed by EAB by fall 2013, following 2 seasons of exposure to the local EAB population. Both blue ash and black ash, therefore, were excluded from the analysis of survivorship between 2017 and 2022. Mortality caused by EAB between 2017 and 2022 varied for Chinese ash, green ash, and white ash (Fig. 4.1). Chinese ash had the lowest survival after 5 years (10%; CI = 3.4 to 29.3%), followed by green ash (32.1%; CI = 18.8 to 55.1%), and white ash (79%; CI = 64.5 to 97.2%) (Fig. 4.2). Throughout the study period, the probability of a green ash dying was 45% lower than Chinese ash (HR = 0.55; CI = 0.30 to 0.99; $P = 0.045$), while the chance of a white ash dying was 89% lower than Chinese ash (HR = 0.11; CI = 0.04 to 0.30; $P < 0.001$) (Fig. 4.2).

Canopy Condition and Signs of EAB Infestation: When we evaluated Plantation A trees in August 2022, we noted a slight amount of canopy thinning (15%) on 2 blue ash trees, while 3 other blue ash had 10% to 15% dieback. In contrast, 3 of the 12 live green ash trees were in poor condition with at least 60% canopy dieback. Of the 4 Chinese ash alive in 2022, 3 had declining

canopies, with 20 to 55% transparency or dieback. Six of the 22 live white ash were severely declining with ≥ 65% canopy dieback. On several white ash, we noted wound periderm, new sapwood, and bark growing over old EAB larval galleries.

Holes left by woodpeckers preying on late instar EAB larvae were observed on a few trees as early as August 2012 and by 2021, trees of all species in Plantation A had at least one distinct woodpecker hole (Fig. 4.3A,B). Between 2017 and 2021, average density of current-year woodpecker holes differed among ash species (excluding black ash) ($\chi^2 = 51.84$; d.f. = 3; $P < 0.0001$) and was lower on blue ash than on the other 3 species (Fig. 4.3A). White ash had fewer woodpecks per m^2 than Chinese ash, while woodpeck density on green ash was intermediate (Fig. 4.3A). Density of new woodpecks tallied annually increased substantially between 2017 and 2018, particularly on Chinese ash and green ash, before declining in 2019 (Fig. 4.3B).

Between 2017 and 2021, exit holes left by emerged EAB adults were tallied on at least one individual of all ash species (Fig. 4.3C,D). Exit hole density from 2017 to 2022 differed among years ($\chi^2 = 56.02$; d.f. = 1; $P < 0.001$) and among the 4 ash species ($\chi^2 = 60.42$; d.f. = 3; $P < 0.001$). On average, the density of current-year exit holes from 2017 to 2021 was lower on blue ash than on the other 3 species, while white ash had fewer exits than Chinese and green ash, which did not differ from each other (Fig. 4.3C). Density of EAB adult exit holes increased markedly in 2020 and 2021, particularly on Chinese and green ash (Fig. 4.3D), many of which were dead in 2022.

Radial Growth: Radial growth rates of trees in Plantation A generally increased as the young trees became established within 2 to 3 yr of planting. Total radial growth from 2007 to 2021 differed among ash species ($F = 14.69$; d.f. = 3,70; $P < 0.001$) and was highest for Chinese ash and lowest for blue ash (Table 4.1). Annual growth increment, ie ring width, from 2007 to

2021 differed among ash species (χ^2 = 15.95; d.f. = 3,96; P < 0.001) (Fig. 4A). Annual growth averaged across the 14-yr period (Fig. 4.4A) was lower for blue ash than for other species, while Chinese ash grew faster than white ash, and green ash growth was intermediate. Annual radial growth of Chinese ash increased substantially from 2007 to 2013, peaked in 2015, then declined through 2021, a period when many trees died (Fig. 4.4B). In contrast, annual radial growth of green ash, white ash, and blue ash growth remained relatively consistent over time (Fig. 4.4B). During the last full year of growth preceding mortality, width of growth rings in Chinese ash and green ash was lower than the average radial growth of the 3 preceding years, declining by 21.6 ± 6.4% and 14.6 ± 7.1%, respectively.

Plantation B

Every green ash tree in Plantation B had been colonized by EAB and most had multiple signs of infestation, while Manchurian ash trees, intermixed with the green ash, were largely ignored by EAB. On average, DBH of the live green ash (16.1 ± 1.27 cm) in 2022 was higher than that of the paired Manchurian ash trees (12.2 ± 0.93 cm) (F = 6.268; d.f. = 1,22; P = 0.02). Average annual growth increment (ring width) from 2011 to 2021 was 63% higher for green ash than Manchurian ash (F = 74.01; d.f. = 1,294; P < 0.001) (Fig. 4.5).

The ranked abundance of woodpecker holes observed on tree trunks was higher for green ash than for Manchurian ash (W = 137.5; P < 0.001). Nearly all green ash (91%) had woodpecker holes and 58% of those trees were ranked as 3, indicating more than 6 woodpecks were visible (Fig. 4.6). In contrast, 91% of the Manchurian ash had no visible woodpecker holes while 2 trees were ranked as either 1 or 2 (up to 6 woodpecker holes) (Fig. 4.6). Presence and abundance of epicormic sprouts on green ash and Manchurian ash followed a similar pattern. Every green ash had at least one epicormic sprout and 67% of the green ash trees were assigned a rank of 3,

indicating > 6 epicormic sprouts were visible. Epicormic sprouts were less common on Manchurian ash than on green ash trees ($W = 139.5$; $P < 0.001$). Six Manchurian ash trees (25%) were ranked as 1 (1 to 3 epicormic shoots) but no sprouts were observed on 75% of the Manchurian ash (Fig. 4.6).

Fall Webworm Presence: Seven of the 12 Manchurian ash trees we evaluated in Plantation B in August 2022 were infested by fall webworm. Despite their close proximity to infested Manchurian ash, none of the live green ash examined in Plantation B had any evidence of fall webworm. Additionally, none of the ash trees in Plantation A were infested by fall webworm.

Discussion

Common garden studies with multiple tree species exposed to the same site and environmental conditions are valuable for evaluating interspecific differences in growth, survival, and vulnerability to insect pests, including EAB. Previous common garden trials to assess EAB host preference or suitability of North American ash species have provided useful information, although possible complications related to saplings originally grafted onto green ash root stock or trees stressed by transplant shock or drought have been noted (Rebek et al. 2008, Rigsby et al. 2014, Subburayalu and Sydnor 2018). Evaluations of EAB adult or larval feeding on detached leaves or in cut sections of trunks or branches circumvent any inducible responses of live trees, while artificial inoculations of EAB eggs or larvae into live trees fail to account for ovipositional preferences of female beetles or suitability of host trees for neonate or early instar larvae (Anulewicz et al. 2007, 2008, Pureswaran and Poland 2009, Schowalter and Ring 2017, Subburayalu and Sydnor 2018, Kelly et al. 2020, Gosner et al. 2023). Ash species evaluated in our plantations were grown from seed and irrigated until well-established, negating

any potential influence of root stock and minimizing stress that could affect EAB host selection. Because the ash species were planted in complete randomized blocks, female beetles selected and oviposited on their preferred hosts each year, while densities of holes left by woodpeckers preying on late-stage larvae (Lindell et al. 2008) and adult EAB exit holes served as proxies for larval presence and successful development (McCullough 2020).

Black ash was clearly the most preferred and vulnerable EAB host of all the species tested in our study, a result consistent with the nearly complete mortality of overstory black ash reported from field studies (Klooster et al. 2014, Engelken and McCullough 2020, Siegert et al. 2021). Every black ash tree in our plantation was heavily colonized within 1 to 2 yr of exposure to EAB. On a few occasions, we observed adult EAB beetles fly around other ash species in Plantation A before landing on a black ash tree. In a previous study with 5 ash species, densities of larval galleries on debarked black ash trees exposed to EAB for 2 yr were approximately 3-fold higher than what could be supported by the available phloem, leading to mortality of more than 90% of the larvae due to intraspecific competition for phloem (Tanis and McCullough 2015).

The strong attraction of adult EAB beetles, particularly ovipositing females, to black ash likely involves multiple factors including host volatiles, visual cues, and physical characteristics such as flaky bark (Rodriguez-Saona et al. 2006, Bartels et al. 2008, deGroot et al. 2008, Crook and Mastro 2010, Grant et al. 2010, Crook et al. 2012, Poland and McCullough 2014). Because the serpentine EAB larval galleries typically extend further horizontally on black ash, each larva damages more area, and fewer EAB larvae are required to kill black ash than other species (McCullough 2020, Siegert et al. 2023). This feeding pattern may at least partially reflect mechanical aspects of xylem tissue that also contribute to the suitability of black ash splints for

indigenous basketry (Siegert et al. 2023). When saplings of 26 *Fraxinus* species were inoculated with EAB eggs in a greenhouse, black ash trees exhibited no defensive response and nearly all larvae on black ash successfully developed to the fourth instar (Kelly et al. 2020). Based on the ongoing spread of EAB, the preference of EAB adults for black ash, and the particularly high vulnerability of this native species, recent projections suggest black ash will be functionally extirpated across its native range by mid-century (Siegert et al. 2023). Loss of this unique species will not only cascade through ecosystems but will affect indigenous people from dozens of Native American and First Nation tribes who have harvested black ash for basketry and ceremonial purposes for generations (McCullough 2013, COSEWIC 2018, Bolen 2020, Siegert et al. 2023).

In contrast to black ash, the continuing persistence of healthy blue ash in Plantation A is both remarkable and consistent with other field or common garden settings (Tanis and McCullough 2012, 2015, Spei and Kashian 2017, Cippolini and Morton 2023). During a decade or more of exceptionally high EAB densities in southeast Michigan, every white ash tree in 2 woodlots with a mix of hardwood species was killed by EAB but more than 60% of blue ash, in all diameter classes, remained healthy (Tanis and McCullough 2012). Similarly, 68 to 93% of blue ash were alive and appeared healthy in 2015 in 6 other post-invasion sites in southeast Michigan compared with 17 to 56% survival of white ash (Spei and Kashian 2017). In 2 Ohio stands surveyed in 2021, 90% of blue ash trees appeared healthy with no evidence of EAB infestation (Cipollini and Morton 2023) despite at least 12 yr of EAB presence in the area (USDA APHIS 2024, EAB.info 2025). In Missouri forests, canopy dieback caused by EAB infestation has been observed on mature blue ash on sites with thin, poor soils that frequently experience droughty conditions, while in areas with better soils, large vigorous blue ash are

growing near white ash killed by EAB several years ago (J. Guldin, USDA Forest Service, pers. comm.).

Phylogenetically, blue ash occurs in section Dipetalae with only two other *Fraxinus* species, *F. anomala* and *F. dipetala*, both native to the southwestern US and Mexico (Hisinger et al. 2013, Wallander 2008). The relatively close phylogenetic relationship, particularly between blue ash and *F. anomala* (single-leaf ash) which are geographically discrete, indicates these species diverged as they adapted to different environments (Hisinger et al. 2013). Unique traits of blue ash include monoecious reproduction as well as morphological or physiological characteristics. For example, fertilization increased nitrogen concentration and chlorophyl index in young blue ash but not in white ash or Manchurian ash, while application of paclobutrazol, a gibberellin inhibitor, reduced radial growth and internode distance on blue ash and Manchurian ash but not white ash (Tanis et al. 2015). Autofluorescence indicative of phenolics, which can act as defensive or anti-feedant compounds, signal molecules, or precursors to defensive compounds, was detected with fluorescent confocal laser scanning microscopy in phloem samples from blue ash and Manchurian ash trees, but not green ash (Tanis 2013). A continuous layer of sclerenchymatous cells in phloem, which could presumably affect feeding EAB larvae, was observed in blue ash and Manchurian ash, but these cells were sporadic and discontinuous in green ash (Tanis 2013). In laboratory or greenhouse studies, EAB larvae inoculated into saplings or cut sections of blue ash had lower survival or slower development compared with other ash species (Peterson et al. 2015, Olsen and Rieske 2019, Kelly et al. 2020).

Although blue ash has been less commonly used in landscapes compared to green ash or white ash (Poland and McCullough 2006), it is an attractive tree with a straight upright form that requires little pruning and foliage that turns a vibrant yellow in autumn. Annual radial growth of

blue ash was consistently lower than the other ash species in our plantation, but in urban or residential areas with limited space, this may be a positive attribute. Given the persistence of healthy blue ash in areas initially invaded by EAB 15 to 20 yr ago, this native species warrants consideration as a viable tree for urban forests and perhaps for restoration efforts in post-invasion sites.

Green ash and white ash are native to forests across much of the eastern and central regions of the US and cultivars of both species have long been popular landscape trees within and beyond their native range (Poland and McCullough 2006, Klooster et al. 2018, Hudgins et al. 2021). Phylogenetically, both green and white ash occur in section *Melioides* with at least 8 other species native to the US, Canada or Mexico (Hisinger et al. 2013, Wallander 2008). Although millions of green ash and white ash have been killed in North America by EAB (eg Knight et al. 2013, Herms and McCullough 2014, Klooster et al. 2014, Smith et al. 2015, Cipollini and Morton 2023), when healthy trees of both species co-occur, green ash is consistently more highly preferred and colonized earlier than white ash (Anulewicz et al. 2007, Limback 2010, Tanis and McCullough 2015). We found the same pattern in Plantation A; by 2022, EAB had killed more than 60% of the green ash but only 3 white ash trees. The density of EAB exit holes on white ash was less than half that recorded on green ash or Chinese ash in most years and most (63%) white ash had less than 30% canopy dieback in 2022. When Robinett and McCullough (2019) evaluated more than 800 white ash trees, ranging from 10 to 44 cm DBH, in 28 stands across southeast and central Michigan in 2015 (> 12 yr post-EAB invasion), 66% of the white ash basal area was alive and 83% of the live trees had healthy canopies while less than 10% of the green ash in adjacent or nearby stands remained alive. They also noted that white ash often produced wound periderm around old EAB larval galleries, then laid down new sapwood and

bark, effectively reestablishing phellogen and cambial integrity over the injury. We observed this response, which may contribute to the persistence of colonized trees, on most white ash trees in Plantation A, but it was rare on green ash or Chinese ash trees. Kelly et al. (2020) reported minimal host defense by white ash saplings inoculated with EAB eggs, suggesting the ability to effectively heal over EAB larval galleries may develop as trees grow and mature. Despite the resilience and ability to recover from at least some level of injury caused by EAB larval feeding, long-term survival of white ash in Plantation A is hard to predict. A high proportion of the EAB adults emerging from trees within or near our plantations may be attracted to these white ash especially as those trees are increasingly stressed by larval galleries. Moreover, given the high mortality of more preferred hosts, EAB females may have little choice but to oviposit on the white ash trees.

Green ash in Plantation A lived substantially longer than black ash, indicative of differences in EAB host preference and vulnerability between the two species. Green ash trees colonized by EAB in our plantations often produced epicormic shoots and basal sprouts, a trait also commonly observed in forested settings (Kashian 2016, Engelken and McCullough 2020, Engelken et al. 2020, Siegert et al. 2021). Kashian (2016) attributed green ash persistence in post-invasion sites in southeast Michigan to the growth of basal sprouts, along with seed production by young trees. In other post-invasion green ash stands in Michigan, however, lateral ingrowth by non-ash overstory trees took over canopy gaps, reducing light available to support the growth of young ash saplings or sprouts into the overstory (Burr and McCullough 2014). We originally hypothesized that the 2 ash species native to Asia, Chinese ash and Manchurian ash, would largely escape high rates of EAB colonization and mortality, given the co-evolutionary history shared by these species and EAB (Liu et al. 2003, 2007, Wei et al.

2004, Herms and McCullough 2014, Orlova-Bienkowskaja and Volkovitsh 2018, McCullough 2020). Reports from China have indicated EAB-caused mortality of both Manchurian and Chinese ash is sporadic and associated with drought stress, poor growing conditions or occurred in plantations with a mix of Asian and North American ash species (Liu et al. 2003, Wei et al. 2004, Wang et al. 2010, Dang et al. 2022). Inoculating small saplings in a greenhouse with EAB eggs resulted in strong defensive responses by both Manchurian ash and Chinese ash and no larvae on either species survived to the fourth instar (Kelly et al. 2020).

Manchurian ash, classed in the *Fraxinus* section which includes the European species *F. excelsior* and *F. angustifolia*, as well as North American black ash (Hisinger et al. 2013, Wallander 2008), overlaps the native range of EAB in northeast China and the Russian Far East (Hisinger et al. 2013). In previous field trials with young ash species, EAB larval survival, development and adult emergence were consistently lower on Manchurian ash than on North American species (Rebek et al. 2008, Tanis and McCullough 2015, Showalter et al. 2018) and in bioassays with detached foliage, adult beetles did poorly when provided with leaves from Manchurian ash (Miller and McMahan 2022). Low survival of early instar EAB larvae on Manchurian ash has been attributed to various phloem traits, including oxidative stress and sclerenchymatous cells, along with phenolics or other metabolites in phloem (Tanis 2013, Rigsby et al. 2014, Villari et al. 2016, Showalter et al. 2018, Qu et al. 2021).

Manchurian ash trees growing in Plantation B remained vigorous and had minimal evidence of EAB colonization, consistent with our hypothesis. Beetles that emerged from highly preferred black ash and green ash trees growing in both Plantation B and Planation A would have had ample opportunity to colonize the Manchurian ash between 2010 and 2022. While we cannot

determine whether female beetles ignored or were repelled by the Manchurian ash, there were few or no EAB galleries, EAB exits or epicormic sprouts on any of the trees we examined.

Given the close phylogenetic relationship between Manchurian ash and black ash in section *Fraxinus* (Hisinger et al. 2013, Wallander 2008), the stark contrast in EAB host preference and suitability of black ash seems counterintuitive. Paleogeographical reconstruction has indicated black ash likely originated in Asia but eventually emerged at the end of the upper Miocene as boreotropical forests in the Northern Hemisphere contracted late in the Oligocene era (Yihong 1995, Wen 1999, Donoghue and Smith 2004, Hisinger et al. 2013). In a previous common garden study that included the horticultural cultivar Northern Treasure, a hybrid of Manchurian ash and black ash grafted onto green ash root stock, Rebek et al. (2008) found the hybrid was highly vulnerable to EAB, indicating the cultivar lacked constitutive resistance mechanisms of Manchurian ash.

In contrast to the EAB resistance demonstrated by Manchurian ash, this non-native species was attractive to fall webworm, a polyphagous defoliator native to North America. During our evaluations in August 2022, late instar fall webworm larvae were feeding on many of the Manchurian ash trees in Plantation B but we saw no evidence of this defoliator on adjacent green ash or any of the other North American ash trees. Fall webworm can feed on more than 600 species, including many hardwood trees (Nie et al. 2023). In the Great Lakes region of the US, the single generation of fall webworm that feeds in mid to late summer rarely affects tree health, although the large leaf-enclosing webs are unsightly on landscape or roadside trees (Schowalter and Ring 2017). Fall webworm, however, is an important invasive pest that continues to expand its range in many regions of Europe, Asia, and North Africa (Nie et al. 2023). While Manchurian ash was more attractive to fall webworm than native ash species, there

are few insect pests native to eastern North America that would pose a serious risk to ash trees, presumably including Manchurian ash (Drooz 1985, Ives and Wong 1988, Johnson and Lyon 1988). Given the attractive form, climate hardiness, and consistent resistance to EAB displayed by Manchurian ash in virtually all North American trials, this species represents a viable option for landscapes or perhaps reforestation in North America.

In contrast to Manchurian ash, Chinese ash trees in Plantation A were not resistant to EAB. By 2022, the 4 Chinese ash trees that remained alive were heavily colonized, severely declining, and appeared likely to succumb to EAB within 1 to 2 yr. Densities of woodpecks and EAB adult exits, indicative of larval presence and successful development, respectively, were similar on Chinese ash and green ash, indicating female EAB beetles preferentially oviposited on these two species, while white ash was less preferred and blue ash was rarely colonized.

Chinese ash is in the *Ornus* section, dominated by other species native to Asia and despite some geographic overlap, is phylogenetically distinct from Manchurian ash (Hisinger et al. 2013, Wallander 2008). Taxonomic complexity of the *Ornus* section, which includes both *F. chinensis* along with Korean ash (*Fraxinus chinensis* subsp. *rhynchophylla* (Hance) A.E. Murray First published in Kalmia 13: 6 (1983)) (Kew Royal Botanical Gardens 2024), was previously noted, including observations of diploid and hexaploid populations within *F. chinensis* (Kelly et al. 2020). Studies in China and Far Eastern Russia indicate *F. chinensis* var. *rhynchopyhlla* is highly resistant to EAB (Zhao et al. 2005, Duan et al. 2012, Zong et al. 2014) and in a comparison of metabolites and genes, Qu et al. (2021) identified unique defensive compounds in *F. chinensis* var. *rhynchophylla*.

It is not clear why Chinese ash trees in our plantation were so attractive and vulnerable to EAB. All the trees were planted as bare root whips, negating potential root stock effects, and like

other trees in Plantation A, irrigated until well-established. There was no evidence of dieback caused by cold winter temperatures or signs that other environmental stress affected the trees. Foliage, bark, and twig characteristics were consistent with descriptions and photos of Chinese ash in its native range and we have no reason to believe this was a different species. Chinese ash trees in Plantation A thrived for at least ten years with annual radial growth rates that were consistently higher than those of green ash or white ash until around 2018, when we suspect increasing EAB larval densities and diminished phloem area caused growth to drop. Whether compounds associated with EAB resistance in *F. chinensis* var. *rhynchophylla* are present in similar levels or ratios in *F. chinensis* or if high growth rates of the trees in Plantation A reduced resource allocation to defensive responses is unknown. Further research to assess interactions of EAB and Chinese ash in North America seems warranted, especially given the expanding interest in Asian ash species for restoration or as landscape and amenity trees in North America or Europe (Lévesque et al. 2023, Roloff et al. 2018).

Tables

Table 4.1. Mean (±SE), minimum and maximum annual increment (mm) and total radial growth (mm) of trees in Plantation A from 2011 to 2021, averaged by species. Thirty trees per species were originally planted in 2007 but four blue ash, one Chinese ash and five white ash saplings that were broken by wind or between 2007 and 2010 were excluded from analysis.

Ash species	Annual (±SE) increment (mm)			Total Radial Growth (mm)
	Mean	Minimum	Maximum	
Blue	2.65 (0.18)	0.89 (0.10)	4.43 (0.25)	13.0 (1.13)
Chinese	4.77 (0.30	1.28 (0.11)	8.21 (0.63)	27.1 (2.68)
Green	4.18 (0.20)	1.57 (0.21)	6.58 (0.34)	21.61 (1.42)
White	3.65 (0.18)	1.18 (0.15)	5.59 (0.30)	20.23 (1.20)

Figures

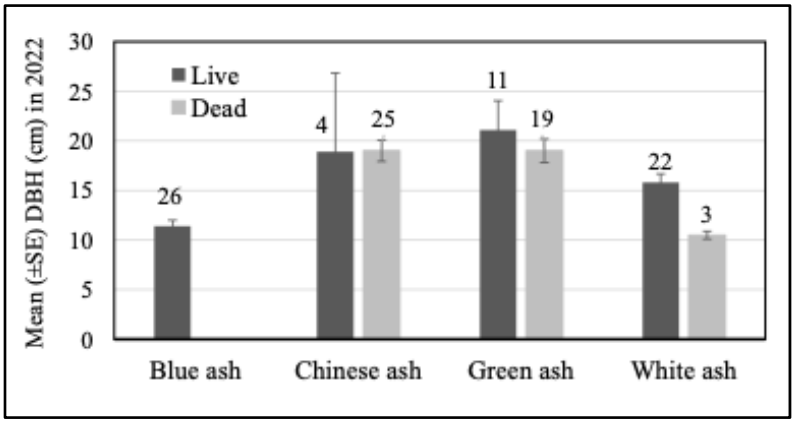

Figure 4.1. Mean (±SE) DBH (cm) and numbers (above bars) of live and dead ash trees killed by emerald ash borer by species in Plantation A recorded in August 2022. No black ash trees were alive in 2022. Of the 30 trees per species planted in 2007, four blue ash, one Chinese ash and five white ash were broken by wind or ice by 2010 and were excluded from analyses.

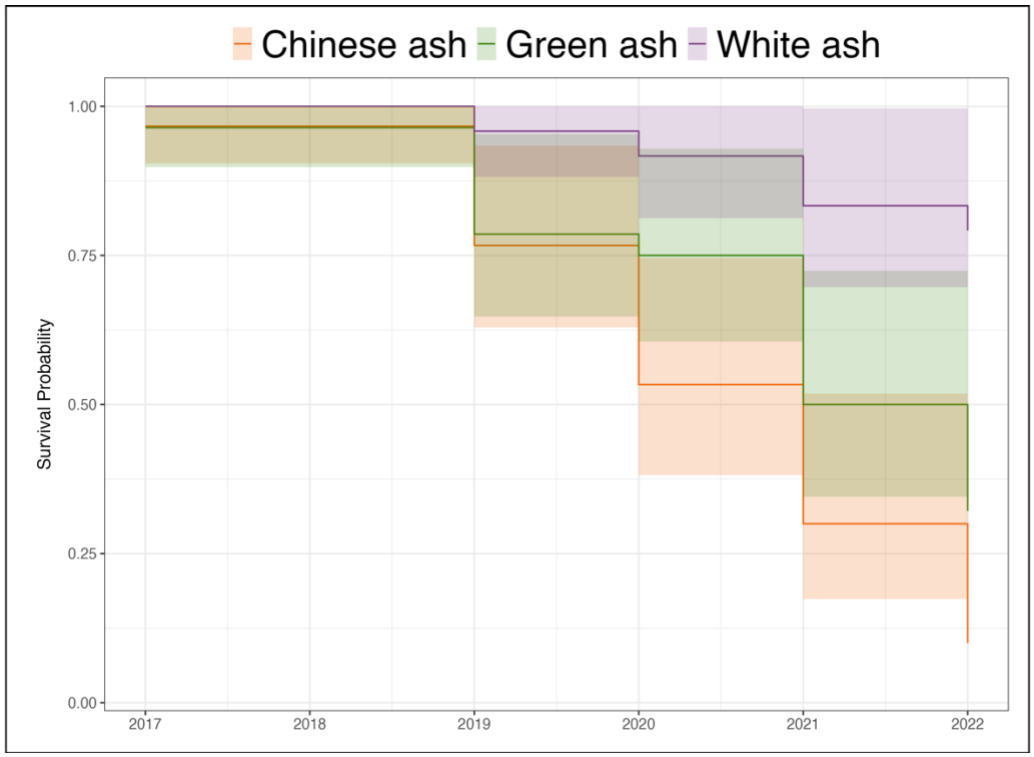

Figure 4.2. Survivorship curves from 2017 to 2022 for Chinese ash, green ash, and white ash in Plantation A. Shading represents the 95% CI. Black ash and blue ash were excluded; all black ash were dead by 2013 while no blue ash died during this period. (N=25 to 30 trees per species).

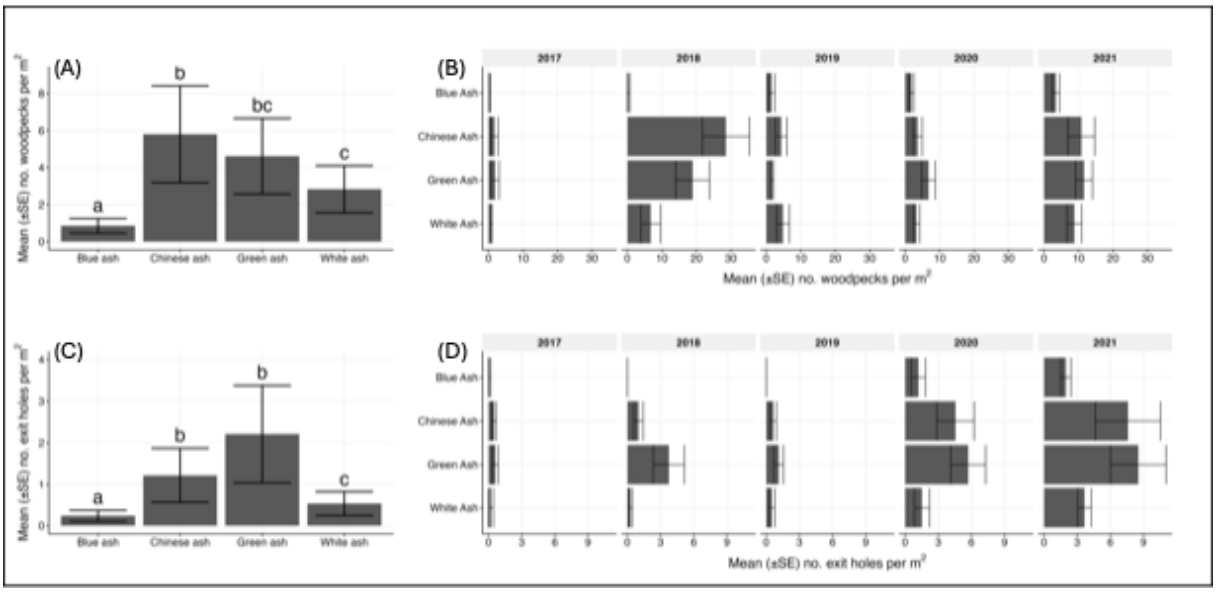

Figure 4.3. (A) Mean (±SE) density of woodpecks from 2017-2022 averaged by species and (B) mean (±SE) woodpeck density recorded annually from 2017 to 2021 for four ash species in Plantation A. (C) Mean (±SE) density of exit holes left by emerged emerald ash borer adults from 2017-2022 averaged by species and (D) mean (±SE) density of exit holes recorded annually from 2017 to 2021 for ash species in Plantation A. Letters above bars in (A) and (C) indicate significant differences among species ($P < 0.05$). (N=25 to 30 trees per species).

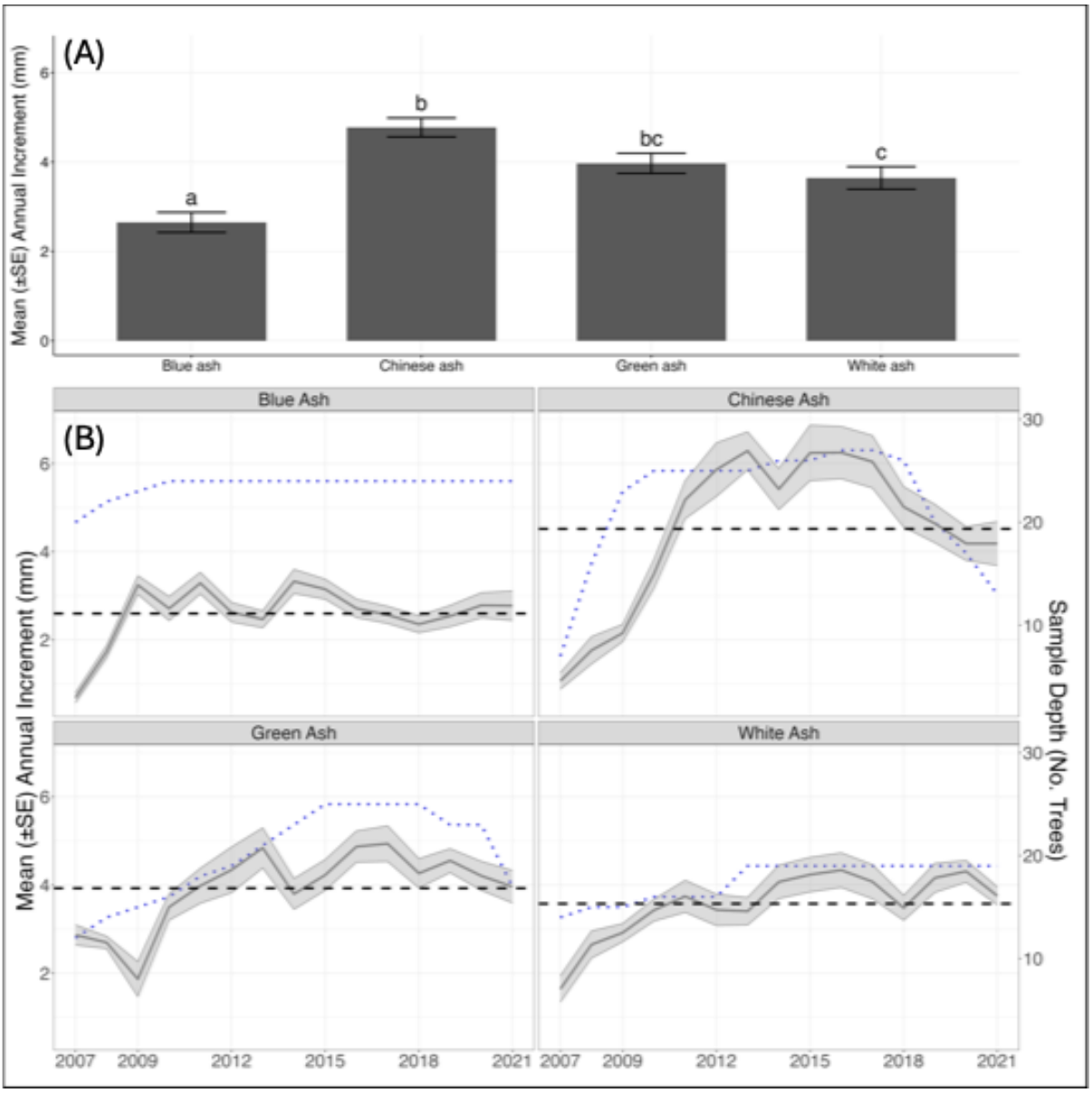

Figure 4.4. (A) Annual radial growth increment (mm) averaged (±SE) by ash species between 2007 and 2021 for trees in Plantation A. Letters above bars indicate significant differences among ash species ($P < 0.05$). (B) Mean (±SE) annual radial growth increment (mm) (grey line with shading) from 2007 to 2021 of four ash species in Plantation A and sample depth (number of trees contributing annually to the mean (blue dotted line) (right panels). Black dashed lines depict average annual increment from 2007 to 2021 for each species.

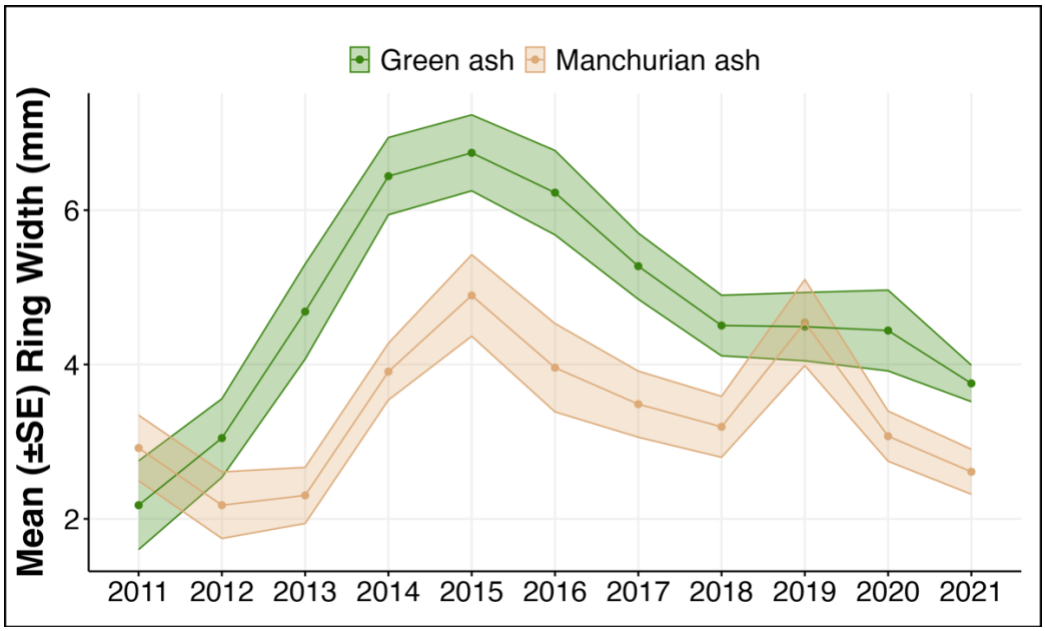

Figure 4.5. Mean (±SE) annual radial growth increment from 2011 to 2021 for green ash and Manchurian ash trees in Plantation B. (N=12 trees per species).

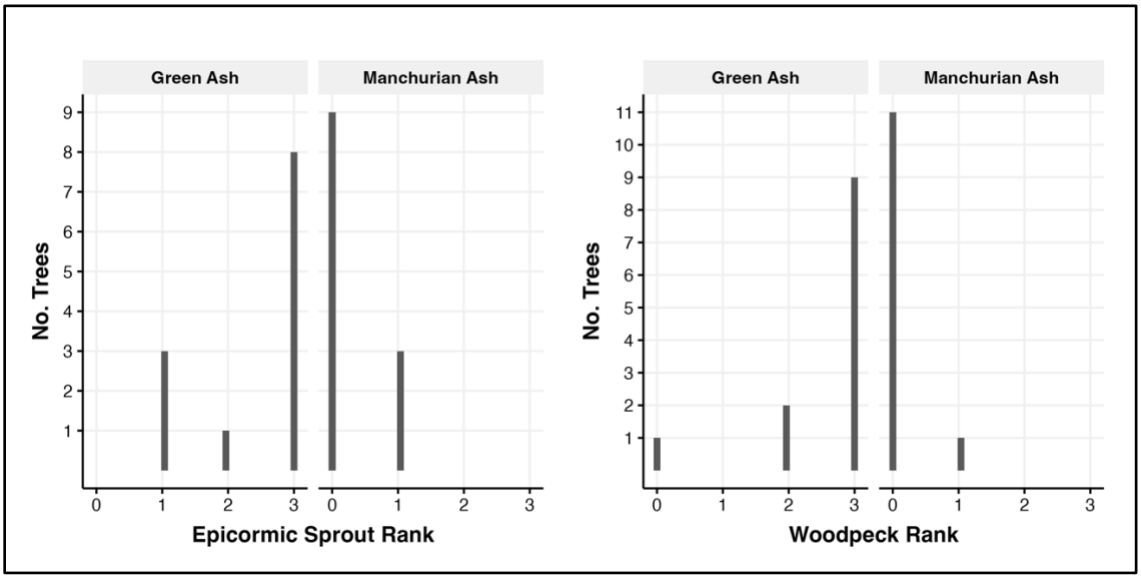

Figure 4.6. Histograms depicting the number of green ash and Manchurian ash trees in Plantation B assigned to ranked categories based on abundance of epicormic sprouts (A) and woodpecks (B) observed on the lower 2 m of the trees. (N=12 trees per species).

LITERATURE CITED

Andrews, A. W. 1916. (list of Cerambycidae), p. 97-100, in: Results of the Mershon Expedition to the Charity Islands, Lake Huron: Coleoptera. Mich. Geol. & Biol. Surv., Publ. 20:67-108.

Allison JD, Borden JH, Seybold SJ. 2004. A review of the chemical ecology of the Cerambycidae (Coleoptera). *Chemoecology.* 14: 3–4. https://doi.org/10.1007/s00049-004-0277-1.

Anulewicz, A.C. and D.G. McCullough. 2012. Development of emerald ash borer (*Agrilus planipennis*) in novel ash (*Fraxinus* spp.) hosts. p. 141–142, In: G. Parra, D. Lance, V. Mastro, R. Reardon and C. Benedict, compilers. Proc. National Emerald Ash Borer Res. Tech. Dev. Mtg, Oct. 12–13, 2011. Wooster, Ohio. USDA Forest Service.

Anulewicz, A.C., D.G. McCullough, and D.L. Cappaert. 2007. Emerald ash borer (*Agrilus planipennis*) density and canopy dieback in three North American ash species. *Arboric. Urban For*. 33: 338–349.

Anulewicz, A.C., D.G. McCullough, D.L. Cappaert, and T.M. Poland. 2008. Host range of the emerald ash borer (*Agrilus planipennis* Fairmaire) (Coleoptera: Buprestidae) in North America: Results of multiple choice field experiments. *Environ. Entomol*. 37: 230–241.

Aukema, J.E., B. Leung, K. Kovacs, C. Chivers, K.O. Britton, J. Englin, S.J. Frankel, R.G. Haight, T.P. Holmes, A. Liebhold, D.G. McCullough, and B. Von Holle. 2011. Economic impacts of non-native forest insects in the continental United States. *PLOS One.* 6(9): e24587.

Aukema, J. E., D.G. McCullough, B. Von Holle, A.M. Liebhold, K. Britton, and S.J. Frankel. Historical accumulation of nonindigenous forest pests in the continental United States. 2010. *Biosience*. 60(11).

Battles J.J., and T.J. Fahey. 2000. Gap dynamics following forest decline: A case study of red spruce forests. *Ecological Applications*. 10(3).

Baranchikov, Y., E. Mozolevskaya, G. Yurchenko, and M. Kenis. 2008. Occurrence of the emerald ash borer, *Agrilus planipennis* in Russia and its potential impact on European forestry. EPPO Bull.38: 233–238.

Bartels, D., D. Williams, J. Ellenwood, and F. Sapio. 2008. Accuracy assessment of remote sensing imagery for mapping hardwood trees and emerald ash borer-stressed ash trees. p. 63–65, In: V. Mastro, D. Lance, R. Reardon, and G. Parra, compilers. Emerald Ash Borer Research and Technology Development Meeting, Oct. 23–24, 2007, Pittsburgh, PA. U.S. Department of Agriculture, Forest Service Publication FHTET-2008-07.Morgantown, WV.

Benedict, L., and R. David 2004. Handbook for black ash preservation reforestation/regeneration .Mohawk Council of Akwesasne, Department of the Environment.

Benedict, M.A., and Frelich, L.E. 2008. Stands factors affecting black ash ring growth in northern Minnesota. *For. Ecol.Manage*., 255:3489-3493.

Bolen, A. 2020. A silent killer.National Museum of the American Indian 2191: 8–15.

Bolker, B. 2025. GLMM FAQ. https://bbolker.github.io/mixedmodels-misc/glmmFAQ.html. Accessed Mar. 2025.

Bolton. N., J. Shannon, J. Davis, M. Van Girnsven, J.N. Noh, S. Schooler, R. Kolka, T. Pypker, and J. Wagenbrenner. 2018. Methods to improve survival and growth of planted alternative species seedlings in black ash ecosystems threatened by emerald ash borer. *Forests*. 9(3).

Boudreault, L., Chagnon, C., Gauthier-Nolett, L., Durand-Nolett, M., Gill, D., Flamand-Hubert, M., and A. Achim. 2024. Physical and mechanical properties affecting the suitability of black ash wood for W8banaki basketry. *Can J. For. Res.* 54(10).

Bowen, A.K.M., and M.H.H. Stevens. 2018. Predicting the effects of emerald ash borer (*Agrilus planipennis* Buprestidae) on hardwood swamp forest structure and composition in southern Michigan. *J. Torrey Bot. Soc.* 145: 41-54.

Brooks, M.E., K. Kristensen, K.J. van Benthem, A. Magnusson, C.W. Berg, A. Nielsen, H.J. Skaug, M. Bolker, and B.M. 2017. glmmTMB balances speed and flexibility among packages for zero-inflated generalized linear mixed modeling. *The R Journal.* 9(2): 378–400. https://doi.org/10.32614/RJ-2017-066.

Bunn, A., M. Korpela, F. Biondi, F. Campelo, P. Mérian, F. Qeadan, and C. Zang. 2010. dplR: Dendrochronology Program Library in R. R package version 1.7.4, https://CRAN.R-project.org/package=dplR.

Burr, S.J., and D.G. McCullough. 2014. Condition of green ash (*Fraxinus pennsylvanica*) overstory and regeneration at three stages of the emerald ash borer invasion wave. *Can. J. For. Res.* 44: 768–776.

Calcagno V (2020). glmulti: Model selection and multimodel inference made easy. R package version 1.0.8, https://CRAN.R-project.org/package=glmulti.

Cappaert, D., D.G. McCullough, T.M. Poland and N.W. Siegert. 2005. Emerald ash borer in North America: a research and regulatory challenge. *Am. Entomol.* 51(3): 152-165.

Chadde, S.W. 2016. Michigan flora: Upper Peninsula. Orchard Innovations.

Chadde, S.W. 2019. Wetland plants of the upper Midwest: A field guide to the aquatic and wetland plants of Michigan, Minnesota and Wisconsin. Orchard Innovations.

Cianciolo, T.R., Diamond, J.S., McLaughlin, D.L., Slesak, R.A., D'Amato, A.W., and Palik, B.J. 2021. Hydrologic variability in black ash wetlands: Implications for vulnerability to emerald ash borer. *Hydrol. Process*. 35.

Cipollini, D., and E. Morton. 2023. The persistence of blue ash in the aftermath of emerald ash borer may be due to adult oviposition preferences and reduced larval performance. *Agric. For. Entomol*. 25(4): 584–589. https://doi.org/10.1111/afe.12582.

Cipollini, D., Q. Wang, J.G.A. Whitehill, J.R. Powell, P. Bonello, and D.A. Herms. 2011. Distinguishing defensive characteristics in the phloem of ash species resistant and susceptible to emerald ash borer. *J. Chem. Ecol.* 37: 450–459.

Cook, B. 2014. Michigan forest types and their ecology. https://msaf.forest.mtu.edu/Business/MSAFguide-2010/1-4-ForestTypes.html. Accessed Apr. 2025.

COSEWIC [Committee on the status of Endangered Wildlife in Canada]. 2014. Assessment and status report on blue ash *Fraxinus quadrangulata* in Canada. Committee on the Status of Endangered Wildlife in Canada. Ottawa xiii + 58 pp. (Species at Risk Public Registry). https://www.canada.ca/en/environment-climate-change/services/species-risk-public-registry/cosewic-assessments-status-reports/blue-ash-2014.html. Accessed Dec. 2024.

COSEWIC [Committee on the status of Endangered Wildlife in Canada]. 2018. Black ash (*Fraxinus nigra*): Assessment and status report. https://www.canada.ca/en/environment-climate-change/services/species-risk-public-registry/cosewic-assessments-status-reports/black-ash-2018.html. Accessed Dec. 2024.

Costanza, K.K.L., Livingston, W.H., Kashian, D.M., Slesak, R.A., Tardif, J. C., Dech, J.P., et al. 2017. The precarious state of a cultural keystone species: Tribal and biological assessments of the role and future of black ash. *J. For.* 115. 435-446.

Costilow KC, Knight K.S., Flower C.E.. 2017. Disturbance severity and canopy position control the radial growth response of maple trees (Acer spp.) in forests of northwest Ohio impacted by emerald ash borer (Agrilus planipennis). *Annals of Forest Science*. 74:10. https://doi.org/10.1007/s13595-016-0602-1.

Crook, D.J. and V. C. Mastro. 2010. Chemical ecology of the emerald ash borer *Agrilus planipennis. J Chem Ecol*. 36: 101–112.

Crook, D.J., A. Khrimian, A. Cosse, I. Fraser, and V.C. Mastro. 2012. Influence of trap color and host volatiles on capture of the emerald ash borer (Coleoptera: Buprestidae). *J. Econ. Entomol*. 105: 429–437.

Curkovic, T., D. Arraztio, A. Huerta, R. Rebolledo, A. Cheuquel, A. Contreras, J. G. Millar. Generic pheromones identified from northern hemisphere Cerambydicae (Coleoptera) are attractive to native longhorn beetles from central-southern Chile. *Insects.* 13.

D'Amato, A., Palik, B., Slesak, R., Edge, G., Matula, C., and Bronson, D. 2018. Evaluating adaptive management options for black ash forests in the face of emerald ash borer invasion. *Forests*. 9: 348.

Dang, Y. Wie, K., Xiaoyi, W., Duan, J.J., D.E. Jennings, and T.M. Poland. 2022. Introduced plants induce outbreaks of a native pest and facilitate invasion in the plants' native range: Evidence from the emerald ash borer. *J. Ecol.*110: 593-604.

Davis, J.C., Shannon, J.P., Bolton, N.W., Kolka, R.K., and T.G. Pypker. 2016. Vegetation responses to simulated emerald ash borer infestation in *Fraxinus nigra* dominated wetlands of upper Michigan, USA. *Can. J. For. Res.* 47: 319-330.

deGroot, P., G. G. Grant, T. M. Poland, R. Scharbach, L. Buchan, R. W. Nott, L. MacDonald, and D. Pitt. 2008. Electrophysiological response and attraction of emerald ash borer to green leaf volatiles (GLVs) emitted by host foliage. *J. Chem. Ecol*. 34: 1170–1179.

Diamond, A.K., and M.R. Emery 2011. Black ash (*Fraxinus nigra* Marsh.): Local ecological knowledge of stands characteristics and morphology associated with basket-grade specimens in New England (USA). *Econ. Bot.* 65: 422-426.

Diamond J.S, D. L. McLaughlin, R.A. Slesak, et al. 2018. Forested versus herbaceous wetlands: Can management mitigate ecohydrologic regime shifts from invasive emerald ash borer? *J. Environ. Manage.* 222: 436–446.

Dodds K.J., D.D. Dubois, and E.R. Hoebeke. 2010. Trap type, lure placement, and habitat effects on Cerambycidae and Scolytinae (Coleoptera) catches in the northeastern United States. *J. Econ. Entomol.* 103: 698–707. https://doi.org/10.1603/EC09395.

Donoghue, M. J., and S. A. Smith. 2008. Patterns in the assembly of temperate forests around the Northern Hemisphere. Philos. *Trans. R. Soc. Lond., B, Biol. Sci.* 359: 1633–1644.

Dray S., and A. Dufour (2007). The ade4 Package: Implementing the duality diagram for ecologists. *Journal of Statistical Software*. 2(4). 1-20.

Drooz, A.T. 1988. Insects of Eastern Forests. US Dept. of Agriculture Forest Service Misc. Publ. No. 1426. Washington, DC. 608 p.

Dumais D, Prévost M. 2014. Physiology and growth of advance Picea rubens and Abies balsamea regeneration following different canopy openings. *Tree Physiology*. 34:194–204.

Duan, J. J., G. Yurchenko, and R. W. Fuester. 2012. Occurrence of emerald ash borer (Coleoptera: Buprestidae) and biotic factors affecting its immature stages in the Russian Far East. *Environ. Entomol*.41: 245–254.

EAB.info [Emerald ash borer information network]. 2025. Michigan State University Departments of Entomology and Forestry.Available online: http://www.emeraldashborer.info/. Accessed Jan. 2024.

Engelken, P. J., and D. G. McCullough. 2020a. Riparian forest conditions along three northern Michigan rivers following emerald ash borer invasion. *Can. J. For. Res.* 50: 800–810.

Engelken PJ, McCullough DG. 2020b. Species Diversity and Assemblages of Cerambycidae in the Aftermath of the Emerald Ash Borer (Coleoptera: Buptrestidae) Invasion in Riparian Forests of Southern Michigan. *Environ. Entomol*. 49(2):391–404.

Engelken, P. J., M. E. Benbow, and D. G. McCullough. 2020. Legacy effects of emerald ash borer on riparian forest vegetation and structure. *Forest Ecol. Manag.* 457.

Erdmann, G.G., Crow, T.R., Peterson, R.M., and Wilson, C.D. 1987. *Managing black ash in the Lake States*. USDA Forest Service.

Evans HF, Moraal LG, Pajares JA. 2007. Biology, ecology and economic importance of Buprestidae and Cerambycidae. Bark and Wood Boring Insects in Living Trees in Europe, A Synthesis. Springer. p. 447-498.

Eyles, A., W. Jones, K. Riedl, D. Cipollini, S. Schwartz, K. Chan, D. A. Herms, and P. Bonello. 2007. Comparative phloem chemistry of Manchurian (*Fraxinus mandshurica*) and two North American ash species (*Fraxinus americana* and *Fraxinus pennsylvanica*). *Chem. Ecol.* 33: 1430–1448.

Fan, J., O. Denux, c. Courtin, A. Bernard, M. Javal, J.G. Millar, L.M. Hanks, and A. Roques. 2019. Multi-component blends for trapping native and exoctic longhorn beetles at potential points-of-entry and in forests. *J. Pest. Sci.* 92: 281-297.

Flower, C. E., K. S. Knight, and M. A. Gonzalez-Meler. 2013. Impacts of the emerald ash borer (*Agrilus planipennis* Fairmaire) induced ash (*Fraxinus* spp.) mortality on forest carbon cycling and successional dynamics in the eastern United States. *Biol.Invasions*. 15: 931–944.

Fraver S., A.W. D'Amato, M. Reinikainen, et al. 2022. Stand dynamics and structure of old-growth *Fraxinus nigra* stands in northern Minnesota, USA. *Can. J. For. Res*. 52: 910–919.

Gandhi, K. J. K., A. M. Smith, D. M. Hartzler, and D. A. Herms. 2014. Indirect effects of emerald ash borer-induced ash mortality and canopy gap formation on epigaeic beetles. *Environ. Entomol*. 43: 546–555.

Gosner, M. M., A. Perret-Gentil, E. Britt, V. Queloz, G. Glauser, T. Ladd, A. D. Roe, M. Cleary, M. Liziniewicz, L. R. Nielsen, S. K. Ghosh, P. Bonello, and M. Eisenring. 2023. A glimmer of hope – ash genotypes with increased resistance to ash dieback pathogen show cross-resistance to emerald ash borer. *New Phytol.* 240: 1219–1232.

Gosling D.C.L. 1973. An annotated list of the Cerambycidae of Michigan (Coleoptera) Part I, Introduction and the subfamilies Parandrinae, Prioninae, Spondylinae, Aseminae, and Cerambycinae. *Great Lakes Entomol.* 6(3). https://doi.org/10.22543/0090-0222.1182.

Gosling D.C.L. 1983. New state records of cerambycidae from michigan (Coleoptera). The Great Lakes Entomologist. 16(4). https://doi.org/10.22543/0090-0222.1486.

Gosling DCL. 1986. Ecology of the Cerambycidae (Coleoptera) of the Huron Mountains in Northern Michigan. *Great Lakes Entomol.*19(3). https://doi.org/10.22543/0090-0222.1571.

Gosling DCL, Gosling NM. 1976. An annotated list of the Cerambycidae of Michigan (Coleoptera) Part II, the Subfamilies Lepturinae and Lamiinae. *Great Lakes Entomol.*10(1). https://doi.org/10.22543/0090-0222.1292.

Graham E.E., Mitchell R.F., Reagel P.F., et al. 2010. Treating panel traps with a fluoropolymer enhances their efficiency in capturing cerambycid beetles. *J. Econ. Entomol.* 103(3):641–647.

Graham EE, Poland TM, McCullough DG, et al. 2012. A Comparison of Trap Type and Height for Capturing Cerambycid Beetles (Coleoptera). *J. Econ. Entomol.* 105(3):837–846.

Grant, G. G., K. L. Ryall, D. B. Lyons, and M. M. Abou-Zaid. 2010. Differential response of male and female emerald ash borers (Col., Buprestidae) to (Z)-3-hexenol and Manuka oil. *J Appl. Entomol.* 134: 26–33.

Griffith, R. S. 1991. *Fraxinus americana*. In: Fire Effects Information System, [Online]. U.S. Department of Agriculture, Forest Service, Rocky Mountain Research Station, Fire Sciences Laboratory (Producer). Available online: https://www.fs.usda.gov/database/feis/plants/tree/fraame/all.html.Accessed Dec. 2024.

Gucker, C. L. 2005a. *Fraxinus nigra*. In: Fire Effects Information System, [Online].U.S. Department of Agriculture, Forest Service, Rocky Mountain Research Station, Fire Sciences Laboratory (Producer). https://www.fs.usda.gov/database/feis/plants/tree/franig/all.html Accessed Dec. 2024.

Gucker, C. L. 2005b. *Fraxinus pennsylvanica*. In: Fire Effects Information System, [Online]. U.S. Department of Agriculture, Forest Service, Rocky Mountain Research Station, Fire Sciences Laboratory (Producer).Available online: https://www.fs.usda.gov/database/feis/plants/tree/frapen/all.html. Accessed Dec. 2024.

Haack RA. 2017. Feeding Biology of Cerambycids. In: Cerambycidae of the World: Biology and Pest Managment. CRC Press. p. 105–133

Haack RA, Keena MA, Eyre D. 2017. 2 Life History and Population Dynamics of Cerambycids. In: Cerambycidae of the World: Biology and Pest Managment. Taylor and Francis Group. p. 71–105

Haack R. A., T. R. Petrice, and A. C. Wiedenhoeft. 2010. Incidence of bark and wood-boring insects in firewood: A survey at Michigan's Mackinac bridge. *J. Econ. Entomol.*103: 1682-1692.

Hammond HEJ, Langor DW, Spence JR. 2017. Changes in saproxylic beetle (Insecta: Coleoptera) assemblages following wild.f.ire and harvest in boreal Populus forests. *For. Ecol. and Manage.* 401:319–329. https://doi.org/10.1016/j.foreco.2017.07.013.

Handley K., J. Hough-Goldstein, L.M. Hanks, J.G. Millar, and V. D'Amico. Species richness and phenology of cerambycid beetles in urban forest fragments of northern Delaware. 2015. *Ann. Entomol. Soc. Am.* 1-12.

Hanks LM. 1999. Influence of the larval host plant on reproductive strategies of cerambycid beetles. *Annu. Rev. Entomol.* 44(1):483–505. https://doi.org/10.1146/annurev.ento.44.1.483.

Hanks LM, Millar JG. 2013. Field bioassays of cerambycid pheromones reveal widespread parsimony of pheromone structures, enhancement by host plant volatiles, and antagonism by components from heterospecifics. *Chemoecology.* 23(1):21–44. https://doi.org/10.1007/s00049-012-0116-8.

Hanks LM, Millar JG, Mongold-Diers JA, et al. 2012. Using blends of cerambycid beetle pheromones and host plant volatiles to simultaneously attract a diversity of cerambycid species. *Can. J. For. Res.* 42(6):1050–1059. https://doi.org/10.1139/x2012-062.

Hartig, F. 2022. DHARMa: Residual Diagnostics for Hierarchical (Multi-Level / Mixed) Regression Models. R package version 0.4.6, https://CRAN.R-project.org/package=DHARMa.

Hauer, R. J., and W. D. Peterson. 2017. Effects of emerald ash borer on municipal forestry budgets. Landsc. *Urban Plan*.157: 98–105.

Herms, D. A., and D. G. McCullough. 2014. Emerald ash borer invasion of North America: History, biology, ecology, impacts, and management. *Ann. Rev. Entomol*. 59: 13–30.

Hissinger, D.D., J. Basak, M. Gaudeul, C. Cruaud, P. Bertolino, N. Frascaria-Lacoste and J. Bousquet. 2013. Phylogeny and biogeographic history of ashes (Fraxinus, Oleaceae) highlight the roles of migration and vicariance in the diversification of temperate trees. *PLOS One.* 8: e804431.

Hoven BM, Knight KS, Peters VE, et al. 2020. Release and suppression: forest layer responses to emerald ash borer (Agrilus planipennis)-caused ash death. *Annals of Forest Science*. 77:10.

Hudgins, E. J., F. H. Koch, M. J. Ambrose, and B. Leung. 2021. Hotspots of pest-induced US urban tree death, 2020–2050. *J. Appl. Ecol*. 58: 2918–2929.

Ives, W.G.H. and H.R. Wong. 1988. Tree and Shrub Insect of the Prairie Provinces. Canadian For. Serv. Info. Rep. NOR-X-292.327 p.

Iwabuchi, K. Mating behavior of Xylotrechus pyrrhoderus Bates (Coleoptera: Cerambycidae) 1. Behavioral sequences and existence of the male sex pheromone. *Appl. Entomol. Zool*. 17, 494–500

Johnson, W.T. and H.H. Lyon. 1988. Insects That Feed on Trees and Shrubs. Cornell Univ. Press. Ithaca, NY.556 p.

Karamanski. T.J. 1989. Deep woods frontier: A history of logging in northern Michigan. Wayne State University Press.

Kashian, D. M. 2016. Sprouting and seed production may promote persistence of green ash in the presence of the emerald ash borer. *Ecosphere*. 7: e01332.

Kelly, L. J., W. Plumb, D. W. Carey and M. E. Mason. 2020. Convergent molecular evolution among ash species resistant to emerald ash borer. *Nat. Ecol. Evol*. 4: 1–13.

Kew Royal Botanical Gardens. 2024. Plants of the world online. Available online: https://powo.science.kew.org/taxon/urn:lsid:ipni.org:names:922141-1. Accessed Dec. 2024.

Klooster, W., K. Gandhi, L. Long, et al. 2018. Ecological impacts of emerald ash borer in forests at the epicenter of the invasion in North America. *Forests*. 9(5): 250. https://doi.org/10.3390/f9050250.

Klooster, W.S., D.A. Herms, K.S. Knight, C.P. Herms, D.G. McCullough, A. Smith, K.J.K. Gandhi and J. Cardina. 2014. Ash (*Fraxinus* spp.) mortality, regeneration, and seed bank dynamics in mixed hardwood forests following invasion by emerald ash borer (*Agrilus planipennis*). *Biol. Invasions*.16: 859-873.

Kneeshaw DD, Bergeron Y. 1998. Canopy Gap Characteristics and Tree Replacement in the Southeastern Boreal Forest. *Ecology*. 79:783–794.

Knight, K. S., J. P. Brown, and R. P. Long. 2013. Factors affecting the survival of ash (*Fraxinus* spp.) trees infested by emerald ash borer (*Agrilus planipennis*). *Biol. Invasions*. 15: 371–383.

Kolka, R.K., D'Amato, A.W., Wagenbrenner, J.W., Slesak, R.A., Pypker, T.G., Youngquist, M.B., Grinde, A.R., Palik, B.J. 2018. Review of ecosystem level impacts of emerald ash borer on black ash wetlands: What does the future hold? *Forests.* 9.

Kovacs, K. F., R. D. Haight, D. G. McCullough, R. J. Mercader, N. A. Siegert, and A. M. Liebhold. 2010. Cost of potential emerald ash borer damage in U.S. communities, 2009–2019. *Ecol. Econ.* 69: 569–578.

Kovacs, K. F., R. G. Haight, R. J. Mercader, and D. G. McCullough. 2014. A bioeconomic analysis of an emerald ash borer invasion of an urban forest with multiple jurisdictions. Resour. *Energy Econ.* 36: 270–289.

Kovacs, K. F., R. J. Mercader, R. G. Haight, N. W. Siegert, D. G. McCullough, and A. M. Liebhold. 2011. The influence of satellite populations of emerald ash borer on projected economic costs in U.S. communities, 2010–2020. *J. Environ. Manage*. 92: 2170–2181.

Krzemien, S., W. M. Robertson, P. J. Engelken, and D. G. McCullough. 2024. Observations of reduced ET and persistent elevated water table beneath a riparian forest gap following emerald ash borer invasion and tree mortality. *Hydrol. Processes*. 38: e15117.

Lacey ES, Millar JG, Moreira JA, et al. 2009. Male-Produced Aggregation Pheromones of the Cerambycid Beetles Xylotrechus colonus and Sarosesthes fulminans. *J. Chem. Ecol.* 35:733–740.

Lacey ES, Moreira JA, Millar JG, et al. 2007. Male-produced aggregation pheromone of the cerambycid beetle *Neoclytus mucronatus mucronatus*. *Entomologia Exp Applicata.* 122:171–179.

Langor DW, Hammond HEJ, Spence JR, et al. 2008. Saproxylic insect assemblages in Canadian forests: diversity, ecology, and conservation. *Can Entomol.* 140:453–474.

Larson, D., P. Engelken, D. G. McCullough, and M. Benbow. 2023. Emerald ash borer invasion of riparian forests alters organic matter and bacterial subsidies to south Michigan headwater streams. *Can. J. Fish. Aquat. Sci.* 80: 298–312.

Legendre, P., and E. Gallagher. 2001. Ecologically meaningful transformations for ordination of species data. *Oecologia*. 129: 271-280.

Lenth, R. 2023. emmeans: Estimated Marginal Means, aka Least-Squares Means. R package version 1.8.5, https://CRAN.R-project.org/package=emmeans.

Levesque, M., J. I. B. Eduardo, and V. Queloz. 2023. Potential alternative tree species to *Fraxinus excelsior* in European forests. *Front. For. Glob.Change.*

Liebhold, A.M., J.M. Kean. 2019. Eradication and containment of non-native forest insects: success and failures. *J. Pest Sci.*92: 83-91

Limback, C. K. 2010. Tree vigor and its relation to emerald ash borer (*Agrilus planipennis* Fairmaire) adult host preference and larval development on green and white ash trees. M.S. thesis, Dept. of Entomology, Michigan State University.98 p.

Lindell, C.A. D. G. McCullough, D. Cappaert, and M. B. Melinda. 2008. Factors influencing woodpecker predation on emerald ash borer. Am. Midl. Nat.159: 434-444.

Lingafelter, S. W. 2007. Illustrated key to the longhorned woodboring beetles of the eastern United States. Special Publication No. 3. Coleopterists Society, North Potomac, MD.

Linsley EG. 1959. Ecology of Cerambycidae. Annu. Rev. Entomol. 4(1):99–138. https://doi.org/10.1146/annurev.en.04.010159.000531.

Liu, H., L. S. Bauer, D. L. Miller, T. Zhao, R. Gao, L. Song, Q. Luan, R. Jin, and C. Gao. 2007. Seasonal abundance of *Agrilus planipennis* (Coleoptera: Buprestidae) and its natural enemies *Oobius agrili* (Hymenoptera: Encyrtidae) and *Tetrastichus planipennisi* (Hymenoptera: Eulophidae) in China. *Biol. Control.* 42: 61–71.

Liu, H., L. S. Bauer, R. Gao, T. Zhao, and T. R. Petrice. 2003. Exploratory survey for the emerald ash borer, *Agrilus planipennis* (Coleoptera: Buprestidae), and its natural enemies in China. *Great Lakes Entomol.* 36(2).

Looney CE, D'Amato AW, Fraver S, et al. 2018. Interspecific competition limits the realized niche of *Fraxinus nigra* along a waterlogging gradient. *Can. J. For. Res.* 48(11):1292–1301. https://doi.org/10.1139/cjfr-2018-0023.

Lorimer CG, Frelich LE. 1994. Natural Disturbance Regimes in Old-Growth Northern Hardwoods: Implications for Restoration Efforts. J*ournal of Forestry.* 92(1):33–38. https://doi.org/10.1093/jof/92.1.33.

Lovett. G.M., M. Weiss, A.M. Liebhold, et al. 2016. Nonative forest insects and pathogens in the United States: Impacts and policy options. *Ecol. App.* 26: 1437-1455

Mathieu R.D.R., D.G. McCullough. 2025. Long-term survival and radial growth of four North American and two Asian ash species in a common garden exposed to emerald ash borer invasion. *Environ. Entomol.*

McCullough, D. G. 2013. Will we kiss our ash goodbye? *Am. For.* 118: 16–23.

McCullough, D. G. 2020. Beyond eradication: challenges, tactics, and integrated management of emerald ash borer. *Int. J. For. Res*.15 p.

McCullough, D.G., R. Mercader. Evaluation of potential strategies to SLow ash mortality (SLAM) caused by emerald ash borer (*Agrilus planipennis*): SLAM in urban forest. *Int. J. Pest. Manag.* 58: 9-23

McCullough, D. G., T. M. Poland, A. C. Anulewicz, and D. Cappaert. 2009a. Emerald ash borer (Coleoptera: Buprestidae) attraction to stressed or baited ash trees. *Environ. Entomol.* 38: 1668–1679.

McCullough, D. G., T. M. Poland, D. Cappaert, and A. C. Anulewicz. 2009b. Emerald ash borer (*Agrilus planipennis*) attraction to ash trees stressed by girdling, herbicide, and wounding. *Can. J. For. Res.* 39: 1331–1345.

McKenney, D. W., J. H. Pedlar, D. Yemshanov, D. B. Lyons, K. L. Campbell, and K. Lawrence. 2012. Estimates of the potential cost of emerald ash borer (*Agrilus planipennis* Fairmaire) in Canadian municipalities. *Arboric. Urban For.* 38: 81–91.

Mercader, R. J., N. W. Siegert, and D. G. McCullough. 2012. Estimating the influence of population density and dispersal behavior on the ability to detect and monitor *Agrilus planipennis* (Coleoptera: Buprestidae) populations. *J. Econ. Entomol.* 105: 272–281.

Mercader, R. J., N. W. Siegert, A. M. Liebhold, and D. G. McCullough. 2011. Simulating the influence of the spatial distribution of host trees on the spread of the emerald ash borer, *Agrilus planipennis*, in recently colonized sites. *Popul. Biol.* 53: 271–285.

Miller DR. 2006. Ethanol and (-)-a-Pinene: Attractant Kairomones for Some Large Wood-Boring Beetles in Southeastern USA. *J. Chem. Ecol.* 32: 779-794.

Miller, F., and E. McMahan. 2022. Examining resistance of Asian, European, and North American ash and elm species to the emerald ash borer (*Agrilus planipennis*) (Coleoptera: Buprestidae). *Great Lakes Entomol.* 55.

Nie, P., R. Yang, R. Cao, X. Hu, and J. Feng. 2023. Niche and range shifts of the fall webworm (*Hyphantria cunea* Dury) in Europe imply its huge invasion potential in the future. *Insects* 14: 316. https://doi.org/10.3390/insects14040316.

Oksanen J., G. Simpson, F. Blanchet, et al. 2024. _vegan: Community Ecology Package_. R package version 2.6-6, https://CRAN.R-project.org/package=vegan.

Olson, D. G., and L. K. Rieske. 2019. Host range expansion may provide enemy-free space for the highly invasive emerald ash borer. *Biol. Invasions*. 20: 1–11.

Orlova-Bienkowskaja, M. J., and M. G. Volkovitsh. 2018. Are native ranges of the most destructive invasive pests well known? A case study of the native range of emerald ash borer, *Agrilus planipennis* (Coleoptera: Buprestidae). *Biol. Invasions.* 20: 1275–1286.

Palik, B.J., D'Amato, A.W., and Slesak, R.A. 2021. Wide-spread vulnerability of black ash (*Fraxinus nigra* marsh.) wetlands in Minnesota USA to loss of tree dominance from invasive emerald ash borer. *Forestry. 94*: 455-463.

Palik, B.J., Ostry, M.E., Venette, R.C., and Abdela, E. 2012. Tree regeneration in black ash (*Fraxinus nigra*) stands exhibiting crown dieback in Minnesota. *For. Ecol. Manage. 269*: 26-30

Peters, M. P., A. M. Prasad, S. N. Matthews, and L. R. Iverson. 2020.Climate change tree atlas, Version 4. U.S. Forest Service, Northern Research Station and Northern Institute of Applied Climate Science, Delaware, OH. https://www.nrs.fs.fed.us/atlas.

Peterson, D. L., J. J. Duan, J. S. Yaninek, M. D. Ginzel, and C. S. Sadof. 2015. Growth of larval *Agrilus planipennis* (Coleoptera: Buprestidae) and fitness of *Tetrastichus planipennisi* (Hymenoptera: Eulophidae) in blue ash (*Fraxinus quadrangulata*) and green ash (*F. pennsylvanica*). *Environ. Entomol*. 44: 1512–1521.

Poland, T. M., and D. G. McCullough. 2006. Emerald ash borer: invasion of the urban forest and the threat to North America's ash resource. *J. For.* 104: 118–124.

Poland, T. M., and D. G. McCullough. 2014. Comparison of trap types and colors for capturing emerald ash borer adults at different population densities. *Environ. Entomol.* 43(1): 157–170.

Poland, T.M., D. Rassati. 2019. Improved biosecurity surveillance of non-native forest insects: a review of current methods. *J. Pest Sci.* 92: 37-49.

Pureswaran, D. S., and T. M. Poland. 2009. Host selection and feeding preferences of *Agrilus planipennis* (Coleoptera: Buprestidae) on ash (*Fraxinus* spp.). *Environ. Entomol.* 38: 757–765.

Qu, L., J. Li, R. Wang, X. Wang, T. Zhao, Y. Chen, and L. Wang. 2021. Metabolic and transcriptional profiling of *Fraxinus chinensis* var. *rhynchophylla* unravels possible constitutive resistance against *Agrilus planipennis*. *Forests.* 12: 1373. https://doi.org/10.3390/f12101373.

R Core Team. 2024. R: A language and environment for statistical computing.R Foundation for Statistical Computing, Vienna, Austria. https://www.R-project.org.

Rebek, E.J., D.A. Herms, and D.R. Smitley. 2008. Interspecific variation in resistance of emerald ash borer (Coleoptera: Buprestidae) among North American and Asian ash (*Fraxinus* spp.). *Environ. Entomol.* 43: 242–246.

Rigsby, C.M., V.L. Muilenburg, T. Tarpeu, D.A. Herms, and D.F. Cipollini. 2014. Oviposition preferences of *Agrilus planipennis* Fairmaire (Coleoptera: Buprestidae) for different ash species support the mother knows best hypothesis. *Ann. Entomol. Soc. Am.* 107: 773–781.

Robinett, M.A., and D.G. McCullough. 2019. White ash (*Fraxinus americana*) survival in the core of the emerald ash borer (*Agrilus planipennis*) invasion. *Can. J. For. Res.* 49: 510–520.

Rodriguez-Saona, C., T.M. Poland, J.R. Miller, L.L. Stelinski, G.G. Grant, P. de Groot, L. Buchan, and L. MacDonald. 2006. Behavioral and electrophysiological responses of the emerald ash borer, *Agrilus planipennis*, to induced volatiles of Manchurian ash, *Fraxinus mandshurica*. *Chemoecology.* 16: 75–86.

Roloff, A., S. Gilner, R. Kniesel, and D. Zhang. 2018. Interesting and new tree species for European cities. *J. For. Landsc. Res.* (3):1: 1-7.

Roques, A. L. Ren, D. Rassati, et al. 2023. Worldwide tests of generic attractants, a promising tool for early detection of non-native cerambycid species. *Neobiota*. http://hdl.handle.net/2067/49749.

Sadof. C. S., D. G. McCullough, and M. D. Ginzel. 2023. Urban ash management and emerald ash borer (Coleoptera: Buprestidae): facts, myths, and an operational synthesis. *J. Integr. Pest Manag.*14: 1-13.

Schmeelk TC, Millar JG, Hanks LM. 2016. Influence of Trap Height and Bait Type on Abundance and Species Diversity of Cerambycid Beetles Captured in Forests of East-Central Illinois. *J. Econ. Entomol.* 109:1750–1757.

Schrader, G., R. Baker, Y. Baranchikov, L. Dumouchel, K.S. Knight, D.G. McCullough, M.J. Orlova-Bienkowskaja, S. Pasquali, and G. Gilioli. 2021. How does the emerald ash borer (*Agrilus planipennis*) affect ecosystem service and biodiversity components in invaded areas? EPPO Bull. DOI: 10.1111/epp.12734.

Schowalter, T.D., and D.R. Ring. 2017. Biology and management of the fall webworm, *Hyphantria cunea* (Lepidoptera: Erebidae). *J. Integr. Pest Manag.* 8: 1–6.

Schowalter, D.N., C. Villari, D.A. Herms, and P. Bonello. 2018. Drought stress increased survival and development of emerald ash borer larvae on coevolved Manchurian ash and implicates phloem-based traits in resistance. Agric. For. Entomol. 20: 170–179.

Schute, L. A, D.J. Mladenoff, T.R. Crow, K.C. Merrick, D.T. Cleland. 2007. Homogenization of northern U.S. Great Lakes forests due to land use. *Landscp. Ecolo.* 22: 1089-1103.

Seymour, R.S, A.S. White 2002. Natural disturbance regimes in northeastern North America—evaluating silvicultural systems using natural scales and frequencies. *For. Ecol. Manag*. 155: 357-367

Shannon, J., Van Grinsven, M., Davis, J., Bolton, N., Noh, N., Pypker, T., et al. 2018. Water level controls on sap flux of canopy species in black ash wetlands. *Forests. 9*: 147-.

Siegert, N.W., D. G. McCullough, D. W. Williams, I. Fraser, T. M. Poland, and S. J. Pierce. 2010. Dispersal of *Agrilus planipennis* (Coleoptera: Buprestidae) from discrete epicenters in two outlier sites. *Environ. Entomol.* 39: 253-265.

Siegert, N.W., D.G. McCullough, A.M. Liebhold, and F.W. Telewski. 2014. Dendrochronological reconstruction of the epicenter and early spread of emerald ash borer in North America. *Divers. Distrib.* 20: 847–858.

Siegert, N.W., D.G. McCullough, T. Luther, L. Benedict, S. Crocker, K. Church, and J. Banks. 2023. Biological invasion threatens keystone species indelibly entwined with indigenous cultures. *Front. Ecol. Environ.* 21: 310-316

Siegert, N.W., P.J. Engelken, and D.G. McCullough. 2021. Changes in demography and carrying capacity of green ash and black ash ten years after emerald ash borer invasion of two ash-dominant forests. *For. Ecol. Manage.* 494.

Slesak, R.A., Lenhart, C.F., Brooks, K.N., D'Amato, A.W., Palik, B.J. 2014. Water table response to harvesting and simulated emerald ash borer mortality in black ash wetlands in Minnesota, USA. *Can. J. For. Res.* 44: 961-968.

Smith, A., D.A. Herms, R.P. Long, and K.J.K. Gandhi. 2015. Community composition and structure had no effect on forest susceptibility to invasion by the emerald ash borer (Coleoptera: Buprestidae). *Can. Entomol.* 147: 318–332.

Spei, B.A., and D.M. Kashian. 2017. Potential for persistence of blue ash in the presence of emerald ash borer in southeastern Michigan. *For. Ecol. Manage.* 392: 137–143.

Speer, J.H. 2010. Fundamentals of tree-ring research. University of Arizona Press, Tucson, USA.

Springer, A., and Dech, J.P. 2019. Regeneration of black ash (Fraxinus nigra Marsh.) in hardwood swamps of the Great Lakes – St. Lawrence Forest Region. *The Forestry Chron.* 97.

Subburayalu S. K., and D. Sydnor. 2018. Results and implications following a twelve-year monitoring of ash (*Fraxinus* spp.) mortality due to *Agrilus planipennis* in an urban forest plantation. AUF. 44: 154-160.

Tanis, S.R. 2013. Host plant interactions between emerald ash borer and North American and Asian *Fraxinus* species. Ph.D. dissertation. Dept. of Forestry, Michigan State University.174 p.

Tanis, S.R., and D.G. McCullough. 2012. Differential persistence of blue ash and white ash following emerald ash borer invasion. *Can. J. For. Res.*42: 1542–1550.

Tanis, S.R., and D.G. McCullough. 2015. Host resistance of five *Fraxinus* species to *Agrilus planipennis* (Coleoptera: Buprestidae) and effects of paclobutrazol and fertilization. *Environ. Entomol.* 44: 287–299.

Tanis, S.R., D.G. McCullough, and B.M. Cregg. 2015. Effects of paclobutrazol and fertilizer on the physiology, growth and biomass allocation of three *Fraxinus* species. *Urban For. Urban Greening*. 14: 590–598.

Tardif, J., and Bergeron, Y. 1993. Radial growth of *Fraxinus nigra* in a Canadian boreal floodplain in response to climatic and hydrological fluctuations. *J. Veg. Sci. 4*. 751-758.

Tardif, J., and Bergeron, Y. 1999. Population dynamics of *Fraxinus nigra* in response to flood level variations, in northwestern Quebec. *Ecol. Monog.* 69. 107-125.

Therneau, T.M., and P.M. Grambusch. 2000. *Modeling survival data: extending the Cox model*. Springer, New York.ISBN 0-387-98784-3.

Tluczek, A. R., D. G. McCullough, and T. M. Poland. 2011. Influence of host stress on emerald ash borer (Coleopter:Buprestidae) adult density, development, and distribution in *Fraxinus pennsylvanica* trees. *Environ. Entomol.* 40: 357-366.

Toczydlowski, A.J.Z., Slesak, R.A., Kolka, R.K., Venterea, R.T., D'Amato, A.W., and Palik, B.J. (2020). Effect of simulated emerald ash borer infestation on nitrogen cycling in black ash (*Fraxinus nigra*) wetlands in northern Minnesota, USA. *For. Ecol. and Manage. 458*.

Uchytil RJ. 1991. Abies balsamea. In: Fire Effects Information System. [accessed 2025 Mar 3]. https://www.fs.usda.gov/database/feis/plants/tree/abibal/all.html.

Ulyshen, M.D., W.S. Klooster, W.T. Barrington, and D.A. Herms. 2011. Impacts of emerald ash borer-induced tree mortality on leaf litter arthropods and exotic earthworms. *Pedobiologia* .54: 261–265.

Ulyshen MD, Lucky A, Work TT. 2020. Effects of prescribed fire and social insects on saproxylic beetles in a subtropical forest. *Sci Rep.* 10(1):9630. https://doi.org/10.1038/s41598-020-66752-wlori.

USDA-APHIS [U.S. Department of Agriculture Animal and Plant Health Inspection Service]. 2011. Risk assessment of the movement of firewood within the United States. U.S. Department of Agriculture, Animal and Plant Health Inspection Service, Plant Protection and Quarantine, Center for Plant Health Science and Technology, Plant Epidemiology and Risk Analysis Laboratory, Raleigh, NC.111 p. https://www.fs.usda.gov/Internet/FSE_DOCUMENTS/stelprdb5331675.pd.f.. Accessed Jan. 2025.

USDA-APHIS [U.S. Department of Agriculture Animal and Plant Health Inspection Service]. 2024.Emerald ash borer (EAB) known infested counties. https://www.aphis.usda.gov/plant-pests-diseases/eab/eab-infestation-map. Accessed Jan. 2025.

Villari, C., D.A. Herms, J.G.A. Whitehill, D. Cipollini, and P. Bonello. 2016. Progress and gaps in understanding mechanisms of ash tree resistance to emerald ash borer; a model for wood-boring insects that kill angiosperms. *New Phytol.* 209: 63–79.

Wallander, E. 2008. Systematics of *Fraxinus* (Oleaceae) and evolution of dioecy. Plant Syst. Evol.273: 25-49.

Walters R.S., and H.W. Yawney. 1990. *Acer rubrum* L. *Silvics of North America, Hardwoods*. USDA For. Serv. Agriculture Handbook 654, vol 2.

Wang, X.Y., Z.Q. Yang, J.R. Gould, Y.N. Zhang, G.J. Liu, and E. Liu. 2010. The biology and ecology of the emerald ash borer, *Agrilus planipennis*, in China. *J. Insect Sci.*10: 128.

Ward, S.F., Leibhold, A.M., Morin, R.S., Frei, S. 2021. Population dynamics of ash across the eastern USA following invasion by emerald ash borer. *For. Ecol. Manag.* 479.

Wei, X.D., Y. Reardon, J.H. Wu, and S. Sun. 2004. Emerald ash borer, *Agrilus planipennis* Fairmaire (Coleoptera: Buprestidae), in China: a review and distribution survey. *Acta Entomol. Sinica.* 47: 679–685.

Weber, C.R, J.G. Cohen, and M.A. Kost. 2007. Natural community abstract for Northern Hardwood Swamp. Michigan Natural Features Inventory, Lansing, MI. 9 pp. Whitney 1987

Williams, M. 1989 Americans and their forests: a historical geography. Cambridge University Press, Cambridge, UK

Wilson, C.J., L. Labbate, T. R. Petrice, T.M. Poland, D.G. Mccullough. 2025. Ongoing regeneration of ash and co-occuring species 20 years following invasion by emerald ash borer. *For. Ecol. Manag.* 580:122546.

Windmuller-Campione, M. A., M.B., Russell, R.A. Slesak, M. Lochner. 2021. Regeneration responses in black ash (*Fraxinus nigra*) wetlands: implications for forest diversification to address emerald ash borer (*Agrilus planipennis*). *New Forests*. 52(4): 537-558

Wright, J.W., and Rauscher, M.H. 1990. *Fraxinus nigra* Marsh. *Silvics of North America, Hardwoods*. USDA For. Serv. Agriculture Handbook 654, vol 2, pp. 344-347.

Wen, J. 1999. Evolution of eastern Asian and eastern North American disjunct distributions in flowering plants. Annu. Rev. Ecol. Syst.30: 421–455.

Yanega, D.1996. Field guide to northeastern longhorned beetles (Coleoptera: Cerambycidae). Illinois Natural History Survey. Champaign. 174 pp.

Yihong, W. 1995. Study on ecology of *Fraxinus mandshurica*. *J. For*. Res.6: 61–64.

Yougquist, M.B., Eggert, S.L., D'Amato, A.W., Palik, B.J., and Slesak, R.A. (2017). Potential Effects of Foundation Species Loss on Wetland Communities: A Case Study of Black Ash Wetlands Threatened by Emerald Ash Borer. *Wetlands.* 37(4) 787–799.

Zhao, T., R. Gao, H. Liu, S.L. Bauer, and Q. Sun. 2005. Host range of emerald ash borer, *Agrilus planipennis* Fairmaire, its damage and the countermeasures. *Acta Entomol.* Sin.48: 594-599.

Zong, S., J. Lin, T. Wang, and Y. Luo. 2014. Resistance of eight species of ash trees to emerald ash borer and their mechanisms. *Am. J. Agric. For.* 2: 302–308.

APPENDIX A: CHAPTER ONE SUPPLMENTAL TABLES AND FIGURES

Supplemental Tables

Table S1.1. Model equations for mixed models, with response and predictors detailed in the first column, and corresponding estimates in the second column.

Model Formula	Fit Equation
Seedling density predicted by Invasion Status (three-level factor) with stand as a random effect and area sampled as a model offset	$Seedling\ Density_{ij} = e^{9.822-(Invasion\ Status_{Post-Invasion})_{ij}*0.669+(Invasion\ Status_{Pre-Invasion})_{ij}*1.197+U_i+W_{ij}} + log(3e\text{-}4)$ $U_i \sim \mathrm{N}(0, 1.56 * 10^{-12})$ $W_{ij} \sim \mathrm{N}(0, 0.035)$

Table S1.2. Stand diameter distribution table with mean (SE) stem density (trees · ha^{-1}) across five-centimeter size classes. Trees above 45 cm are excluded from this table due to their exceedingly low density.

Status	Species	DBH Size Class							
		10	15	20	25	30	35	40	45
Post-Invasion	***Fraxinus nigra***	**16.6 (6.4)**	**5.4 (3.1)**	**0.7 (0.7)**	**0 (0)**	**0 (0)**	**0 (0)**	**0 (0)**	**0 (0)**
	Abies balsamea	44.4 (17.9)	24.5 (8.3)	3.5 (2.2)	0 (0)	0 (0)	0 (0)	0 (0)	0 (0)
	Acer rubrum	25.9 (13.3)	10.2 (4.5)	3.4 (2.3)	2.7 (1.5)	0.7 (0.7)	0 (0)	1.4 (0.9)	0.7 (0.7)
	Acer saccharinum	9.5 (9.5)	6.1 (6.1)	1.4 (1.4)	0.7 (0.7)	0 (0)	0 (0)	0 (0)	0 (0)
	Acer saccharum	0 (0)	0 (0)	0 (0)	0 (0)	0 (0)	0 (0)	0 (0)	0.8 (0.8)
	Betula alleghaniensis	2 (1.5)	1.4 (0.9)	1.4 (0.9)	1.4 (0.9)	0 (0)	0 (0)	0 (0)	0 (0)
	Betula papyrifera	4.2 (1.6)	3.5 (1.6)	1.6 (1.6)	1.4 (0.9)	0 (0)	0 (0)	0 (0)	0 (0)
	Fraxinus pennsylvanica	1.4 (0.9)	0 (0)	0 (0)	0 (0)	0 (0)	0 (0)	0 (0)	0 (0)
	Ostrya virginiana	0 (0)	0 (0)	0 (0)	0 (0)	0 (0)	0 (0)	0 (0)	0 (0)
	Picea mariana	3.4 (2.7)	2 (1.5)	4.8 (3.2)	1.4 (0.9)	0 (0)	0 (0)	0.7 (0.7)	0 (0)
	Pinus strobus	0 (0)	0 (0)	0 (0)	0 (0)	0.7 (0.7)	0 (0)	0 (0)	0 (0)
	Populus balsamifera	8.1 (5.5)	7.7 (5.8)	5.7 (4.2)	1.4 (1.4)	0 (0)	0 (0)	0 (0)	0 (0)
	Populus deltoides	0.7 (0.7)	0 (0)	0 (0)	0 (0)	0 (0)	0 (0)	0 (0)	0 (0)
	Populus grandidentata	0 (0)	0.7 (0.7)	0 (0)	0 (0)	0 (0)	0 (0)	0 (0)	0 (0)
	Populus tremuloides	0 (0)	1.4 (1.4)	1.4 (1.4)	2.7 (2.7)	2.7 (2.7)	0 (0)	0 (0)	0 (0)
	Quercus bicolor	0.7 (0.7)	0 (0)	0 (0)	0 (0)	0 (0)	0 (0)	0 (0)	0 (0)
	Quercus rubra	0 (0)	0 (0)	0 (0)	0 (0)	0 (0)	0 (0)	0 (0)	0 (0)
	Thuja occidentalis	8.3 (3.6)	7.5 (4.2)	12.2 (5.2)	6.8 (3.2)	4.8 (2.6)	2 (1.5)	0.7 (0.7)	0.7 (0.7)
	Tilia americana	1.4 (0.9)	0 (0)	1.4 (1.4)	0 (0)	0 (0)	0 (0)	0.7 (0.7)	0 (0)
	Tsuga canadensis	0 (0)	0 (0)	0 (0)	0 (0)	0 (0)	0 (0)	0 (0)	0 (0)
	Ulmus americana	6.8 (4.7)	6.1 (2.7)	3.9 (3.2)	0.7 (0.7)	0 (0)	0 (0)	0 (0)	0 (0)
	Ulmus rubra	0.7 (0.7)	0 (0)	0 (0)	0 (0)	0 (0)	0 (0)	0 (0)	0 (0)

Table S1.2 (cont'd).
Stand diameter distribution table with mean (SE) stem density (trees · ha^{-1}) across five-centimeter size classes. Trees above 45 cm are excluded from this table due to their exceedingly low density.

Invasion Status	Species	DBH Size Class							
		10	15	20	25	30	35	40	45
Mid Invasion	***Fraxinus nigra***	**118.3 (28.1)**	**67.4 (22.4)**	**26.1 (22.1)**	**24.5 (16.3)**	**4.9 (3.3)**	**0 (0)**	**0 (0)**	**0 (0)**
	Abies balsamea	65.3 (17.5)	12 (5.1)	0 (0)	3.3 (3.3)	0 (0)	0 (0)	0 (0)	0 (0)
	Acer rubrum	6.5 (4.8)	13.1 (5.5)	3.6 (2.2)	0 (0)	3.3 (3.3)	0 (0)	1.6 (1.6)	0 (0)
	Acer saccharinum	0 (0)	0 (0)	0 (0)	0 (0)	0 (0)	0 (0)	0 (0)	0 (0)
	Acer saccharum	0 (0)	0 (0)	0 (0)	0 (0)	0 (0)	0 (0)	0 (0)	0 (0)
	Betula alleghaniensis	5.2 (3.4)	6.5 (3.1)	6.5 (3.1)	0 (0)	0 (0)	0 (0)	0 (0)	0 (0)
	Betula papyrifera	19.6 (14.3)	11.7 (7.5)	8.7 (5.4)	3.6 (2.2)	0 (0)	0 (0)	0 (0)	0 (0)
	Fraxinus pennsylvanica	13.1 (9.5)	6.5 (4)	4.9 (4.9)	3.3 (3.3)	0 (0)	1.6 (1.6)	0 (0)	0 (0)
	Ostrya virginiana	0 (0)	0 (0)	0 (0)	0 (0)	0 (0)	0 (0)	0 (0)	0 (0)
	Picea mariana	0 (0)	0 (0)	0 (0)	0 (0)	0 (0)	0 (0)	0 (0)	0 (0)
	Pinus strobus	0 (0)	0 (0)	0 (0)	0 (0)	0 (0)	0 (0)	0 (0)	0 (0)
	Populus balsamifera	1.9 (1.9)	9.3 (7.5)	1.9 (1.9)	3.3 (2)	0 (0)	0 (0)	0 (0)	0 (0)
	Populus deltoides	0 (0)	0 (0)	0 (0)	0 (0)	0 (0)	0 (0)	0 (0)	0 (0)
	Populus grandidentata	0 (0)	1.9 (1.9)	0 (0)	0 (0)	0 (0)	0 (0)	0 (0)	0 (0)
	Populus tremuloides	1.6 (1.6)	0 (0)	0 (0)	0 (0)	0 (0)	0 (0)	0 (0)	0 (0)
	Quercus bicolor	0 (0)	0 (0)	0 (0)	0 (0)	0 (0)	0 (0)	0 (0)	0 (0)
	Quercus rubra	0 (0)	0 (0)	0 (0)	0 (0)	0 (0)	0 (0)	0 (0)	0 (0)
	Thuja occidentalis	31 (25.3)	19.6 (8.4)	45.7 (20.8)	13.4 (6.6)	6.8 (4.8)	4.9 (3.3)	1.6 (1.6)	0 (0)
	Tilia americana	0 (0)	0 (0)	0 (0)	0 (0)	0 (0)	0 (0)	0 (0)	0 (0)
	Tsuga canadensis	0 (0)	0 (0)	0 (0)	0 (0)	0 (0)	0 (0)	0 (0)	0 (0)
	Ulmus americana	3.3 (2)	1.6 (1.6)	0 (0)	0 (0)	0 (0)	0 (0)	0 (0)	0 (0)
	Ulmus rubra	0 (0)	0 (0)	0 (0)	0 (0)	0 (0)	0 (0)	0 (0)	0 (0)

Table S1.2 (cont'd).
Stand diameter distribution table with mean (SE) stem density (trees · ha^{-1}) across five-centimeter size classes. Trees above 45 cm are excluded from this table due to their exceedingly low density.

Invasion Status	Species	DBH Size Class							
		10	15	20	25	30	35	40	45
Pre Invasion	***Fraxinus nigra***	**144.6 (44.7)**	**96.8 (14.2)**	**73.5 (21)**	**28 (11.8)**	**8.2 (6.9)**	**5.8 (4.6)**	**4.7 (3)**	**0 (0)**
	Abies balsamea	21 (7.5)	15.2 (7)	1.2 (1.2)	2.3 (2.3)	0 (0)	0 (0)	0 (0)	0 (0)
	Acer rubrum	17.5 (9)	10.5 (6.1)	4.7 (3)	0 (0)	0 (0)	1.2 (1.2)	0 (0)	0 (0)
	Acer saccharinum	3.5 (2.4)	0 (0)	0 (0)	0 (0)	0 (0)	0 (0)	0 (0)	0 (0)
	Acer saccharum	12.8 (6.1)	5.8 (3.9)	1.2 (1.2)	1.2 (1.2)	1.2 (1.2)	0 (0)	0 (0)	0 (0)
	Betula alleghaniensis	22.2 (13.3)	3.5 (2.4)	1.2 (1.2)	1.2 (1.2)	1.2 (1.2)	0 (0)	0 (0)	0 (0)
	Betula papyrifera	0 (0)	0 (0)	0 (0)	0 (0)	0 (0)	0 (0)	0 (0)	0 (0)
	Fraxinus pennsylvanica	38.5 (15.3)	36.2 (15.9)	12.8 (5)	2.3 (2.3)	2.3 (2.3)	1.2 (1.2)	1.2 (1.2)	2.3 (2.3)
	Ostrya virginiana	1.2 (1.2)	0 (0)	0 (0)	0 (0)	0 (0)	0 (0)	0 (0)	0 (0)
	Picea mariana	1.2 (1.2)	3.5 (2.4)	0 (0)	0 (0)	0 (0)	0 (0)	0 (0)	0 (0)
	Pinus strobus	0 (0)	0 (0)	0 (0)	0 (0)	0 (0)	0 (0)	0 (0)	0 (0)
	Populus balsamifera	5.8 (5.8)	21 (21)	10.5 (10.5)	0 (0)	0 (0)	0 (0)	0 (0)	0 (0)
	Populus deltoides	0 (0)	0 (0)	0 (0)	0 (0)	0 (0)	0 (0)	0 (0)	0 (0)
	Populus grandidentata	0 (0)	0 (0)	0 (0)	0 (0)	0 (0)	0 (0)	0 (0)	0 (0)
	Populus tremuloides	28 (22.8)	18.7 (14.8)	8.2 (5.9)	7 (3.7)	5.8 (2.9)	0 (0)	1.2 (1.2)	0 (0)
	Quercus bicolor	0 (0)	0 (0)	0 (0)	0 (0)	0 (0)	0 (0)	0 (0)	0 (0)
	Quercus rubra	1.2 (1.2)	1.2 (1.2)	0 (0)	0 (0)	0 (0)	0 (0)	0 (0)	0 (0)
	Thuja occidentalis	0 (0)	4.7 (3.5)	14 (8.1)	16.3 (10.7)	7 (4.9)	2.3 (2.3)	3.5 (2.4)	0 (0)
	Tilia americana	23.3 (11.6)	7 (3.3)	1.2 (1.2)	1.2 (1.2)	1.2 (1.2)	0 (0)	1.2 (1.2)	0 (0)
	Tsuga canadensis	2.3 (2.3)	0 (0)	1.2 (1.2)	1.2 (1.2)	1.2 (1.2)	2.3 (1.5)	0 (0)	0 (0)
	Ulmus americana	23.3 (14.1)	7 (5.8)	3.5 (1.6)	1.2 (1.2)	0 (0)	0 (0)	0 (0)	0 (0)
	Ulmus rubra	0 (0)	0 (0)	0 (0)	0 (0)	0 (0)	0 (0)	0 (0)	0 (0)

Supplemental Figures

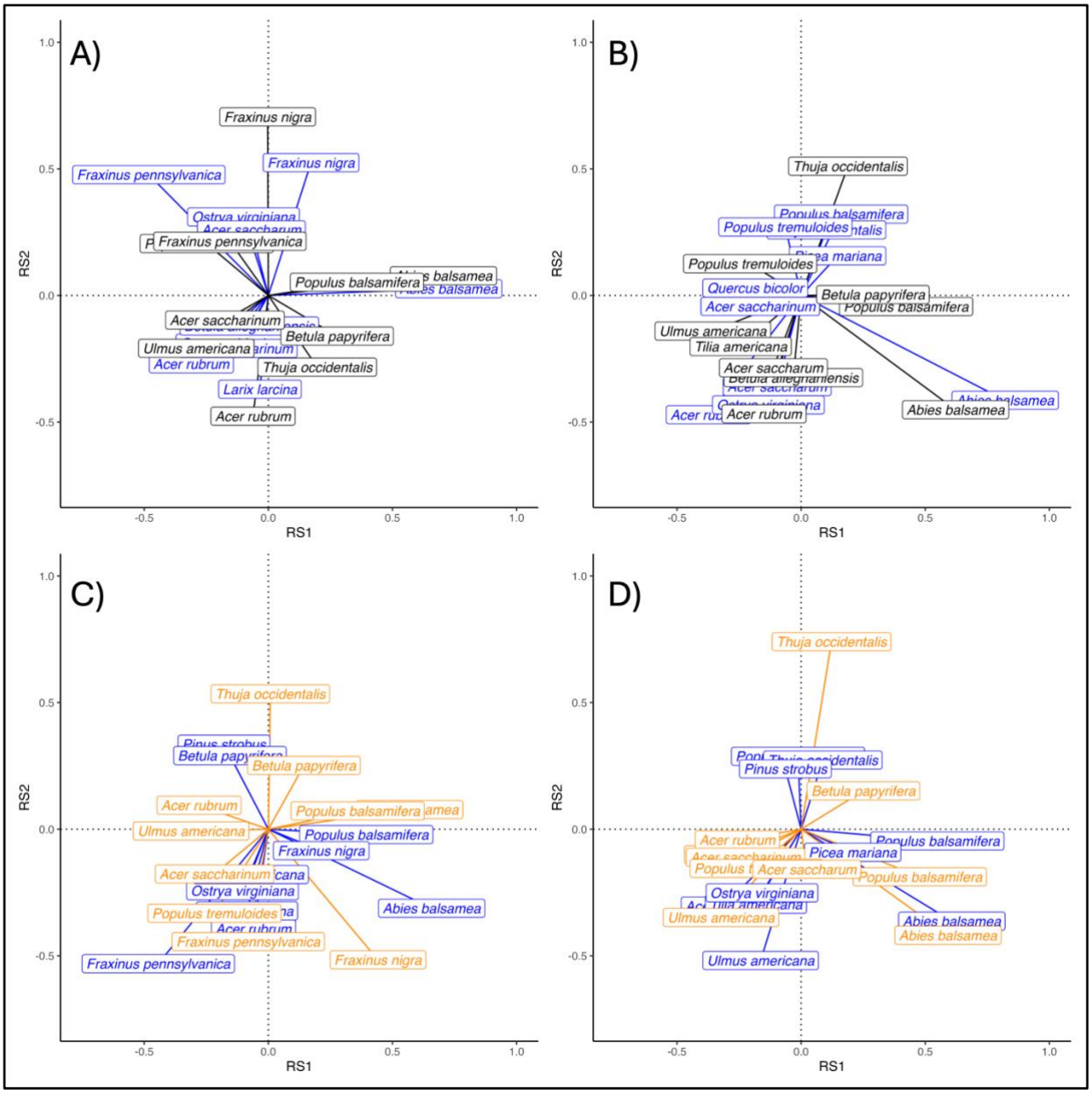

Figure S1.1. Plots displaying the contributions of species to the CoIA canonical space and the relationships between species in the different size classes, with overstory species (blue text) compared to recruit species (black text) with black ash included (A) and excluded (B) from analysis, and overstory species compared to sapling species (orange text) including (C) and excluding ash (D). Distance of species names from the center of the plots represents the amount of influence each species has on the CoIA plot, and closeness of different species of different colors represents how correlated these species were. For example, in plot A, *Fraxinus nigra* is heavily influence the CoIA plot, and the generally overstory black ash were represented similarly in our overstory and recruit communities.

APPENDIX B: CHAPTER TWO SUPPLMENTAL TABLES AND FIGURES

Supplemental Tables

Table S2.1. Model equations for mixed models, with response and predictors detailed in the first column, and corresponding estimates in the second column.

Model	Fit Equation
Mean overstory black ash ring width predicted by tree age with a random effect for stand	$\log(y_{ij}) = Mean\ Ring\ Width_{ij} * 0.005 - 11.2 + U_i + W_{ij}$ $U_i \sim \mathrm{N}(0,0.015)$ $W_{ij} \sim \mathrm{N}(0,0.056)$
Mean overstory black ash DBH predicted by tree age with a random effect for stand	$\log(y_{ji}) = DBH_{ij} * -0.005 + 11.9 + U_{ij} + W_{ij}$ $U_i \sim \mathrm{N}(0,0.012)$ $W_{ij} \sim \mathrm{N}(0,0.052)$
Mean black ash recruit ring width predicted by tree age with a random effect for stand	$\log(y_{ij}) = Mean\ Ring\ Width_{ij} * 0.019 - 37.13 + U_i + W_{ij}$ $U_i \sim \mathrm{N}(0,0.012)$ $W_{ij} \sim \mathrm{N}(0,0.039)$
Mean black ash recruit DBH predicted by tree age with a random effect for stand	$\log(y_{ij}) = Mean\ Ring\ Width_{ij} * 0.019 - 37.13 + U_i + W_{ij}$ $U_i \sim \mathrm{N}(0,0.012)$ $W_{ij} \sim \mathrm{N}(0,0.039)$
Average balsam fir standard ring width predicted by Pre-Post-2015 (two level factor) and Invasion Strata (three level factor) with stand as a random effect	y_{ij} $= 0.73 + (Pre/Post_{mean.rwi.pre})_{ij} * 0.73$ $+ (Invasion\ Status_{Mid-Invasion})_{ij} * 0.009$ $+ (Invasion\ Status_{Pre-Invasion})_{ij} * 0.83 + U_i + W_{ij}$ $U_i \sim \mathrm{N}(0,1.56 * 10^{-12})$ $W_{ij} \sim \mathrm{N}(0,0.035)$
Standard radial growth after 2015 predicted by tree species (black ash / balsam fir) and Invasion Strata (three level factor)	y_{ij} $= 0.722 + (Species_{Black\ Ash})_{ij} * 0.6264$ $- (Invasion\ Status_{Mid-Invasion})_{ij} * 0.04 + 0.17$ $* (Invasion\ Status_{Pre-Invasion})_{ij} - 0.869 * (Species_{Black\ Ash})_{ij}$ $* (Invasion\ Status_{Mid-Invasion})_{ij} - 0.7385 * (Species_{Black\ Ash})_{ij}$ $* (Invasion\ Status_{Pre-Invasion})_{ij} + U_i + W_{ij}$ $U_i \sim \mathrm{N}(0, 0.127)$ $W_{ij} \sim \mathrm{N}(0,0.0454)$

APPENDIX C: CHAPTER THREE SUPPLMENTAL TABLES AND FIGURES

Supplemental Tables

Table S3.1. Model equations for mixed models, with response and predictors detailed in the first column, and corresponding estimates in the second column.

Model Formula	Fit Model Equation
Live black ash basal area predicted by Invasion Status (two-level factor), with a random effect for Stand	$Black\ Ash\ BA_{ij}$ $= StatusPre_{ij} * -4.6487 + 4.9769 + U_i + W_{ij}$ $U_i \sim \mathrm{N}(0, 4.16e-10)$ $W_{ij} \sim \mathrm{N}(0, 9.7e-10)$
Total snag basal area predicted by Invasion Status (two-level factor), with a random effect for stand	$Total\ Snag\ BA_{ij}$ $= StatusPre_{ij} * -4.302 + 8.876 + U_i + W_{ij}$ $U_i \sim \mathrm{N}(0, 5.85)$ $W_{ij} \sim \mathrm{N}(0, 11.58)$
Black ash snag basal area predicted by Invasion Status (two-level factor), with a random effect for stand	$Black\ Ash\ Snag\ BA_{ij}$ $= StatusPre_{ij} * -5.163 + 5.571 + U_i + W_{ij}$ $U_i \sim \mathrm{N}(0, 6.05e-10)$ $W_{ij} \sim \mathrm{N}(0, 1.62)$
Total cerambycids caught predicted by Invasion Status (two-level factor), with a random effect for Stand and Year.	$Total\ Caught_{ijk}$ $= StatusPre_{ijk} * -15.4 + 53.5 + U_{ij}^{Stand} + U_{ik}^{Year} + W_{ijk}$ $U_{ij}^{Stand} \sim \mathrm{N}(0, 0.003)$ $U_{ik}^{Year} \sim N(0, 91.2)$ $W_{ij} \sim \mathrm{N}(0, 810.6)$
Total cerambycids caught predicted by Trap Placement (two-level factor), with a random effect for Stand and Year.	$Total\ Caught_{ijk}$ $= GroundTrap_{ijk} * -7 + 25.44 + U_{ij}^{Stand} + U_{ik}^{Year} + W_{ijk}$ $U_{ij}^{Stand} \sim \mathrm{N}(0, 0.001)$ $U_{ik}^{Year} \sim N(0, 27.18)$ $W_{ij} \sim \mathrm{N}(0, 335.2)$

Table S3.1 (cont'd).
Model equations for mixed models, with response and predictors detailed in the first column, and corresponding estimates in the second column.

Model Formula	Fit Model Equation
Cerambycid species richness predicted by Invasion Status(two-level factor), with a random effect for Stand and Year.	$Species\ Richness_{ijk} = StatusPre_{ijk} * -0.367 + 11.67 + U_{ij}^{Stand} + U_{ik}^{Year} + W_{ijk}$ $U_{ij}^{Stand} \sim \mathrm{N}(0, 0.90)$ $U_{ik}^{Year} \sim N(0, 1.66e-8)$ $W_{ij} \sim \mathrm{N}(0, 11.1)$
Cerambycid species richness predicted by Trap Placement (two-level factor), with a random effect for Stand and Year.	$Species\ Richness_{ijk} = GroundTrap_{ijk} * -1.44 + 6.43 + U_{ij}^{Stand} + U_{ik}^{Year} + W_{ijk}$ $U_{ij}^{Stand} \sim \mathrm{N}(0, 0.35)$ $U_{ik}^{Year} \sim N(0, 9.36e-9)$ $W_{ij} \sim \mathrm{N}(0, 4.86)$
Coarse woody debris volume (CWD) predicted by Invasion status (two-level factor) and an interaction with Decay Class (four-level factor), with a random effect for stand.	$CWD\ Volume_{ij} = 10.601 - 1.697 * StatusPre_{ij} + 5.780 * DecayClass2_{ij} + 33.406 * DecayClass3_{ij} + 15.087 \cdot DecayClass4_{ij} + 8.301 \cdot StatusPre_{ij} * DecayClass2_{ij} - 13.824 * StatusPre * DecayClass3_{ij} - 10.765 * StatusPre_{ij} * DecayClass4_{ij} + U_i + W_{ij}$ $U_i \sim N(0, 115.8)$ $W_{ij} \sim N(0, 132.8)$

Table S3.2.
Species with new county records by subfamily and tribe, for the subfamily Cerambycinae. County names with new records are shown along with sources for previous known county records.

Subfamily	Tribe	Species	Authority	New County Records	Source(s)
Cerambycinae	Anaglyptini	*Crytophorus verrucosus*	Olivier	Baraga, Dickinson, Gogebic, Iron	Gosling (1973), Pellmyr (1985), Downie and Arnett (1996), Hubbard and Schwarz (1878)
	Callidiini	*Phymatodes aereus*	Newman	Baraga, Menominee, Ontonagon	Gosling (1973)
	Clytini	*Clytus ruricola*	Olivier	Baraga, Dickinson, Iron, Menominee, Ontonagon	Gosling (1973), MacRae and Rice (2007), Downie and Arnett (1996), Hubbard and Schwarz (1878)
		Glycobius speciosus	Say	Gogebic, Iron, Menominee	Gosling (1973), Holland (2009)
		Neoclytus acuminatus	Fabricius	Dickinson, Menominee	Gosling (1973), Andrews (1923), BugGuide, Hubbard and Schwarz (1878)
		Sarosesthes fulminans	Fabricius	Iron	Gosling (1973), Andrews (1923), BugGuide, Hubbard and Schwarz (1878)
		Xylotrechus colonus	Fabricius	Baraga, Dickinson, Gogebic, Iron, Menominee	Gosling (1973), Andrews (1923), Downie and Arnett (1996), Hubbard and Schwarz (1878)
		Xylotrechus integer	Fabricius	Baraga	Ruesink and Parsons (2021)
	Trachyderini	*Purpuricenus humeralis*	Fabricius	Dickinson	Gosling (1973), Andrews (1916), Downie and Arnett (1996)

Table S3.2 (cont'd).
Species with new county records by subfamily and tribe, for the subfamily Lamiinae. County names with new records are shown along with sources for previous known county records

Subfamily	Tribe	Species	Authority	New County Records	Source(s)
Lamiinae	Acanthocinini	*Astylopsis macula*	Say	Menominee	Gosling and Gosling (1976), Andrews (1923), Downie and Arnett (1996), Hubbard and Schwarz (1878)
		Astylopsis sexguttata	Say	Dickinson	Gosling and Gosling (1976), Andrews (1923), Hubbard and Schwarz (1878)
		Urgleptes querci	Fitch	Menominee, Ontonagon	Gosling and Gosling (1976), Andrews (1916), Downie and Arnett (1996), Hubbard and Schwarz (1878)
	Acanthoderini	*Aegomorphus modestus*	Gyllenhal	Baraga, Dickinson	Gosling and Gosling (1976), Downie and Arnett (1996), Hubbard and Schwarz (1878)
	Monochamini	*Microgoes oculatus*	LeConte	Dickinson, Iron	Gosling and Gosling (1976), Downie and Arnett (1996), Hubbard and Schwarz (1878)

Table S3.2 (cont'd).
Species with new county records by subfamily and tribe, for the subfamily Lepturinae. County names with new records are shown along with sources for previous known county records

Subfamily	Tribe	Species	Authority	New County Records	Source(s)
Lepturinae	Lepturini	*Pygoleptura nigrella*	Say	Baraga	Gosling and Gosling (1976), Andrews (1923), Downie and Arnett (1996), Hubbard and Schwarz (1878)
		Strangalepta abbreviata	Germar	Menominee	Gosling and Gosling (1976), Andrews (1923), Downie and Arnett (1996), Hubbard and Schwarz (1878)
		Trigonarthris minnesotana	Casey	Baraga, Dickinson	Gosling and Gosling (1976), Hatch (1924)
		Trigonarthris proxima	Say	Gogebic	Gosling and Gosling (1976), Andrews (1923), Hubbard and Schwarz (1878)
	Oxymirini	*Anthophylax attenuatus*	Halderman	Baraga	Gosling and Gosling (1976), Downie and Arnett (1996), Hubbard and Schwarz (1878)
	Rhagiini	*Centrodera decolorata*	Harris	Ontonagon	Gosling and Gosling (1976), Hubbard and Schwarz (1878)
		Gaurotes cyanipennis	Say	Baraga, Mackinac	Gosling and Gosling (1976), Andrews (1923), Downie and Arnett (1996), Hubbard and Schwarz (1878)
		Stenocorus schaumii	LeConte	Ontonagon	Gosling and Gosling (1976), BugGuide